



Volume 6, Issue 2, Year 2023

ISSN: 2645-9000

Owner

IZMIR DEMOCRACY UNIVERSITY

Chief Editor

Prof. Dr. Günay ÖZTÜRK

Vice Editors

Assoc. Prof. Tuğba KESKİN GÜNDOĞDU

Assoc. Prof. Sema ÇARIKÇI

Journal Contact: Izmir Democracy University Natural and Applied Sciences Journal

E-mail: idunas@idu.edu.tr

Web: <https://dergipark.org.tr/en/pub/idunas>

Publisher: Izmir Democracy University

EDITORIAL BOARD

Head of Editorial Board: Prof. Dr. Günay OZTURK

Vice Editor: Assoc. Prof. Tuğba KESKİN GÜNDOĞDU

Vice Editor: Assoc. Prof. Sema ÇARIKÇI

Departmental Editor: Assist. Prof. Gizem KALELİ CAN

Publishing Editor: Assist. Prof. Gizem KALELİ CAN

English Language Editor: Dr. Kudret ÖKTEM

Layout Editor: Bengü GÜNGÖR

International Editorial Board Member: Prof. Dr. Elza Maria Morais Fonseca/ Polytechnic Ins of Porto

International Editorial Board Member: Prof. Dr. Ercan Yılmaz/ Abant İzzet Baysal University

International Editorial Board Member: Prof. Dr. Fatih İnci/ Standford University

International Editorial Board Member: Prof. Dr. Hariharan Muthusamy/Nat Ins of Tech.-Uttarakhand

International Editorial Board Member: Prof. Dr. Kemal Polat/ Abant İzzet Baysal University

International Editorial Board Member: Prof. Dr. Murat Şimşek/İnönü University

International Editorial Board Member: Prof. Dr. Sinan Akgöl/ Ege University

International Editorial Board Member: Prof. Dr. Soner Çakmak/ Hacettepe University

International Editorial Board Member: Assoc. Dr. Elif Güngör /Balıkesir University

International Editorial Board Member: Asst. Selma Çelen Yüçetürk/Balıkesir University

International Editorial Board Member: Prof. Dr. Cihan Özgür/ Izmir Democracy University

International Editorial Board Member: Prof. Dr. Timur Canel / Kocaeli University

International Editorial Board Member: Prof. Dr. İrem Bağlan/ Kocaeli University

International Editorial Board Member: Prof. Dr. Bengü Bayram/Balıkesir University

International Editorial Board Member: Assoc.. Dr. Zeynel Abidin Çil/ Izmir Democracy University

International Editorial Board Member: Assoc.. Dr. Damla Kızılay / Izmir Democracy University

International Editorial Board Member: Assoc. Dr. Mine Güngörmüşler/ İzmir Economy University

International Editorial Board Member: Dr. Gülizar Çalışkan/ Izmir Democracy University

International Editorial Board Member: Assoc.. Dr. Müge İşleten Hoşoğlu/ Gebze Tech. Uni.

International Editorial Board Member: Assoc.. Dr. Gözde Duman Taç/ Ege University

International Editorial Board Member: Dr. Sıdıka Tuğçe Dağlıoğlu/ Ege University

International Editorial Board Member: Asst. Prof. Hilal Betül Kaya Akkale/Manisa Celal Bayar Uni.

INDEXES AND DATABASES

IDUNAS is indexed by 4 national and international databases.

INDEXED DATABASES	
ACARINDEX	https://www.acarindex.com/search?type=article&q=Natural+and+Applied+Sciences+Journal
Academic Resource Index ResearchBib	https://journalseeker.researchbib.com/view/issn/2645-9000
Google Scholar	https://scholar.google.com.tr/scholar?q=izmir+democracy+university+natural+and+applied+sciences+journal&hl=tr&as_sdt=0&as_vis=1&oi=scholart
Ideal Online	https://www.idealonline.com.tr/IdealOnline/
APPLIED DATABASES	
Directory of Research Journals Indexing	http://olddrji.lbp.world/
Directory of Academic and Scientific Journals	https://ojs.europubpublications.com/ojs/index.php
OJOP	https://www.ojop.org/

ABOUT

Natural & Applied Sciences Journal is an international open access, peer-reviewed, free of cost academic journal that includes articles and reviews on natural and applied sciences. It is published twice a year in June and December. Our journal accepts only English content from the second issue.

AIM & SCOPE

It aims to contribute to the knowledge of the field of natural and applied sciences by publishing qualified scientific studies in the field.

Natural & Applied Sciences Journal is an international open access, peer-reviewed, free of cost academic journal that includes articles and reviews on natural and applied sciences published by İzmir Democracy University. It is published twice a year in June and December. Our journal accepts only English content from the second issue.

PERIODS

June and December

ETHICAL PRINCIPLES AND PUBLICATION POLICY

All articles submitted for publication in the journal must conform to the ethical rules of scientific research. The authors of each article are required to sign the Copyright Form confirming that they have granted permission for their work to be published in Natural and Applied Science Journal. Publication will not take place, even if the manuscript is accepted without this form. Authors are solely responsible for the content of their articles and any responsibilities they may incur regarding copyrights. The work submitted to the journal should not have been published in any language, in any journal, or in the process of being evaluated in any other publication.

Articles should be prepared in accordance with the general ethical rules specified by DOI and DOAJ. Plagiarism Control All articles submitted to Natural and Applied Science Journal are checked using the iThenticate plagiarism detection software. Based on the similarity report generated by the software, the editorial board determines whether the article should be submitted to peer review or rejected.

PRICE POLICY

No fee is charged from the author or institution under any name.

INTERNATIONAL STANDARDS FOR AUTHORS

RESPONSIBLE RESEARCH PUBLICATION

A position statement developed at the 2nd World Conference on Research Integrity, Singapore, July 22-24, 2010.

Elizabeth Wager & Sabine Kleinert

Contact details: liz@sideview.demon.co.uk
sabine.kleinert@lancet.com

SUMMARY

- The research being reported should have been conducted in an ethical and responsible manner and should comply with all relevant legislation.
- Researchers should present their results clearly, honestly, and without fabrication, falsification, or inappropriate data manipulation.
- Researchers should strive to describe their methods clearly and unambiguously so that their findings can be confirmed by others.
- Researchers should adhere to publication requirements that submitted work is original, is not plagiarized, and has not been published elsewhere.
- Authors should take collective responsibility for submitted and published work.
- The authorship of research publications should accurately reflect individuals' contributions to the work and its reporting.

- Funding sources and relevant conflicts of interest should be disclosed.

Cite this as: Wager E & Kleinert S (2011) Responsible research publication: international standards for authors. A position statement developed at the 2nd World Conference on Research Integrity, Singapore, July 22-24, 2010. Chapter 50 in: Mayer T & Steneck N (eds) Promoting Research Integrity in a Global Environment. Imperial College Press / World Scientific Publishing, Singapore (pp 309-16). (ISBN 978-981-4340-97-7)

INTRODUCTION

Publication is the final stage of research and therefore a responsibility for all researchers. Scholarly publications are expected to provide a detailed and permanent record of research. Because publications form the basis for both new research and the application of findings, they can affect not only the research community but also, indirectly, society at large. Researchers therefore have a responsibility to ensure that their publications are honest, clear, accurate, complete and balanced, and should avoid misleading, selective or ambiguous reporting. Journal editors also have responsibilities for ensuring the integrity of the research literature and these are set out in companion guidelines.

This document aims to establish international standards for authors of scholarly research publications and to describe responsible research reporting practice. We hope these standards will be endorsed by research institutions, funders, and professional societies; promoted by editors and publishers; and will aid in research integrity training.

Responsible research publication

1 Soundness and reliability

1.1 The research being reported should have been conducted in an ethical and responsible manner and follow all relevant legislation. [See also the Singapore Statement on Research Integrity, www.singaporestatement.org]

1.2 The research being reported should be sound and carefully executed.

1.3 Researchers should use appropriate methods of data analysis and display (and, if needed, seek, and follow specialist advice on this).

1.4 Authors should take collective responsibility for their work and for the content of their publications. Researchers should check their publications carefully at all stages to ensure methods and findings are reported accurately. Authors should carefully check calculations, data presentations, typescripts/submissions, and proofs.

2 Honesty

2.1 Researchers should present their results honestly and without fabrication, falsification, or inappropriate data manipulation. Research images (e.g. micrographs, X-rays, pictures of electrophoresis gels) should not be modified in a misleading way.

2.2 Researchers should strive to describe their methods and to present their findings clearly and unambiguously. Researchers should follow applicable reporting guidelines. Publications should provide sufficient detail to permit experiments to be repeated by other researchers.

2.3 Reports of research should be complete. They should not omit inconvenient, inconsistent, or inexplicable findings or results that do not support the authors' or sponsors' hypothesis or interpretation.

2.4 Research funders and sponsors should not be able to veto publication of findings that do not favor their product or position. Researchers should not enter agreements that permit the research sponsor to veto or control the publication of the findings (unless there are exceptional circumstances, such as research classified by governments because of security implications).

2.5 Authors should alert the editor promptly if they discover an error in any submitted, accepted or published work. Authors should cooperate with editors in issuing corrections or retractions when required.

2.6 Authors should represent the work of others accurately in citations and quotations.

2.7 Authors should not copy references from other publications if they have not read the cited work.

3 Originality

3.1 Authors should adhere to publication requirements that submitted work is original and has not been published elsewhere in any language. Work should not be submitted concurrently to more than one publication unless the editors have agreed to co-publication. If articles are co-published this fact should be made clear to readers.

3.2 Applicable copyright laws and conventions should be followed. Copyright material (e.g. tables, figures, or extensive quotations) should be reproduced only with appropriate permission and acknowledgement.

3.3 Relevant previous work and publications, both by other researchers and the authors' own, should be properly acknowledged, and referenced. The primary literature should be cited where possible.

3.4 Data, text, figures, or ideas originated by other researchers should be properly acknowledged and should not be presented as if they were the authors' own. Original wording taken directly from publications by other researchers should appear in quotation marks with the appropriate citations.

3.5 Authors should inform editors if findings have been published previously or if multiple reports or multiple analyses of a single data set are under consideration for publication elsewhere. Authors should provide copies of related publications or work submitted to other journals.

3.6 Multiple publications arising from a single research project should be clearly identified as such and the primary publication should be referenced. Translations and adaptations for different audiences should be clearly identified as such, should acknowledge the original source, and

should respect relevant copyright conventions and permission requirements. If in doubt, authors should seek permission from the original publisher before republishing any work.

4 Appropriate authorship and acknowledgement

4.1 The research literature serves as a record not only of what has been discovered but also of who made the discovery. The authorship of research publications should therefore accurately reflect individuals' contributions to the work and its reporting.

4.2 In cases where major contributors are listed as authors while those who made less substantial, or purely technical, contributions to the research or to the publication are listed in an acknowledgement section, the criteria for authorship and acknowledgement should be agreed at the start of the project. Ideally, authorship criteria within a particular field should be agreed, published and consistently applied by research institutions, professional and academic societies, and funders. While journal editors should publish and promote accepted authorship criteria appropriate to their field, they cannot be expected to adjudicate in authorship disputes. Responsibility for the correct attribution of authorship lies with authors themselves working under the guidance of their institution. Research institutions should promote and uphold fair and accepted standards of authorship and acknowledgement. When required, institutions should adjudicate in authorship disputes and should ensure that due process is followed.

4.3 Researchers should ensure that only those individuals who meet authorship criteria (i.e. made a substantial contribution to the work) are rewarded with authorship and that deserving authors are not omitted. Institutions and journal editors should encourage practices that prevent guest, gift, and ghost authorship.

Note:

- Guest authors are those who do not
- Gift authors are those who do meet accepted authorship criteria but are listed because of their seniority, reputation or supposed influence not
- Ghost authors are those who meet authorship criteria but are not listed meet accepted authorship criteria but are listed as a personal favor or in return for payment

4.4 All authors should agree to be listed and should approve the submitted and accepted versions of the publication. Any change to the author list should be approved by all authors including any who have been removed from the list. The corresponding author should act as a point of contact between the editor and the other authors and should keep co-authors informed and involve them in major decisions about the publication (e.g. responding to reviewers' comments).

4.5 Authors should not use acknowledgements misleadingly to imply a contribution or endorsement by individuals who have not, in fact, been involved with the work or given an endorsement.

5 Accountability and responsibility

5.1 All authors should have read and be familiar with the reported work and should ensure that publications follow the principles set out in these guidelines. In most cases, authors will be expected to take joint responsibility for the integrity of the research and its reporting. However, if authors take responsibility only for certain aspects of the research and its reporting, this should be specified in the publication.

5.2 Authors should work with the editor or publisher to correct their work promptly if errors or omissions are discovered after publication.

5.3 Authors should abide by relevant conventions, requirements, and regulations to make materials, reagents, software, or datasets available to other researchers who request them. Researchers, institutions, and funders should have clear policies for handling such requests. Authors must also follow relevant journal standards. While proper acknowledgement is expected, researchers should not demand authorship as a condition for sharing materials.

5.4 Authors should respond appropriately to post-publication comments and published correspondence. They should attempt to answer correspondents' questions and supply clarification, or additional details where needed.

6 Adherence to peer review and publication conventions

6.1 Authors should follow publishers' requirements that work is not submitted to more than one publication for consideration at the same time.

6.2 Authors should inform the editor if they withdraw their work from review or choose not to respond to reviewer comments after receiving a conditional acceptance.

6.3 Authors should respond to reviewers' comments in a professional and timely manner.

6.4 Authors should respect publishers' requests for press embargos and should not generally allow their findings to be reported in the press if they have been accepted for publication (but not yet published) in a scholarly publication. Authors and their institutions should liaise and cooperate with publishers to coordinate media activity (e.g. press releases and press conferences) around publication. Press releases should accurately reflect the work and should not include statements that go further than the research findings.

7 Responsible reporting of research involving humans or animals

7.1 Appropriate approval, licensing or registration should be obtained before the research begins and details should be provided in the report (e.g. Institutional Review Board, Research Ethics Committee approval, national licensing authorities for the use of animals).

7.2 If requested by editors, authors should supply evidence that reported research received the appropriate approval and was carried out ethically (e.g. copies of approvals, licenses, participant consent forms).

7.3 Researchers should not generally publish or share identifiable individual data collected in the course of research without specific consent from the individual (or their representative). Researchers should remember that many scholarly journals are now freely available on the internet and should therefore be mindful of the risk of causing danger or upset to unintended readers (e.g. research participants or their families who recognize themselves from case studies, descriptions, images, or pedigrees).

7.4 The appropriate statistical analyses should be determined at the start of the study and a data analysis plan for the prespecified outcomes should be prepared and followed. Secondary or post hoc analyses should be distinguished from primary analyses and those set out in the data analysis plan.

7.5 Researchers should publish all meaningful research results that might contribute to understanding. In particular, there is an ethical responsibility to publish the findings of all clinical trials. The publication of unsuccessful studies or experiments that reject a hypothesis may help prevent others from wasting time and resources on similar projects. If findings from small studies and those that fail to reach statistically significant results can be combined to produce more useful information (e.g. by meta-analysis) then such findings should be published.

7.6 Authors should supply research protocols to journal editors if requested (e.g. for clinical trials) so that reviewers and editors can compare the research report to the protocol to check that it was carried out as planned and that no relevant details have been omitted. Researchers should follow relevant requirements for clinical trial registration and should include the trial registration number in all publications arising from the trial.

INTERNATIONAL STANDARDS FOR EDITORS

RESPONSIBLE RESEARCH PUBLICATION

A position statement developed at the 2nd World Conference on Research Integrity, Singapore, July 22-24, 2010.

Sabine Kleinert & Elizabeth Wager

Contact details: sabine.kleinert@lancet.com

liz@sideview.demon.co.uk

Cite this as: Kleinert S & Wager E (2011) Responsible research publication: international standards for editors. A position statement developed at the 2nd World Conference on Research Integrity, Singapore, July 22-24, 2010. Chapter 51 in: Mayer T & Steneck N (eds) Promoting Research Integrity in a Global Environment. Imperial College Press / World Scientific Publishing, Singapore (pp 317-28). (ISBN 978-981-4340-97-7)

Summary

- Editors are accountable and should take responsibility for everything they publish

- Editors should make fair and unbiased decisions independent from commercial consideration and ensure a fair and appropriate peer review process
- Editors should adopt editorial policies that encourage maximum transparency and complete, honest reporting
- Editors should guard the integrity of the published record by issuing corrections and retractions when needed and pursuing suspected or alleged research and publication misconduct
- Editors should pursue reviewer and editorial misconduct
- Editors should critically assess the ethical conduct of studies in humans and animals
- Peer reviewers and authors should be told what is expected of them
- Editors should have appropriate policies in place for handling editorial conflicts of interest

Introduction

As guardians and stewards of the research record, editors should encourage authors to strive for, and adhere themselves to, the highest standards of publication ethics. Furthermore, editors are in a unique position to indirectly foster responsible conduct of research through their policies and processes. To achieve the maximum effect within the research community, ideally all editors should adhere to universal standards and good practices. While there are important differences between different fields and not all areas covered are relevant to each research community, there are important common editorial policies, processes, and principles that editors should follow to ensure the integrity of the research record.

These guidelines are a starting point and are aimed at journal editors in particular. While books and monographs are important and relevant research records in many fields, guidelines for book editors are beyond the scope of these recommendations. It is hoped that in due course such guidelines can be added to this document.

Editors should regard themselves as part of the wider professional editorial community, keep themselves abreast of relevant policies and developments, and ensure their editorial staff is trained and kept informed of relevant issues.

To be a good editor requires many more principles than are covered here. These suggested principles, policies, and processes are particularly aimed at fostering research and publication integrity.

Editorial Principles

1. Accountability and responsibility for journal content

Editors have to take responsibility for everything they publish and should have procedures and policies in place to ensure the quality of the material they publish and maintain the integrity of the published record (see paragraphs 4-8).

2. Editorial independence and integrity

An important part of the responsibility to make fair and unbiased decisions is the upholding of the principle of editorial independence and integrity.

2.1 Separating decision-making from commercial considerations

Editors should make decisions on academic merit alone and take full responsibility for their decisions. Processes must be in place to separate commercial activities within a journal from editorial processes and decisions. Editors should take an active interest in the publisher's pricing policies and strive for wide and affordable accessibility of the material they publish.

Sponsored supplements must undergo the same rigorous quality control and peer review as any other content for the journal. Decisions on such material must be made in the same way as any other journal content. The sponsorship and role of the sponsor must be clearly declared to readers.

Advertisements need to be checked so that they follow journal guidelines, should be clearly distinguishable from other content, and should not in any way be linked to scholarly content.

2.2 Editors' relationship to the journal publisher or owner

Editors should ideally have a written contract setting out the terms and conditions of their appointment with the journal publisher or owner. The principle of editorial independence should be clearly stated in this contract. Journal publishers and owners should not have any role in decisions on content for commercial or political reasons. Publishers should not dismiss an editor because of any journal content unless there was gross editorial misconduct, or an independent investigation has concluded that the editor's decision to publish was against the journal's scholarly mission.

2.3 Journal metrics and decision-making

Editors should not attempt to inappropriately influence their journal's ranking by artificially increasing any journal metric. For example, it is inappropriate to demand that references to that journal's articles are included except for genuine scholarly reasons. In general, editors should ensure that papers are reviewed on purely scholarly grounds and that authors are not pressured to cite specific publications for non-scholarly reasons.

3. Editorial confidentiality

3.1 Authors' material

If a journal operates a system where peer reviewers are chosen by editors (rather than posting papers for all to comment as a pre-print version), editors must protect the confidentiality of authors' material and remind reviewers to do so as well. In general, editors should not share submitted papers with editors of other journals, unless with the authors' agreement or in cases of alleged misconduct (see below). Editors are generally under no obligation to provide material to lawyers for court cases. Editors should not give any indication of a paper's status with the journal to anyone other than the authors. Web-based submission systems must be run in a way that prevents unauthorized access.

In the case of a misconduct investigation, it may be necessary to disclose material to third parties (e.g., an institutional investigation committee or other editors).

3.2 Reviewers

Editors should protect reviewers' identities unless operating an open peer review system. However, if reviewers wish to disclose their names, this should be permitted.

If there is alleged or suspected reviewer misconduct it may be necessary to disclose a reviewer's name to a third party.

General editorial policies

4. Encourage maximum transparency and complete and honest reporting

To advance knowledge in scholarly fields, it is important to understand why particular work was done, how it was planned and conducted and by whom, and what it adds to current knowledge. To achieve this understanding, maximum transparency and complete and honest reporting are crucial.

4.1 Authorship and responsibility

Journals should have a clear policy on authorship that follows the standards within the relevant field. They should give guidance in their information for authors on what is expected of an author and, if there are different authorship conventions within a field, they should state which they adhere to.

For multidisciplinary and collaborative research, it should be apparent to readers who has done what and who takes responsibility for the conduct and validity of which aspect of the research. Each part of the work should have at least one author who takes responsibility for its validity. For example, individual contributions and responsibilities could be stated in a contributor section. All authors are expected to have contributed significantly to the paper and to be familiar with its entire content and ideally, this should be declared in an authorship statement submitted to the journal.

When there are undisputed changes in authorship for appropriate reasons, editors should require that all authors (including any whose names are being removed from an author list) agree

these in writing. Authorship disputes (i.e., disagreements on who should or should not be an author before or after publication) cannot be adjudicated by editors and should be resolved at institutional level or through other appropriate independent bodies for both published and unpublished papers. Editors should then act on the findings, for example by correcting authorship in published papers.

Journals should have a publicly declared policy on how papers submitted by editors or editorial board members are handled (see paragraph on editorial conflicts of interest: 8.2).

4.2 Conflicts of interest and role of the funding source

Editors should have policies that require all authors to declare any relevant financial and non-financial conflicts of interest and publish at least those that might influence a reader's perception of a paper, alongside the paper. The funding source of the research should be declared and published, and the role of the funding source in the conception, conduct, analysis, and reporting of the research should be stated and published.

Editors should make it clear in their information for authors if in certain sections of the journal (e.g., commissioned commentaries or review articles) certain conflicts of interest preclude authorship.

4.3 Full and honest reporting and adherence to reporting guidelines

Among the most important responsibilities of editors is to maintain a high standard in the scholarly literature. Although standards differ among journals, editors should work to ensure that all published papers make a substantial new contribution to their field. Editors should discourage so-called 'salami publications' (i.e., publication of the minimum publishable unit of research), avoid duplicate or redundant publication unless it is fully declared and acceptable to all (e.g., publication in a different language with cross-referencing), and encourage authors to place their work in the context of previous work (i.e., to state why this work was necessary/done, what this work adds or why a replication of previous work was required, and what readers should take away from it).

Journals should adopt policies that encourage full and honest reporting, for example, by requiring authors in fields where it is standard to submit protocols or study plans, and, where they exist, to provide evidence of adherence to relevant reporting guidelines. Although devised to improve reporting, adherence to reporting guidelines also makes it easier for editors, reviewers, and readers to judge the actual conduct of the research.

Digital image files, figures, and tables should adhere to the appropriate standards in the field. Images should not be inappropriately altered from the original or present findings in a misleading way.

Editors might also consider screening for plagiarism, duplicate or redundant publication by using anti-plagiarism software, or for image manipulation. If plagiarism or fraudulent image manipulation is detected, this should be pursued with the authors and relevant institutions (see paragraph on how to handle misconduct: 5.2)

5. Responding to criticisms and concerns

Reaction and response to published research by other researchers is an important part of scholarly debate in most fields and should generally be encouraged. In some fields, journals can facilitate this debate by publishing readers' responses. Criticisms may be part of a general scholarly debate but can also highlight transgressions of research or publication integrity.

5.1 Ensuring integrity of the published record - corrections

When genuine errors in published work are pointed out by readers, authors, or editors, which do not render the work invalid, a correction (or erratum) should be published as soon as possible. The online version of the paper may be corrected with a date of correction and a link to the printed erratum. If the error renders the work or substantial parts of it invalid, the paper should be retracted with an explanation as to the reason for retraction (i.e., honest error).

5.2 Ensuring the integrity of the published record – suspected research or publication misconduct

If serious concerns are raised by readers, reviewers, or others, about the conduct, validity, or reporting of academic work, editors should initially contact the authors (ideally all authors) and allow them to respond to the concerns. If that response is unsatisfactory, editors should take this to the institutional level (see below). In rare cases, mostly in the biomedical field, when concerns are very serious and the published work is likely to influence clinical practice or public health, editors should consider informing readers about these concerns, for example by issuing an 'expression of concern', while the investigation is ongoing. Once an investigation is concluded, the appropriate action needs to be taken by editors with an accompanying comment that explains the findings of the investigation. Editors should also respond to findings from national research integrity organisations that indicate misconduct relating to a paper published in their journal. Editors can themselves decide to retract a paper if they are convinced that serious misconduct has happened even if an investigation by an institution or national body does not recommend it.

Editors should respond to all allegations or suspicions of research or publication misconduct raised by readers, reviewers, or other editors. Editors are often the first recipients of information about such concerns and should act, even in the case of a paper that has not been accepted or has already been rejected. Beyond the specific responsibility for their journal's publications, editors have a collective responsibility for the research record and should act whenever they become aware of potential misconduct if at all possible. Cases of possible plagiarism or duplicate/redundant publication can be assessed by editors themselves. However, in most other cases, editors should request an investigation by the institution or other appropriate bodies (after seeking an explanation from the authors first and if that explanation is unsatisfactory).

Retracted papers should be retained online, and they should be prominently marked as a retraction in all online versions, including the PDF, for the benefit of future readers.

For further guidance on specific allegations and suggested actions, such as retractions, see the COPE flowcharts and retraction guidelines (<http://publicationethics.org/flowcharts>; [http://publicationethics.org/files/u661/Retractions COPE gline final 3 Sept 09 2 .pdf](http://publicationethics.org/files/u661/Retractions%20COPE%20gline%20final%203%20Sept%2009%202.pdf)).

5.3 Encourage scholarly debate

All journals should consider the best mechanism by which readers can discuss papers, voice criticisms, and add to the debate (in many fields this is done via a print or on-line correspondence section). Authors may contribute to the debate by being allowed to respond to comments and criticisms where relevant. Such scholarly debate about published work should happen in a timely manner. Editors should clearly distinguish between criticisms of the limitations of a study and criticisms that raise the possibility of research misconduct. Any criticisms that raise the possibility of misconduct should not just be published but should be further investigated even if they are received a long time after publication. Editorial policies relevant only to journals that publish research in humans or animals.

6. Critically assess and require a high standard of ethical conduct of research

Especially in biomedical research but also in social sciences and humanities, ethical conduct of research is paramount in the protection of humans and animals. Ethical oversight, appropriate consent procedures, and adherence to relevant laws are required from authors. Editors need to be vigilant to concerns in this area.

6.1 Ethics approval and ethical conduct

Editors should generally require approval of a study by an ethics committee (or institutional review board) and the assurance that it was conducted according to the Declaration of Helsinki for medical research in humans but, in addition, should be alert to areas of concern in the ethical conduct of research. This may mean that a paper is sent to peer reviewers with particular expertise in this area, to the journal's ethics committee if there is one, or that editors require further reassurances or evidence from authors or their institutions.

Papers may be rejected on ethical grounds even if the research had ethics committee approval.

6.2 Consent (to take part in research)

If research is done in humans, editors should ensure that a statement on the consent procedure is included in the paper. In most cases, written informed consent is the required norm. If there is any concern about the consent procedure, if the research is done in vulnerable groups, or if there are doubts about the ethical conduct, editors should ask to see the consent form and enquire further from authors, exactly how consent was obtained.

6.3 Consent (for publication)

For all case reports, small case series, and images of people, editors should require the authors to have obtained explicit consent for publication (which is different from consent to take part in research). This consent should inform participants which journal the work will be published in, make it clear that, although all efforts will be made to remove unnecessary identifiers, complete anonymity is not possible, and ideally state that the person described has seen and agreed with the submitted paper.

The signed consent form should be kept with the patient file rather than sent to the journal (to maximize data protection and confidentiality, see paragraph 6.4). There may be exceptions where it is not possible to obtain consent, for example when the person has died. In such cases, a careful consideration about possible harm is needed and out of courtesy attempts should be made to obtain assent from relatives. In very rare cases, an important public health message may justify publication without consent if it is not possible despite all efforts to obtain consent and the benefit of publication outweighs the possible harm.

6.4 Data protection and confidentiality

Editors should critically assess any potential breaches of data protection and patient confidentiality. This includes requiring properly informed consent for the actual research presented consent for publication where applicable (see paragraph 6.3) and having editorial policies that comply with guidelines on patient confidentiality.

6.5 Adherence to relevant laws and best practice guidelines for ethical conduct

Editors should require authors to adhere to relevant national and international laws and best practice guidelines where applicable, for example when undertaking animal research. Editors should encourage registration of clinical trials.

Editorial Processes

7. Ensuring a fair and appropriate peer review process

One of the most important responsibilities of editors is organizing and using peer review fairly and wisely. Editors should explain their peer review processes in the information for authors and also indicate which parts of the journal are peer reviewed.

7.1 Decision whether to review

Editors may reject a paper without peer review when it is deemed unsuitable for the journal's readers or is of poor quality. This decision should be made in a fair and unbiased way. The criteria used to make this decision should be made explicit. The decision not to send a paper for peer review should only be based on the academic content of the paper and should not be influenced by the nature of the authors or the host institution.

7.2 Interaction with peer reviewers

Editors should use appropriate peer reviewers for papers that are considered for publication by selecting people with sufficient expertise and avoiding those with conflicts of interest. Editors should ensure that reviews are received in a timely manner.

Peer reviewers should be told what is expected of them and should be informed about any changes in editorial policies. In particular, peer reviewers should be asked to assess research and publication ethics issues (i.e., whether they think the research was done and reported ethically, or if they have any suspicions of plagiarism, fabrication, falsification, or redundant publication). Editors should have a policy to request a formal conflict of interest declaration from peer reviewers and should ask peer reviewers to inform them about any such conflict of interest at the earliest

opportunity so that they can make a decision on whether an unbiased review is possible. Certain conflicts of interest may disqualify a peer reviewer. Editors should stress confidentiality of the material to peer reviewers and should require peer reviewers to inform them when they ask a colleague for help with a review or if they mentor a more junior colleague in conducting peer review. Editors should ideally have a mechanism to monitor the quality and timeliness of peer review and to provide feedback to reviewers.

7.3 Reviewer misconduct

Editors must take reviewer misconduct seriously and pursue any allegation of breach of confidentiality, non-declaration of conflicts of interest (financial or non-financial), inappropriate use of confidential material, or delay of peer review for competitive advantage. Allegations of serious reviewer misconduct, such as plagiarism, should be taken to the institutional level (for further guidance see: http://publicationethics.org/files/u2/07_Reviewer_misconduct.pdf).

7.4 Interaction with authors

Editors should make it clear to authors what the role of the peer reviewer is because this may vary from journal to journal. Some editors regard peer reviewers as advisors and may not necessarily follow (or even ask for) reviewers' recommendations on acceptance or rejection. Correspondence from editors is usually with the corresponding author, who should guarantee to involve co-authors at all stages. Communicating with all authors at first submission and at final acceptance stage can be helpful to ensure all authors are aware of the submission and have approved the publication. Normally, editors should pass on all peer reviewers' comments in their entirety. However, in exceptional cases, it may be necessary to exclude parts of a review, if it, for example, contains libelous or offensive remarks. It is important, however, that such editorial discretion is not inappropriately used to suppress inconvenient comments.

There should always be good reasons, which are clearly communicated to authors, if additional reviewers are sought at a late stage in the process.

The final editorial decision and reasons for this should be clearly communicated to authors and reviewers. If a paper is rejected, editors should ideally have an appeals process. Editors, however, are not obliged to overturn their decision.

8. Editorial decision-making

Editors are in a powerful position by making decisions on publications, which makes it very important that this process is as fair and unbiased as possible, and is in accordance with the academic vision of the particular journal.

8.1 Editorial and journal processes

All editorial processes should be made clear in the information for authors. In particular, it should be stated what is expected of authors, which types of papers are published, and how papers are handled by the journal. All editors should be fully familiar with the journal policies, vision, and scope. The final responsibility for all decisions rests with the editor-in-chief.

8.2 Editorial conflicts of interest

Editors should not be involved in decisions about papers in which they have a conflict of interest, for example if they work or have worked in the same institution and collaborated with the authors, if they own stock in a particular company, or if they have a personal relationship with the authors. Journals should have a defined process for handling such papers. Journals should also have a process in place to handle papers submitted by editors or editorial board members to ensure unbiased and independent handling of such papers. This process should be stated in the information for authors. Editorial conflicts of interests should be declared, ideally publicly.

TABLE OF CONTENTS

RESEARCH ARTICLES	PAGES
İrem BAĞLAN Analysis of Inverse Coefficient Problem for Euler-Bernoulli Equation with Periodic and Integral Conditions	1 - 8
Bahadır AYTAÇ, Albert GÜVENİŞ Improving the Quantification Accuracy of Tc-99m Mibi Dual-Phase Parathyroid Spect/Ct: A Monte Carlo Simulation Study	9 - 23
Sinan ASLAN Some New Integral Inequalities via Caputo-Fabrizio Fractional Integral Operator	24 - 30
Timur CANEL, Satılmış ÜRGÜN Using CO ₂ Laser, Optimization of Laser Power, Exposure Time and Frequency for Cavity Formation on Hardox Steel Plate	31 - 40
Evrin GÜVEN Homoderivations and Their Impact on Lie Ideals in Prime Rings	41 - 48
Çağla PİLAVCI, Satılmış ÜRGÜN, Yasemin TABAK, Timur CANEL Determination of the CO ₂ Laser Parameters on Dimple Geometry on Al ₂ O ₃ Ceramic Surface	49 - 60
Didem KARALARLIOĞLU CAMCI, Didem YEŞİL, Rasie MEKERA, Çetin CAMCI A Generalization of The Prime Radicals of Rings	61 - 69

IDUNAS	NATURAL & APPLIED SCIENCES JOURNAL	2023 Vol. 6 No. 2 (1-8)
--------	---------------------------------------	----------------------------------

Analysis of Inverse Coefficient Problem for Euler-Bernoulli Equation with Periodic and Integral Conditions

Research Article

İrem Bağlan^{1*} 

¹Department of Mathematics, Kocaeli University, Kocaeli, Türkiye

Author E-mail:

isakinc@kocaeli.edu.tr

ORCID ID: 0000-0002-1877-9791

*Correspondence to: İrem Bağlan, Department of Mathematics, Kocaeli University, Kocaeli, Türkiye

DOI: 10.38061/idunas.1368788

Received: 29.09.2023; Accepted: 09.11.2023

Abstract

The research investigates the solution of the inverse problem of a linear Euler-Bernoulli equation. While finding the solution, Volterra integral equation theory was used. For this purpose, the existence of this problem, its uniqueness, and its constant dependence on the data are demonstrated using the Fourier methods.

Keywords: Fourier method, Periodic conditions, Volterra theorem, Euler-Bernoulli inverse problem.

1. INTRODUCTION

The Euler-Bernoulli problem is common. This problem has been used for many physics and engineering problems. The investigation of various problems concerning 4th order homogeneous, linear, and quasi-linear equations has been one of the most attractive areas for mathematicians and engineers due to their importance in the solution of several engineering problems. Examples of scientists working on this subject can be given [1-4].

The Euler-Bernoulli problem was first developed by Daniel Bernoulli and Leonard Euler. $T(t,x)$ is the displacement at time t and at position x , $\alpha(x)$ is the bending stiffness, and $k(x)>0$ is the linear mass. The transverse motion of an unloaded thin beam is represented by the following fourth-order partial differential equation (PDE):

$$k(x)(\partial^2 T)/(\partial t^2) + \alpha(x)(\partial^4 T)/(\partial x^4) = 0, t > 0, 0 < x < L.$$

The vibration, buckling, and dynamic behavior of various building elements widely used in nanotechnology (nanotube, nanofillers for nanomotors, nanobearings, and nanosprings) and population dynamics, thermoelasticity, medical science, electrochemistry, engineering, wide scope, chemical engineering are represented by the Euler-Bernoulli equations [5-6].

In this problem, the periodic [7] and integral conditions were used [8]. The periodic boundary conditions are highly challenging. The periodic boundary conditions arise from many important applications in heat transfer, and life sciences [8].

The paper is organized as follows. In Section 2, the existence, and the uniqueness of the solution of the problem are proved by using the Fourier method and iteration method. In Section 3, the stability of the method for the solution is shown.

2. MATERIAL AND METHODS

The Fourier Method is a successive approximation method to solve the problem. The Fourier method is one of the very common but highly difficult methods to apply. It is used in all partial type differential equations. Volterra theorem is very difficult to satisfy theory. However, they are very successful methods in analytical solutions. Many scientists have used these methods [3-4].

3. STATEMENT OF SOLUTIONS

The inverse coefficient problem

$$\frac{\partial^2 T}{\partial t^2} + \frac{\partial^4 T}{\partial \chi^4} = j(t)f(\chi, t), \tag{1}$$

the initial condition

$$\begin{aligned} T(\chi, 0) &= \varphi(\chi), \chi \in [0, \pi] \\ T_t(\chi, 0) &= \psi(\chi), \chi \in [0, \pi] \end{aligned} \tag{2}$$

the periodic boundary conditions

$$\begin{aligned} T(0, t) &= T(\pi, t), t \in [0, T] \\ T_\chi(0, t) &= T_\chi(\pi, t), t \in [0, T] \\ T_{\chi\chi}(0, t) &= T_{\chi\chi}(\pi, t), t \in [0, T] \\ T_{\chi\chi\chi}(0, t) &= T_{\chi\chi\chi}(\pi, t), t \in [0, T] \end{aligned} \tag{3}$$

the integral overdetermination data

$$\delta(t) = \int_0^\pi \chi T(\chi, t) d\chi, t \in [0, T]. \tag{4}$$

By applying the Fourier Method, the ensuing model is as follows

$$\begin{aligned} T(\chi, t) &= \frac{1}{2} \left[\varphi_0 + \psi_0 t + \frac{2}{\pi} \int_0^t \int_0^\pi (t-\tau) j(\tau) f(\chi, \tau) d\chi d\tau \right] \\ &+ \sum_{m=1}^\infty \left[\varphi_{cm} \cos(2m)^2 t + \frac{\psi_{cm}}{\pi(2m)^2} \sin(2m)^2 t \right] \cos 2m\chi \end{aligned}$$

$$\begin{aligned}
 & + \sum_{m=1}^{\infty} \left[\frac{2}{\pi(2m)^2} \int_0^t \int_0^{\pi} j(\tau) f(\chi, \tau) \sin(2m)^2 (t - \tau) \cos 2m\chi d\chi d\tau \right] \cos 2m\chi \\
 & + \sum_{m=1}^{\infty} \left[\varphi_{sm} \cos(2m)^2 t + \frac{\psi_{sm}}{\pi(2m)^2} \sin(2m)^2 t \right] \sin 2m\chi \\
 & + \sum_{m=1}^{\infty} \left[\frac{2}{\pi(2m)^2} \int_0^t \int_0^{\pi} j(\tau) f(\chi, \tau) \sin(2m)^2 (t - \tau) \sin 2m\chi d\chi d\tau \right] \sin 2m\chi .
 \end{aligned} \tag{5}$$

Definition 3.1. $\{T(\chi, t), j(t)\}$ is called the solution of the inverse problem (1)-(4).

Theorem 3.2. Let below the assumptions be provided

- (A1) $\delta(t) \in C^2[0, T]$
- (A2) $\varphi(\chi) \in C^3[0, \pi], \psi(\chi) \in C^1[0, \pi]$
- (A3) $f(\chi, t) \in C([0, \pi] \times [0, t])$
- (A4) $0 \neq \int_0^{\pi} \chi T(\chi, t) d\chi, t \in [0, T]$

then the solution of above the problem (1)-(4) has solutions.

Proof. Let the assumptions is verified:

$$\begin{aligned}
 & \varphi(0) = \varphi(\pi), \varphi'(0) = \varphi'(\pi), \\
 & \psi(0) = \psi(\pi), \psi'(0) = \psi'(\pi), \\
 & f(0, t) = f(\pi, t).
 \end{aligned}$$

Since our series (5) is absolutely convergent, it is also uniformly convergent. Naturally, $T(\chi, t), T_{\chi}(\chi, t), T_{\chi\chi}(\chi, t), T_t(\chi, t), T_{tt}(\chi, t)$ are continuous and absolutely convergent.

According to (5) and (A1) to get:

$$\delta''(t) = \int_0^{\pi} \chi T_{tt}(\chi, t) d\chi, t \in [0, T]. \tag{6}$$

From (5) and (6)

$$\begin{aligned}
 j(t) = & \frac{\delta''(t) - \pi \sum_{m=1}^{\infty} (2m) \left[\varphi_{cm} \cos(2m)^2 t + \frac{\psi_{cm}}{\pi(2m)^2} \sin(2m)^2 t \right]}{\int_0^{\pi} \chi f(\chi, t) d\chi} \\
 & - \frac{\pi \sum_{m=1}^{\infty} (2m) \int_0^t f_{sm}(\tau) j(\tau) \sin(2m)^2 (t - \tau) d\tau}{\int_0^{\pi} \chi f(\chi, t) d\chi}
 \end{aligned}$$

The equation given below is the second type of Volterra integral equation:

$$F(t) = \frac{\delta''(t) - \pi \sum_{m=1}^{\infty} (2m)^3 \varphi_{cm} \cos(2m)^2 t + \frac{\psi_{cm}}{\pi} 2m \sin(2m)^2 t}{\int_0^{\pi} \chi f(\chi, t) d\chi}, \tag{7}$$

$$K(t, \tau) = \frac{-\pi \sum_{m=1}^{\infty} (2m) \int_0^t f_{sm}(\tau) j(\tau) \sin(2m)^2 (t - \tau) d\tau}{\int_0^{\pi} \chi f(\chi, t) d\chi}$$

$$j(t) = F(t) + \int_0^t K(t, \tau) j(\tau) d\tau, t \in [0, T] \tag{8}$$

Let show F(t) and the kernel K(t,τ) are continuous in [0,T] and [0,T]x[0,T] respectively,

$$F(t) = \frac{\delta''(t) - \pi \sum_{m=1}^{\infty} (2m)^3 \left(\int_0^{\pi} \varphi(\chi) \sin 2m\chi d\chi \right) \cos(2m)^2 t}{\int_0^{\pi} \chi f(\chi, t) d\chi} + \frac{-\pi \sum_{m=1}^{\infty} \left(\int_0^{\pi} \psi(\chi) \sin 2m\chi d\chi \right) \frac{2m}{\pi} \sin(2m)^2 t}{\int_0^{\pi} \chi f(\chi, t) d\chi},$$

$$F(t) = \frac{\delta''(t) - \pi \sum_{m=1}^{\infty} (2m)^3 \varphi_{cm}'' \cos(2m)^2 t}{\int_0^{\pi} \chi f(\chi, t) d\chi} + \frac{-\pi \sum_{m=1}^{\infty} \psi_{cm}' \frac{2m}{\pi} \sin(2m)^2 t}{\int_0^{\pi} \chi f(\chi, t) d\chi},$$

Taking maximum,

$$\|F(t)\| \leq \frac{2 \left(\|\delta''(t)\| + \pi \sum_{m=1}^{\infty} (\|\varphi''_{cm}\| + \|\psi'_{cm}\|) \right)}{M \pi^2}$$

$$K(t, \tau) = \frac{-2 \sum_{m=1}^{\infty} (2m) \int_0^t \int_0^{\pi} f(\chi, \tau) j(\tau) \sin(2m)^2 (t - \tau) d\chi d\tau}{\int_0^{\pi} \chi f(\chi, t) d\chi}.$$

Taking maximum,

$$\|K(t, \tau)\| \leq \frac{2 \left(\sum_{m=1}^{\infty} (\|f_{cm}\| \|T\|) \right)}{M \pi}.$$

According to (A1)-(A2) and the Weierstrass M test, the kernels F(t) and K(t,τ) are continuous at [0,T] and [0,T]x[0T]. According to Volterra's Theorem, the inverse (1)-(4) problem has only unique solution on [0,T].

4. STABILITY FOR THE PROBLEM

Theorem 4.1. If the data (A1)-(A4) is provided, the solution is constantly dependent on the initial data.

Proof. Let us denote

$$\Delta = \{\varphi, \psi, \kappa, f\},$$

$$\bar{\Delta} = \{\bar{\varphi}, \bar{\psi}, \bar{\kappa}, \bar{f}\},$$

$$\|\Delta\| = (\|\kappa\| + \|\varphi\| + \|\psi\| + \|f\|).$$

$$F(t) - \bar{F}(t) = \frac{\left(\delta''(t) - \bar{\delta}''(t) + \pi \sum_{m=1}^{\infty} (\varphi''_{cm} - \bar{\varphi}''_{cm}) \cos(2m)^2 t \right)}{\int_0^{\pi} \chi f(\chi, t) d\chi} + \frac{\pi \sum_{m=1}^{\infty} (\psi'_{cm} - \bar{\psi}'_{cm}) \cos(2m)^2 t}{\int_0^{\pi} \chi f(\chi, t) d\chi}$$

Taking maximum

$$\|F(t) - \bar{F}(t)\| \leq \frac{2 \left(\|\delta''(t) - \bar{\delta}''(t)\| + \pi \sum_{m=1}^{\infty} (\|\varphi''_{cm} - \bar{\varphi}''_{cm}\| + \|\psi'_{cm} - \bar{\psi}'_{cm}\|) \right)}{M \pi^2} \tag{9}$$

$$K(t, \tau) - \overline{K(t, \tau)} = \frac{\pi \sum_{m=1}^{\infty} \int_0^t (f_{cm})_{\chi} \sin(2m)^2(t - \tau) d\tau}{\int_0^{\pi} \chi f(\chi, t) d\chi}$$

$$\frac{\pi \sum_{m=1}^{\infty} \int_0^t \overline{(f_{cm})_{\chi}} \sin(2m)^2(t - \tau) d\tau}{\int_0^{\pi} \overline{\chi f(\chi, t)} d\chi}$$

Taking maximum

$$\|K(t, \tau) - \overline{K(t, \tau)}\| \leq \frac{2 \left(\|f - \overline{f}\| \|T\| + \|T\| \sum_{m=1}^{\infty} \left(\|(f_{cm})_{\chi} - \overline{(f_{cm})_{\chi}}\| \right) \right)}{M\pi} \tag{10}$$

Using same estimations, we get

$$\|j - \overline{j}\| \leq \|F - \overline{F}\| + \|T\| \|K\| \|j - \overline{j}\| + \|j\| \|K - \overline{K}\|,$$

From (9)-(10)

$$\|j - \overline{j}\| \leq \frac{2}{\pi^2 M (1 - \|T\| \|K\|)} \left\{ \|\delta' - \overline{\delta'}\| + \pi \sum_{m=1}^{\infty} \left(\|\varphi_{cm}'' - \overline{\varphi_{cm}''}\| + \|\psi_{cm}' - \overline{\psi_{cm}'}\| \right) \right\}$$

$$+ \frac{2 \|T\| \|j\|}{\pi^2 M (1 - \|T\| \|K\|)} \|f - \overline{f}\| + \frac{2 \|T\|^2 \|j\|}{\pi^2 M (1 - \|T\| \|K\|)} \sum_{m=1}^{\infty} \left(\|(f_{cm})_{\chi} - \overline{(f_{cm})_{\chi}}\| \right)$$

The difference from the (5)

$$T - \overline{T} = \frac{1}{2} \left[(\varphi_0 - \overline{\varphi_0}) + (\psi_0 - \overline{\psi_0}) t + \frac{2}{\pi} \int_0^t (t - \tau) j(\tau) (f_0 - \overline{f_0}) d\tau \right]$$

$$+ \sum_{m=1}^{\infty} \left[(\varphi_{cm} - \overline{\varphi_{cm}}) \cos(2m)^2 t + \frac{(\psi_{cm} - \overline{\psi_{cm}})}{\pi(2m)^2} \sin(2m)^2 t \right] \cos 2m\chi$$

$$+ \sum_{m=1}^{\infty} \left[\frac{2}{\pi(2m)^2} \int_0^t j(\tau) (f_{cm} - \overline{f_{cm}}) \sin(2m)^2(t - \tau) d\tau \right] \cos 2m\chi$$

$$+ \sum_{m=1}^{\infty} \left[(\varphi_{sm} - \overline{\varphi_{sm}}) \cos(2m)^2 t + \frac{(\psi_{sm} - \overline{\psi_{sm}})}{\pi(2m)^2} \sin(2m)^2 t \right] \sin 2m\chi$$

$$+ \sum_{m=1}^{\infty} \left[\frac{2}{\pi(2m)^2} \int_0^t j(\tau) (f_{sm} - \overline{f_{sm}}) \sin(2m)^2(t - \tau) d\tau \right] \sin 2m\chi$$

Taking maximum

$$\begin{aligned} \|T - \bar{T}\| &\leq \frac{1}{2} \|\varphi_0 - \bar{\varphi}_0\| + \frac{1}{2} \|\psi_0 - \bar{\psi}_0\| \|T\| \\ &+ \sum_{m=1}^{\infty} \frac{1}{(2m)^2} (\|\varphi_{cm} - \bar{\varphi}_{cm}\| + \|\psi_{cm} - \bar{\psi}_{cm}\|) \\ &+ \sum_{m=1}^{\infty} \frac{1}{(2m)^2} (\|f_{cm} - \bar{f}_{cm}\| \|T\| \|j\| + \|f_{sm} - \bar{f}_{sm}\| \|T\| \|j\|) \\ &+ \sum_{m=1}^{\infty} \frac{1}{(2m)^2} (\|\varphi_{sm} - \bar{\varphi}_{sm}\| + \|\psi_{sm} - \bar{\psi}_{sm}\|) \\ &+ \sum_{m=1}^{\infty} \frac{1}{(2m)^2} (\|\bar{f}_{cm}\| \|T\| \|j - \bar{j}\| + \|\bar{f}_{sm}\| \|T\| \|j - \bar{j}\|) \end{aligned}$$

Applying Hölder inequality,

$$\begin{aligned} \|T - \bar{T}\| &\leq \frac{1}{2} \|\varphi_0 - \bar{\varphi}_0\| + \frac{1}{2} \|\psi_0 - \bar{\psi}_0\| \|T\| \\ &+ \frac{\pi^2}{24} \sum_{m=1}^{\infty} (\|\varphi_{cm} - \bar{\varphi}_{cm}\| + \|\psi_{cm} - \bar{\psi}_{cm}\|) \\ &+ \frac{\pi^2}{24} \sum_{m=1}^{\infty} (\|f_{cm} - \bar{f}_{cm}\| \|T\| \|j\| + \|f_{sm} - \bar{f}_{sm}\| \|T\| \|j\|) \\ &+ \frac{\pi^2}{24} \sum_{m=1}^{\infty} (\|\varphi_{sm} - \bar{\varphi}_{sm}\| + \|\psi_{sm} - \bar{\psi}_{sm}\|) \\ &+ \frac{\pi^2}{24} \sum_{m=1}^{\infty} (\|\bar{f}_{cm}\| \|T\| \|j - \bar{j}\| + \|\bar{f}_{sm}\| \|T\| \|j - \bar{j}\|) \\ \|T - \bar{T}\| &\leq M_1 \|\varphi - \bar{\varphi}\| + M_2 \|\psi - \bar{\psi}\| \\ &+ M_3 \|f - \bar{f}\| + M_4 \|\kappa - \bar{\kappa}\| \\ \|T - \bar{T}\| &\leq M_5 \|\Delta - \bar{\Delta}\| \end{aligned}$$

for $\Delta \rightarrow \bar{\Delta}$ then $T \rightarrow \bar{T}$.

5. CONCLUSION

The solution of the inverse coefficient for the linear Euler equation which involves periodic and integral boundary conditions was examined. Although the problem is ill-posed, the results obtained are quite suitable. This article specifically examines periodic boundary conditions, which are more challenging than local boundary conditions in inverse coefficient problems. In this study, results were obtained using the Fourier method. As a result, the applied methods revealed the analytical solution to this problem.

6. ACKNOWLEDGMENTS

We would like to thank the reviewers.

REFERENCES

1. Sharma, P.R., Methi, G. (2012). Solution of two-dimensional parabolic equation subject to non-local conditions using homotopy Perturbation method, *Jour. of App.Com.*, 1, 12-16.
2. Cannon, J. Lin, Y. (1899). Determination of parameter $p(t)$ in Hölder classes for some semilinear parabolic equations, *Inverse Problems*, 4, 595-606.
3. Dehghan, M. (2005). Efficient techniques for the parabolic equation subject to nonlocal specifications, *Applied Numerical Mathematics*, 52(1), 39-62.
4. Dehghan, M. (2001). Implicit Solution of a Two-Dimensional Parabolic Inverse Problem with Temperature Overspecification, *Journal of Computational Analysis and Applications*, 3(4).
5. He X.Q., Kitipornchai S., Liew K.M., (2005). Buckling analysis of multi-walled carbon nanotubes a continuum model accounting for van der Waals interaction, *Journal of the Mechanics and Physics of Solids*, 53, 303-326.
6. Natsuki T., Ni Q.Q., Endo M., (2007). Wave propagation in single-and double-walled carbon nano tubes filled with fluids, *Journal of Applied Physics*, 101, 034319.
7. Ionkin, N.I. (1977). Solution of a boundary value problem in heat conduction with a nonclassical boundary condition, *Differential Equations*, 13, 204-211.
8. Hill G.W. (1886). On the part of the motion of the lunar perigee which is a function of the mean motions of the sun and moon, *Acta Mathematica*, 8, 1-36.

IDUNAS	NATURAL & APPLIED SCIENCES JOURNAL	2023 Vol. 6 No. 2 (9-23)
--------	---------------------------------------	-----------------------------------

Improving the Quantification Accuracy of Tc-99m Mibi Dual-Phase Parathyroid Spect/Ct: A Monte Carlo Simulation Study

Research Article

Bahadır Aytaç^{1*} , Albert Güveniş¹ 

¹Boğaziçi University, Institute of Biomedical Engineering

Author E-mails

bahadir57aytac@gmail.com

B. Aytaç ORCID ID: 0009-0000-6795-8975

A. Güveniş ORCID ID: 0000-0003-0490-5184

*Correspondence to: Bahadır Aytaç, Boğaziçi University, Institute of Biomedical Engineering, İstanbul, Türkiye
DOI: 10.38061/idunas.1325839

Received: 17.07.2023; Accepted: 24.11.2023

Abstract

Quantitative parathyroid SPECT imaging is a technique used in assessing primary hyperparathyroidism that may have potential in the identification and differentiation of parathyroid lesions as well as the estimation of disease severity. Studying the effect of data acquisition parameters on the quantification error is important for maximizing the accuracy of this diagnostic technique. In this study, the effects of different data acquisition parameters, namely the type of collimator, scatter correction status, and reconstruction iteration number on the quantification accuracy were examined using computer simulation. The SIMIND Monte Carlo Simulation and CASToR iterative reconstruction program was used to simulate a commercially available SPECT camera (Siemens Symbia Intevo Gamma Camera) with a crystal size of 29.55cm and 128x128 matrix size. A digital cylindrical phantom filled with water was constructed. A 0.36 cm radius spherical adenoma filled with a uniform 1MBq radioactivity is placed within the phantom. Low-Energy High Resolution (LEHR) and Low Energy Ultra High Resolution (LEUHR) collimator models are tested along with the presence of Scatter correction and differing iteration numbers (x16, x32). An image FOV-based calibration method was used to gather quantitative information and check against the input radioactivity. The inclusion of scatter correction resulted in a 15-20% relative improvement in quantification accuracy while the optimal number of iterations yielded a 10% improvement. Overall, accuracies as high as 7% were observed. The optimization of parameters can provide a significant improvement in quantification accuracy.

Keywords: SPECT, Monte Carlo Simulation, Quantification, Hyperparathyroidism.

1. INTRODUCTION

Primary hyperparathyroidism (PHPT) is among the most common endocrine disorders in the world. The disorder can cause the overproduction of parathyroid hormones (PTH) and an increase of plasma

calcium levels in the blood [13]. It presents itself in the form of irregularities and over-release of PTH. Symptomatic representation of PHPT is commonly seen around the renal system and skeletal structures, with patients suffering from fragility in bones, renal nephrocalcinosis, and renal insufficiency. However, with the improvements in modern medicine and the ability to screen serum calcium levels, it is possible for physicians to gradually shift the PHPT presentation form from symptomatic to asymptomatic presentations [9]. Around 80% to 85% of hyperparathyroidism is caused by parathyroid adenomas, with primary parathyroid hyperplasia (15%) and parathyroid carcinoma (5%) less commonly linked with the disorder [13, 54]. Most patients exhibit adenomas on a single gland while about 20% percent of patients have multiple adenomas on their glands [40].

In normal circumstances, parathyroids are too small to detect, but PHPT causes the glands to increase in size, resulting in an enlarged state that allows imaging [54]. Patients with enlarged glands are generally advised to undergo surgery for the removal of the adenoma. For those patients who are not seen as fit for surgical operation, according to relevant guidelines [9], physicians can follow more conservative approaches such as newer, less invasive surgical interventions [40].

Parathyroid glands are rather small (generally 5x3x1 mm [54] and situated right behind the thyroid glands [22]. This makes imaging difficult. Sonography and Tc99m-Sestamibi scintigraphy are the imaging modalities used for imaging parathyroid glands [54]. Tc99m-Sestamibi is a known substance used in parathyroid imaging and is absorbed by both the adenomas and the thyroid glands. The substance then washes off the thyroid glands and provides a good vision of the adenomas in parathyroids [24].

Quantification of a medical image means gathering not only visual but also numeric information on biological structures such as the concentration of radioactive material within a certain biological structure in units of kilo becquerels per cubic centimeter This allows the user to further understand the properties of pathologies. Research has highlighted the benefits of quantification. [50] uses quantification to observe the effect of delay in Tc99m SPECT/CT imaging of secondary hyperparathyroidism patients. Another study on thyroid imaging Lee et al. ([31]) found that quantitative SPECT/CT measurements were more accurate than the thyroid uptake system (TUS). Some articles in the literature describe quantitative imaging as one of the most promising practices in nuclear medicine [1, 26, 28, 30].

In the case of an adenoma, quantification allows for the observation of not only the radioactivity level, but also properties such as size, shape, position, and volume in a much more precise way. Furthermore, it is possible to assess disease severity [23, 47].

The detection and quantitative analysis of parathyroid adenomas is a studied field that encompasses many approaches. Namely, Listewnik et al. ([32]) used particle swarm optimization with random neighbor topology to achieve 3% voxel size with heavily reduced processing times. Havel et al. ([19]), Khouli et al. ([27]), Robin et al. ([46]), and Wang et al. ([51, 52]) have used quantitative methods to gather information on optimal timing, standard uptake by time, and washout of radionuclides during imaging. Ma et al. ([36]) have employed a semi-quantitative method to analyze the degree of hyperplasia of the parathyroid gland pre-operation. Harris et al. ([17]) were able to localize adenomas with an accuracy within 19mm, demonstrating the viability of quantitative techniques for non-invasive analysis. Razavi et al. ([44]) has used quantitative analysis of parathyroid imaging to test the co-registration combinations of the early and delayed SPECT/CT scans to achieve the most viable pair along with operator variability. Khouli et al. ([29]) has successfully used quantitative analysis in the localization of adenomas.

The consensus is that the accurate acquisition of quantitative data is a critical step in dosimetry and treatment planning in nuclear medicine. However, inaccurate calculation of quantitative measures can cause mistreatment and potential adverse side effects [10]. With the addition of iterative imaging methods that allow for corrections during reconstruction, quantitative imaging has become increasingly prevalent in SPECT imaging.

Single photon emission computed tomography (SPECT) visualizes the radioactivity distribution across the human body on a field of view (FOV). Traditionally, SPECT is seen as a qualitative imaging technique that has low special resolution and high noise in regions of interest [45, 41]. Since the recent development of

iterative reconstruction algorithms, SPECT has joined others as a quantitative imaging modality providing an accurate quantitative representation of radioactivity in the body. Corrections should be performed for maximum accuracy against naturally occurring physical phenomena, such as scattering and attenuation. These phenomena cause inaccuracies in radioactivity readings. Studies show that iterative reconstruction methods paired with correction methods can give much higher quantitative accuracy than their non-iterative counterparts (e.g., filtered back projection) [3, 4, 45]. When performing a SPECT scan, there are many factors to consider: detector properties, collimator models, and randomly occurring physical events such as scattering and attenuation [2]. Furthermore, when simulating a system such as SPECT, the ability to simulate randomly occurring events becomes paramount. Monte Carlo simulation is one algorithm that allows the user to simulate these events and its use in Nuclear Medicine is well documented [11, 55]. Monte Carlo uses random sampling and different numbers of probability density functions (pdf) to model, simulate, and predict complex systems [18].

As quantification becomes important for parathyroid SPECT/CT studies, there is a clinical need to identify the best acquisition and processing parameters that will yield the optimum accuracy. This study aims to address this need for the first time by using a Monte Carlo simulation platform for the Tc-99m sesta-MIBI dual-phase parathyroid SPECT/CT imaging protocol. Monte Carlo simulation allows the determination of optimal parameters while eliminating experimental errors and the expense and inconvenience of using physical systems.

2. METHODS

The following steps have been followed in our study:

- A. Use the previously validated cylindrical digital phantom ([53]) along with the Simind platform to enable multiple parameter testing. An illustration of images obtained using SIMIND is shown in Figure 1.
- B. Define processing acquisition parameters based on previous similar studies.
- C. Analyze the results quantitatively, then find the optimal parameters.
- D. Compare results with previously obtained research findings.

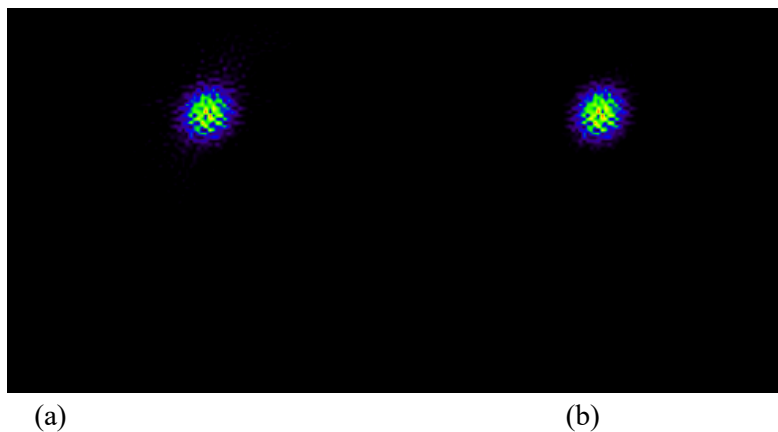


Figure 1. Examples of Siemens Symbia Gamma camera image outputs in transaxial view using LEUHR(a) and LEHR(b) collimators, with a spherical source.

Imaging Modalities that are Simulated

The dual-phase parathyroid Tc-99m-MIBI SPECT imaging protocol was used per previous parathyroid studies [40, 41]. Specifically, Siemens Symbia Intevo Gamma Camera was chosen for the study. Table 1 and Table 2 give the parameters that were selected based on previous studies.

Table 1. SPECT camera specifications used in simulations per previous studies [41].

Camera Parameters	Value
Photon Energy(keV)	140
Upper Window Threshold(keV)	147
Lower Window Threshold(keV)	133
Energy Resolution(140keV)	9.9%
Intrinsic Resolution (140 keV) (cm)	0.3
Source Activity (MBq)	13629
Image Matrix Size	128x128
Number of SPECT Projections	48
SPECT Rotation (3=180)	3
Pixel Size(cm)	0.24
Crystal Thickness	0.95
Crystal Half Length/Radius(cm)	29.55

Siemens Low-Energy High Resolution (LEHR) and Low-Energy ultra-high-resolution (LEUHR) collimators have been used to see the effect of the collimator model on the quantification process (Table 2) [48].

Table 2. Siemens Collimator specifications including septal properties. Sensitivity is set according to Tc99m [41].

Collimator	Hole length (mm)	Septal Thickness (mm)	Hole Diameter (mm)	Sensitivity (cpm/ μ Ci)	System Resolution (100mm)	Septal Penetration (%)
LEHR	24.05	0.16	1.11	202	7.5	1.5
LEUHR	35.08	0.13	1.16	100	6	0.8

A digital cylindrical phantom (Figure 2) was selected for the study. The phantom was chosen for its cylindrical shape to simulate the neck and upper torso area. The phantom has an 11cm cross-section and 30 cm height, which is in line with previous anthropometric measurements of the neck and torso [49]. This allows for simulation of the neck and upper torso area without using an anthropomorphic phantom. The simulated phantom was filled with water. The pixel size for the phantom was 0.24mm according to previous studies ([40, 41]) while the entire phantom is sized 128x128x128 pixels. The adenoma is simulated as a uniform sphere with an offset ~ 1.5 cm from the center situated on the upper central portion of the cylinder. The sphere was sized around a radius of ~ 0.3 cm. The sphere was filled with approximately 1MBq/cc.

SIMIND (Ljungberg n.d.) was selected as the simulation platform for this study. It is a validated simulation platform that utilizes Monte Carlo Simulation. SIMIND enables users to simulate photon emissions through Monte Carlo simulation with possible reconstruction [15].

Simulated imaging studies allow us to test many parameters during testing without the need to travel to medical facilities or use radioactive material, thus being time and cost-effective. These parameters that are used during SPECT imaging such as Energy window, collimator type, etc., can be changed within SIMIND. This allows a comprehensive study of how the image quality behaves concerning acquisition parameters. It is used by ([2]) to simulate a single photon emission as well as being used in quantitative studies [34, 35, 38].

The software Customizable and Advanced Software for Tomographic Reconstruction (CASToR) ([37]) was used for the reconstruction of the images created by SIMIND simulation, CASToR, an open-source project, is created for the iterative reconstruction of emission (SPECT, PET) data. The OSEM algorithms can use differing number of iterations. In this study, 16 and 32 iterations were used with 8 subsets.

Three parameters were chosen for testing their impact on quantification error in hyperparathyroid imaging (Table 3): Collimator type (Low Energy-Ultra High Resolution, Low Energy-High Resolution), iteration number (16, 32), and presence of scatter correction.

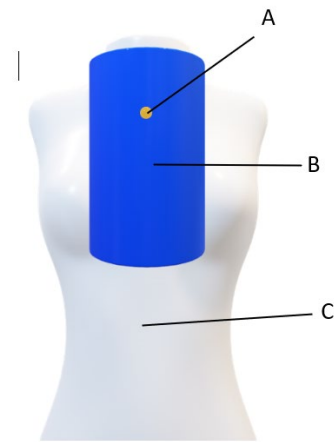


Figure 2. An approximate representation of the way the cylindrical phantom simulates the head and neck area. (A)The radioactive matter (B)The cylindrical phantom (C)A model human torso.

Table 3. The simulation/reconstruction process parameters that are being tested in regard to their effect on quantification accuracy. With parameter Scatter Correction given binary coding. (0-not used,1-used).

Parameters		
Collimator	Iteration	Scatter Corr.
siemens-leuhr	16	0
siemens-leuhr	16	1
siemens-leuhr	32	0
siemens-leuhr	32	1
siemens-lehr	16	0
siemens-lehr	16	1
siemens-lehr	32	0
siemens-lehr	32	1

Attenuation Correction

All SPECT images suffer from attenuation artifacts due to the varying attenuation values of the object between the source and the detector surface. These artifacts affect the quantification of the images and applying methods to correct this effect is a must. To correct this effect, the attenuation coefficients of the object in question need to be known during the reconstruction stage of the image [45]. With the advent of SPECT/CT, which allows the acquisition of both imaging modalities for the patient with presumably shared positional information, gathering attenuation maps has become much more available [43]. During reconstruction, CASToR can perform attenuation correction. This correction has been featured in all images within this study.

Scatter Correction

One of the many factors affecting the SPECT imaging is Compton photon scattering. The Triple-Energy-Window (TEW) method, proposed by Koichi Ogawa, is one of the simplest methods to correct this effect [7, 39]. According to this method, the scattering effect on a certain energy window could be corrected by subtraction of the counts observed in the two neighboring energy windows [7]. This technique allows us to administer scatter correction after the reconstruction, thus giving us a chance to compare it against its non-scatter corrected counterpart. Three energy windows were set-up with the primary photopeak at 140 keV [41].

Table 4. Energy windows utilized in the study. With the central window 133-147 keV and the two neighboring energy windows used in the scatter correction process. The window-width represents the distance between the 140 keV mark and the upper and lower limits of the windows.

Window	Window Limits(keV)	Window Width
1	133-147	%10
2	147-168	%15
3	112-133	%15

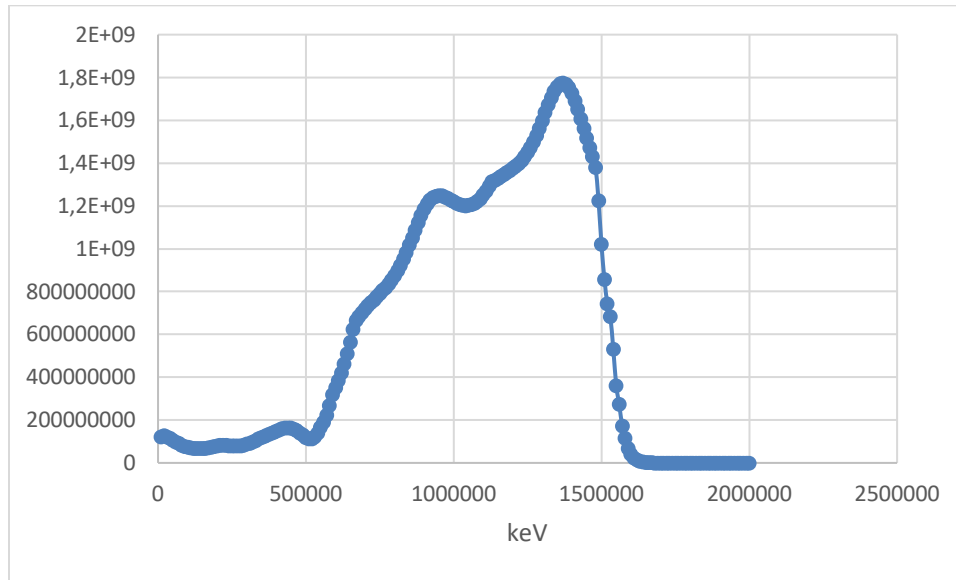


Figure 3. The energy Spectra of the Siemens Symbia Intevo Gamma Camera for LEUHR Collimator, where the triple energy window centered around the 140 keV peak can be observed within the main window and every dot representing an event.

Calibration

In the field of nuclear medicine, there is a significant need for the standardization of dosimetry and characterization of the imaging system. Since there is an abundance of factors that could influence the resulting counts in the output, calibration of the system is crucial for quantitative imaging [10, 14, 16, 53]. In this study, a previously validated image-based calibration protocol was used. This calibration method proposed by ([16]) uses the count numbers in each pixel to create an image-based calibration factor S_{std} . The calibration factor for each image was determined by calibrating the number of counts found in the images to the known input radioactivity. System calibration factor S_{tot} was found by pooling the individual calibration factors gathered from each image.

$$S_{std} = \frac{N_{SPECT}}{A_{mean} \times \Delta T_{acq}} \tag{1}$$

Halty et al. ([16]) suggests using the equation (1) to calculate the individual calibration factor S_{std} . The Halty equation was slightly modified to calibrate the images on a Bq/cc basis. Which might offer a better insight regarding adenomas that are not uniform.

$$S_{std} = \frac{N_{Bq/cc}}{A_{mean} \times \Delta T_{acq}} \tag{2}$$

$$N_{Bq/cc} = \frac{N_{SPECT}}{N_{Voxel} \times 76.62} \tag{3}$$

$N_{Bq/cc}$: The number of counts per cc in the adenoma. The adenoma should be segmented before this measurement is made (as given in the ‘‘Segmentation’’ section).

N_{Voxel} : The number of voxel that adenoma spans. This value along with the $N_{Bq/cc}$ could be found by using quantitative reporting and segmentation algorithms. This value is multiplied by 76.62 to reflect the voxel to cc change in equation (3).

A_{mean} : Mean activity over the acquisition duration ΔT_{acq} .

ΔT_{acq} : The acquisition duration of the image. (33s for this study)

Using equation (2) the individual calibration factors for every image can be found. It was chosen to pool these factors to get a cohesive understanding of the system and gather a singular pooled calibration factor S_{tot} . It was discovered that for better accuracy all image types should be counted in this average, such as images with and without scatter correction, lower and higher iteration, and other image-altering settings.

$$S_{tot} = \frac{\sum_{i=0}^n Sstd_i}{n} \tag{4}$$

Here, n represents the number of images that are being pooled.

One thing to keep in mind with this method is ensuring consistency in iteration numbers when dealing with components such as scatter correction. This means for example if one uses iteration number a with scatter correction, then he/she should also use iteration number a without scatter correction.

Segmentation

For the analysis and segmentation of the radioactive sphere placed within the phantom 3D-Slicer was used [12]. Using various plugins such as quantitative reporting and radiomics, it was possible to observe: the mean radioactivity per voxel, the voxel-wise size of the adenoma, the coordinates of the adenoma center, etc. For segmentation, an auto segmentation algorithm, the OTSU 3D Segmentation algorithm was used[6, 8, 20, 25]. Otsu is a popular non-parametric method in image segmentation and has precedent in the use of medical imaging [6]. The selection to use an auto-segmentation algorithm was made to eliminate the human factor in segmentation, in favor of mathematical algorithms for the most objective segmentation and quantification accuracy.

3. RESULTS

The results (Table 5) show that the change of parameter sets can result in a nearly 20% relative improvement in quantification error, from the highest error rate of 8.7% to the lowest error rate of 7%. The quantification error for the simulated images was found to be around 9% or below which is in line with the desired results of a sub-10% error. When low energy-ultra high-resolution collimator was used with scatter correction and 32 iterations, the error was found to be as low as 7%.

Table 5. Quantification accuracy results of Siemens Symbia Intevo Gamma Camera Using LEUHR and LEHR collimators along with the corresponding process parameter combinations.

Parameters			Quantification Error
Collimator	Iteration	Scatter Corr.	MBq/cc
siemens-leuhr	16	0	7.5%
siemens-leuhr	16	1	7%
siemens-leuhr	32	0	7.3%
siemens-leuhr	32	1	7.1%
siemens-lehr	16	0	8.3%
siemens-lehr	16	1	7.6%
siemens-lehr	32	0	8.5%
siemens-lehr	32	1	8.7%

4. DISCUSSION

This study aims to simulate and observe the effects of differing simulation and processing parameters on the quantification accuracy of hyperactive parathyroid glands using Tc-99m MIBI dual-phase parathyroid SPECT/CT.

According to Hwang et al. (2008), the presence of attenuation and scatter correction can cause a 25 percent difference in the observed radioactivity level in water-filled phantoms which is consistent with our results. A consistent improvement in accuracy was observed when scatter correction was applied to experiments. While the absence of both is stated to cause a nearly 50 percent error rate (Hwang et al. 2008), we consider this as a plausible possibility. Zeintl et al. ([56]) report that using commercial tools a quantification accuracy of 1-4 percent can be achieved. This is consistent also with our observations of around a 7 percent accuracy improvement made with open-source programs such as SIMIND and CASToR.

This study has been conducted with three different simulation and process parameters: the collimator, iterative reconstruction number, and the presence of scatter correction. During the simulation, a uniform adenoma within a digital cylindrical phantom filled with water was used. These experiments with rather simple parameter sets were selected to showcase the quantification capabilities of SPECT imaging and can become a basis for any further studies looking to experiment with other parameters as well as more complicated phantoms and reconstruction algorithms.

An anthropomorphic phantom could be used in this study to better examine real life situations. The current cylindrical phantom provides advantages in having uniform density and low background activity facilitating easier segmentation of the adenoma. However, its lack of biological structures and attenuation poses another limitation of this study.

The number of iterations has also been observed to be effective in improving accuracy. This is reasonable considering the optimization-based reconstruction algorithms (OLEM) used. However, higher iterations also certainly mean higher process times and delayed outputs. Therefore, users should be encouraged to keep a balanced approach when tackling this issue. Therefore, the processing power of the system is seen as highly affecting the processing time, so this should also be considered.

The type of collimator also makes a difference. It was observed that the higher resolution LEUHR collimator results in higher accuracy than LEHR. We observed an accuracy difference of around 1-1.5% percent in relative comparison between these types of collimators. The collimator has shown a consistent difference in accuracy with LEUHR having an accuracy of lower 7 percent while LEHR achieved an accuracy of around 8.5 percent. These results give us an idea about the impact of septal properties on quantitative accuracy, with both collimators operating on low energy. The most significant differences in properties are hole length and septal penetration percentage (Table 2).

Scatter correction influenced the results, by 1-1.5 percent in certain instances. When put into perspective, this is around a 15 percent improvement relative to the accuracy without scatter correction. This puts forward the capabilities and importance of this correction method, as scattering is a factor present in every imaging modality involving photon radiation. In further studies, the importance of scatter correction might be emphasized particularly with biological structures having different attenuation coefficients. Additionally, within the open-source programs SIMIND and CASToR, it is not possible to employ resolution recovery, dead time correction, and partial volume correction which is another limitation in our study. In conclusion, it can be stated with confidence, that the results show that parameters used in imaging have a considerable impact on quantification accuracy.

5. CONCLUSION

This study undertakes for the first time the optimization of quantitative parathyroid SPECT using computer simulation. This study has the potential to advance the use of this technique by improving accuracy.

Quantification is shown to be a method that holds immense potential for the future of medical imaging. It gives the user the ability to identify an adenoma in a precise and accurate manner.

In this study, it was concluded that instrumentation and processing parameters have observable effects on quantification accuracy. The results show that the presence of scatter correction, the number of iterations, and the collimators have impactful effects on quantification accuracy. All parameter values have achieved a sub-10 percent quantification accuracy, demonstrating the viability of SPECT as a quantitative imaging modality.

Resolution recovery, a correction method, used to reduce the necessary dose for imaging during the reconstruction process. It is only available alongside iterative reconstruction. Images created by resolution recovery provide better contrast and resolution while needing less acquisition and processing time [42]. This method should be further examined for its effect on quantification accuracy.

Other correction methods such as dead time correction and partial volume correction may also improve the quality of the image which is proven to be very important in quantitative studies and should be employed in future studies.

The addition of anthropomorphic phantom types to the testing can improve our understanding of this study with scenarios closer to real-life circumstances. It also introduces further challenges, such as segmentation alongside background activity and attenuation.

Simulating and testing different gamma camera models would expand the spectrum of this study encompasses. Since most gamma camera models have different imaging parameters, their effects could also be studied. More clinical studies are also needed to establish the technique.

REFERENCES

1. Anon. (2016). 'EANM'16'. Pp. 1–734 in European journal of nuclear medicine and molecular imaging. Vol. 43.
2. Bahreyni Toossi, M. T., J. Pirayesh Islamian, M. Momenzhad, M. Ljungberg, and S. H. Naseri. (2010). 'SIMIND Monte Carlo Simulation of a Single Photon Emission CT.' *Journal of Medical Physics* 35(1):42–47. doi: 10.4103/0971-6203.55967.
3. Bailey, Dale L., and Kathy P. Willowson. (2013). 'An Evidence-Based Review of Quantitative SPECT Imaging and Potential Clinical Applications'. *Journal of Nuclear Medicine* 54(1):83–89.
4. Bailey, Dale L., and Kathy P. Willowson. (2014). 'Quantitative SPECT/CT: SPECT Joins PET as a Quantitative Imaging Modality'. *European Journal of Nuclear Medicine and Molecular Imaging* 41(SUPPL. 1). doi: 10.1007/s00259-013-2542-4.
5. Bilezikian, John P., Maria Luisa Brandi, Richard Eastell, Shonni J. Silverberg, Robert Udelsman, Claudio Marcocci, and John T. Potts. (2014). 'Guidelines for the Management of Asymptomatic Primary Hyperparathyroidism: Summary Statement from the Fourth International Workshop'. Pp. 3561–69 in *Journal of Clinical Endocrinology and Metabolism*. Vol. 99. Endocrine Society.

6. Bindu, Ch Hima, and K. Satya Prasad. (2012). An Efficient Medical Image Segmentation Using Conventional OTSU Method. Vol. 38.
7. Bong, Jung Kyun, Hye Kyung Son, Jong Doo Lee, and Hee Joung Kim. (2005). 'Improved Scatter Correction for SPECT Images: A Monte Carlo Study'. IEEE Transactions on Nuclear Science 52(5 1):1263–70. doi: 10.1109/TNS.2005.858202.
8. Carvalho, L. E., A. C. Sobieranski, and A. von Wangenheim. (2018). '3D Segmentation Algorithms for Computerized Tomographic Imaging: A Systematic Literature Review'. Journal of Digital Imaging 31(6):799–850.
9. Dandurand, Karel, Dalal S. Ali, and Aliya A. Khan. (2021). 'Primary Hyperparathyroidism: A Narrative Review of Diagnosis and Medical Management'. Journal of Clinical Medicine 10(8).
10. D'Arienzo, M., M. Cazzato, M. L. Cozzella, M. Cox, M. D'Andrea, A. Fazio, A. Fenwick, G. Iaccarino, L. Johansson, L. Strigari, S. Ungania, and P. De Felice. (2016). 'Gamma Camera Calibration and Validation for Quantitative SPECT Imaging with 177Lu'. Applied Radiation and Isotopes 112:156–64. doi: 10.1016/j.apradiso.2016.03.007.
11. Fahey, Frederic H., Kira Grogg, and Georges El Fakhri. (2018). 'Use of Monte Carlo Techniques in Nuclear Medicine.' Journal of the American College of Radiology: JACR 15(3 Pt A):446–48. doi: 10.1016/j.jacr.2017.09.045.
12. Fedorov, Andriy, Reinhard Beichel, Jayashree Kalpathy-Cramer, Julien Finet, Jean-Christophe Fillion-Robin, Sonia Pujol, Christian Bauer, Dominique Jennings, Fiona Fennessy, Milan Sonka, John Buatti, Stephen Aylward, James V Miller, Steve Pieper, and Ron Kikinis. (2012). '3D Slicer as an Image Computing Platform for the Quantitative Imaging Network.' Magnetic Resonance Imaging 30(9):1323–41. doi: 10.1016/j.mri.2012.05.001.
13. Fraser, William D. (2009). 'Hyperparathyroidism'. The Lancet 374(9684):145–58.
14. Frezza, Andrea, Corentin Desport, Carlos Uribe, Wei Zhao, Anna Celler, Philippe Després, and Jean Mathieu Beauregard. (2020). 'Comprehensive SPECT/CT System Characterization and Calibration for 177Lu Quantitative SPECT (QSPECT) with Dead-Time Correction'. EJNMMI Physics 7(1). doi: 10.1186/s40658-020-0275-6.
15. Gustafsson, Johan, Gustav Brodin, and Michael Ljungberg. (2018). 'Monte Carlo-Based SPECT Reconstruction within the SIMIND Framework'. Physics in Medicine & Biology 63(24):245012. doi: 10.1088/1361-6560/aaf0f1.
16. Halty, Adrien, Jean Noël Badel, Olga Kochebina, and David Sarrut. (2018). 'Image-Based SPECT Calibration Based on the Evaluation of the Fraction of Activity in the Field of View'. EJNMMI Physics 5(1). doi: 10.1186/s40658-018-0209-8.
17. Harris, Luke, John Yoo, Albert Driedger, Kevin Fung, Jason Franklin, Daryl Gray, and Ronald Holliday. (2008). 'Accuracy of Technetium-99m SPECT-CT Hybrid Images in Predicting the Precise Intraoperative Anatomical Location of Parathyroid Adenomas'. Head & Neck 30(4):509–17. doi: 10.1002/hed.20727.
18. Harrison, Robert L. (2009). 'Introduction to Monte Carlo Simulation'. Pp. 17–21 in AIP Conference Proceedings. Vol. 1204.

19. Havel, Martin, Vladimir Dedek, Michal Kolacek, and Martin Formanek. (2022). 'Quantitative Analysis in Parathyroid Adenoma Scintigraphy'. *Nuclear Medicine Communications* 43(1):1–7. doi: 10.1097/MNM.0000000000001474.
20. Hima Bindu, Ch. (2009). *An Improved Medical Image Segmentation Algorithm Using Otsu Method*. Vol. 2.
21. Hwang, Andrew B., Benjamin L. Franc, Grant T. Gullberg, and Bruce H. Hasegawa. (2008). 'Assessment of the Sources of Error Affecting the Quantitative Accuracy of SPECT Imaging in Small Animals'. *Physics in Medicine and Biology* 53(9):2233–52. doi: 10.1088/0031-9155/53/9/002.
22. Ilahi, Ali, Erind Muco, and Tahir B. Ilahi. (2022). *Anatomy, Head and Neck, Parathyroid*.
23. Im, Hyung-Jun, In Ki Lee, Jin Chul Paeng, Kyu Eun Lee, Gi Jeong Cheon, Keon Wook Kang, June-Key Chung, and Dong Soo Lee. (2014). 'Functional Evaluation of Parathyroid Adenoma Using 99mTc-MIBI Parathyroid SPECT/CT'. *Nuclear Medicine Communications* 35(6):649–54. doi: 10.1097/MNM.0000000000000102.
24. Jiang, Shu Qin, Ting Yang, Qiong Zou, Lei Xu, Ting Ye, Yin Qian Kang, Wan Ru Li, Ju Jiao, and Yong Zhang. (2020). 'The Role of 99mTc-MIBI SPECT/CT in Patients with Secondary Hyperparathyroidism: Comparison with 99mTc-MIBI Planar Scintigraphy and Ultrasonography'. *BMC Medical Imaging* 20(1). doi: 10.1186/s12880-020-00517-9.
25. Jun, Zhang, and Hu Jinglu. (2008). 'Image Segmentation Based on 2D Otsu Method with Histogram Analysis'. Pp. 105–8 in *Proceedings - International Conference on Computer Science and Software Engineering, CSSE 2008*. Vol. 6.
26. Khouli, Riham El, Martin Lodge, Martha Zeiger, Melin Vranesic, Harvey Ziessman, and Zsolt Szabo. (2015a). 'Quantitative SPECT CT of the Parathyroid with SUV Measurements'. *Journal of Nuclear Medicine* 56(supplement 3):1645.
27. Khouli, Riham El, Martin Lodge, Martha Zeiger, Melin Vranesic, Harvey Ziessman, and Zsolt Szabo. (2015b). 'Quantitative SPECT CT of the Parathyroid with SUV Measurements'. *Journal of Nuclear Medicine* 56(supplement 3):1645.
28. Khouli, Riham El, Evrim Turkbey, Martin Lodge, Melin Vranesic, Harvey Ziessman, Don Spence, Xinhong Ding, Alexander Vija, and Zsolt Szabo. (2017a). 'Standardized Uptake Value Based Assessment of Dual Phase Parathyroid SPECT CT: Promising Role in Equivocal Cases'. *Journal of Nuclear Medicine* 58(supplement 1):101.
29. Khouli, Riham El, Evrim Turkbey, Martin Lodge, Melin Vranesic, Harvey Ziessman, Don Spence, Xinhong Ding, Alexander Vija, and Zsolt Szabo. (2017b). 'Standardized Uptake Value Based Assessment of Dual Phase Parathyroid SPECT CT: Promising Role in Equivocal Cases'. *Journal of Nuclear Medicine* 58(supplement 1):101.
30. Kim, Hyun Joo, Ji In Bang, Ji Young Kim, Jae Hoon Moon, Young So, and Won Woo Lee. (2017). 'Novel Application of Quantitative Single-Photon Emission Computed Tomography/Computed Tomography to Predict Early Response to Methimazole in Graves' Disease'. *Korean Journal of Radiology* 18(3):543–50. doi: 10.3348/kjr.2017.18.3.543.

31. Lee, Hyunjong, Ji Hyun Kim, Yeon Koo Kang, Jae Hoon Moon, Young So, and Won Woo Lee. (2016). 'Quantitative Single-Photon Emission Computed Tomography/Computed Tomography for Technetium Pertechnetate Thyroid Uptake Measurement'. *Medicine (United States)* 95(27). doi: 10.1097/MD.0000000000004170.
32. Listewnik, Maria H., Hanna Piwowarska-Bilska, Krzysztof Safranow, Jacek Iwanowski, Maria Laszczyńska, Maria Chosia, Marek Ostrowski, Bozena Birkenfeld, Dorota Oszutowska-Mazurek, and Przemyslaw Mazurek. (2019). 'Estimation of Parameters of Parathyroid Glands Using Particle Swarm Optimization and Multivariate Generalized Gaussian Function Mixture'. *Applied Sciences (Switzerland)* 9(21). doi: 10.3390/app9214511.
33. Ljungberg, Michael. n.d. The SIMIND Monte-Carlo Program.
34. Ljungberg, Michael, Katarina Sjögren, Xiaowei Liu, Eric Frey, Yuni Dewaraja, and Sven-Erik Strand. (2002). 'A 3-Dimensional Absorbed Dose Calculation Method Based on Quantitative SPECT for Radionuclide Therapy: Evaluation for ¹³¹I Using Monte Carlo Simulation'. *Journal of Nuclear Medicine* 43(8):1101.
35. Ljungberg, Michael, and Katarina Sjögren-Gleisner. (2011). 'The Accuracy of Absorbed Dose Estimates in Tumours Determined by Quantitative SPECT: A Monte Carlo Study'. Pp. 981–89 in *Acta Oncologica*. Vol. 50.
36. Ma, Junhao, Jun Yang, Chuanzhi Chen, Yimin Lu, Zhuochao Mao, Haohao Wang, Yan Yang, Zhongqi Li, Weibin Wang, and Lisong Teng. (2021). 'Use of ^{99m}Tc-Sestamibi SPECT/CT Imaging in Predicting the Degree of Pathological Hyperplasia of the Parathyroid Gland: Semi-Quantitative Analysis'. *Quantitative Imaging in Medicine and Surgery* 11(10):4375–88. doi: 10.21037/qims-21-66.
37. Merlin, Thibaut, Simon Stute, Didier Benoit, Julien Bert, Thomas Carlier, Claude Comtat, Marina Filipovic, Frédéric Lamare, and Dimitris Visvikis. (2018). 'CASToR: A Generic Data Organization and Processing Code Framework for Multi-Modal and Multi-Dimensional Tomographic Reconstruction'. *Physics in Medicine & Biology* 63(18):185005. doi: 10.1088/1361-6560/aadacl.
38. Minarik, D., K. Sjögren Gleisner, and M. Ljungberg. (2008). 'Evaluation of Quantitative ⁹⁰Y SPECT Based on Experimental Phantom Studies'. *Physics in Medicine and Biology* 53(20):5689–5703. doi: 10.1088/0031-9155/53/20/008.
39. Ogawa, Koichi, Yasuo Harata, Takashi Ichihara, Atsushi Kubo, and Shozo Hashimoto. (1991). 'A Practical Method for Position-Dependent Compton-Scatter Correction in Single Photon Emission CT'. *IEEE Transactions on Medical Imaging* 10(3):408–12. doi: 10.1109/42.97591.
40. Oral, Ayscgul, and Albert Guvenis. (2019). 'A Digital Platform for Simulating the Accurate Detectability of Overactive Parathyroid Glands in SPECT/CT Imaging'. in *TIPTEKNO 2019 - Tip Teknolojileri Kongresi*. Institute of Electrical and Electronics Engineers Inc.
41. Oral, Aysegul, and Albert Guvenis. (2021). 'Improving the Detectability of Overactive Glands in Dual-Phase Parathyroid SPECT/CT: A Monte Carlo Simulation Study'. *Biomedical Physics and Engineering Express* 7(4). doi: 10.1088/2057-1976/ac0954.

42. Pagnanelli, Robert, and Salvador Borges-Neto. (2016). 'Technical Aspects of Resolution Recovery Reconstruction'. *Journal of Nuclear Cardiology* 23(1):149–52. doi: 10.1007/s12350-015-0345-7.
43. Patton, James A., and Timothy G. Turkington. (2008). 'SPECT/CT Physical Principles and Attenuation Correction'. *Journal of Nuclear Medicine Technology* 36(1):1. doi: 10.2967/jnmt.107.046839.
44. Razavi, Simin, Blair Ziebarth, Ran Klein, and Wanzhen Zeng. (2018). 'Dual Time-Point Quantitative SPECT-CT Parathyroid Imaging Using a Single Computed Tomography'. *Nuclear Medicine Communications* 39(1):3–9. doi: 10.1097/MNM.0000000000000761.
45. Ritt, Philipp, Hans Vija, Joachim Hornegger, and Torsten Kuwert. (2011). 'Absolute Quantification in SPECT'. *European Journal of Nuclear Medicine and Molecular Imaging* 38(SUPPL. 1).
46. Robin, Philippe, Ran Klein, Jeremy Gardner, Blair Ziebarth, Sadri Bazarjani, Simin Razavi, Lionel S. Zuckier, and Wanzhen Zeng. (2019). 'Quantitative Analysis of Technetium-99m-Sestamibi Uptake and Washout in Parathyroid Scintigraphy Supports Dual Mechanisms of Lesion Conspicuity'. *Nuclear Medicine Communications* 40(5):469–76. doi: 10.1097/MNM.0000000000000996.
47. Suh, Hoon Young, Hee Young Na, So Yeon Park, June Young Choi, Young So, and Won Woo Lee. (2020). 'The Usefulness of Maximum Standardized Uptake Value at the Delayed Phase of Tc-99m Sestamibi Single-Photon Emission Computed Tomography/Computed Tomography for Identification of Parathyroid Adenoma and Hyperplasia'. *Medicine* 99(28):e21176. doi: 10.1097/MD.00000000000021176.
48. Tunninen, Virpi, T. Kauppinen, and H. Eskola. (2017). 'Physical Characteristics of Collimators for Dual-Isotope Imaging with 99mTc and 123I'. Pp. 245–49 in *IFMBE Proceedings*. Vol. 65. Springer Verlag.
49. Vasavada, Anita N., Jonathan Danaraj, and Gunter P. Siegmund. (2008). 'Head and Neck Anthropometry, Vertebral Geometry and Neck Strength in Height-Matched Men and Women'. *Journal of Biomechanics* 41(1):114–21. doi: 10.1016/j.jbiomech.2007.07.007.
50. Wang, Yuhua, Ye Liu, Na Li, Kang Xu, and Wanchun Zhang. (2023a). 'Quantitative Application of Dual-Phase 99mTc-Sestamibi SPECT/CT Imaging of Parathyroid Lesions: Identification of Optimal Timing in Secondary Hyperparathyroidism'. *EJNMMI Physics* 10(1). doi: 10.1186/s40658-023-00548-5.
51. Wang, Yuhua, Ye Liu, Na Li, Kang Xu, and Wanchun Zhang. (2023b). 'Quantitative Application of Dual-Phase 99mTc-Sestamibi SPECT/CT Imaging of Parathyroid Lesions: Identification of Optimal Timing in Secondary Hyperparathyroidism'. *EJNMMI Physics* 10(1). doi: 10.1186/s40658-023-00548-5.
52. Wang, Yuhua, Ye Liu, Na Li, Kang Xu, and Wanchun Zhang. (2023c). 'Quantitative Application of Dual-Phase 99mTc-Sestamibi SPECT/CT Imaging of Parathyroid Lesions: Identification of Optimal Timing in Secondary Hyperparathyroidism'. *EJNMMI Physics* 10(1):29. doi: 10.1186/s40658-023-00548-5.
53. Wevrett, J., A. Fenwick, J. Scuffham, and A. Nisbet. (2017). 'Development of a Calibration Protocol for Quantitative Imaging for Molecular Radiotherapy Dosimetry'. *Radiation Physics and Chemistry* 140:355–60. doi: 10.1016/j.radphyschem.2017.02.053.

54. Wieneke, Jacqueline A., and Alice Smith. (2008). 'Parathyroid Adenoma.' *Head and Neck Pathology* 2(4):305–8. doi: 10.1007/s12105-008-0088-8.
55. Zaidi, Habib. (1999). 'Relevance of Accurate Monte Carlo Modeling in Nuclear Medical Imaging'. *Medical Physics* 26(4):574–608.
56. Zeintl, Johannes, Alexander Hans Vija, Amos Yahil, Joachim Hornegger, and Torsten Kuwert. (2010). 'Quantitative Accuracy of Clinical ^{99m}Tc SPECT/CT Using Ordered-Subset Expectation Maximization with 3-Dimensional Resolution Recovery, Attenuation, and Scatter Correction'. *Journal of Nuclear Medicine* 51(6):921–28. doi: 0.2967/jnumed.109.071571.

IDUNAS	NATURAL & APPLIED SCIENCES JOURNAL	2023 Vol. 6 No. 2 (24-30)
---------------	---	------------------------------------

Some New Integral Inequalities via Caputo-Fabrizio Fractional Integral Operator

Research Article

Sinan ASLAN^{1*} 

¹Ağrı İbrahim Çeçen University, Institute of Graduate Studies, Ağrı-Türkiye

Author E-mail
sinanaslan0407@gmail.com
ORCID ID: 0000-0001-5970-1926

*Correspondence to: Aslan S., Ağrı İbrahim Çeçen University, Institute of Graduate Studies, Ağrı Türkiye
DOI: 10.38061/idunas.1318116

Received: 21.06.2023; Accepted: 31.08.2023

Abstract

On this note, some new integral inequalities were constructed for the product of two integrable functions by using Young's inequality with a well-known classical inequality via the Caputo-Fabrizio fractional integral operator. Some specific cases of the main findings are then given. The main results have the potential to be used in inequality theory.

Keywords: Caputo-Fabrizio fractional integral operator, Young inequality, Inequalities.

1. INTRODUCTION

Definition 1.1 [2] Let $f \in H^1(a, b)$, $b > a$, $\alpha \in [0, 1]$. The definitions of the left and right sides of the Caputo-Fabrizio fractional integral are given as:

$$({}^{CF}I_a^\alpha)(t) = \frac{1-\alpha}{B(\alpha)}f(t) + \frac{\alpha}{B(\alpha)}\int_a^t f(y)dy$$

and

$$({}^{CF}I_b^\alpha)(t) = \frac{1-\alpha}{B(\alpha)}f(t) + \frac{\alpha}{B(\alpha)}\int_t^b f(y)dy$$

where $B(\alpha) > 0$ is normalization function.

Subsequently in the paper, we will denote normalization function as $B(\alpha)$ with $B(0) = B(1) = 1$.

In [4], the authors provided an integral inequality of Hermite-Hadamard type for preinvex functions via Caputo-Fabrizio fractional integral operator as follows.

Theorem 1.2 Let $f: I = [k_1, k_1 + \mu(k_2, k_1)] \rightarrow (0, \infty)$ be a preinvex function on I° and $f \in L[k_1, k_1 + \mu(k_2, k_1)]$. If $\alpha \in [0, 1]$, then the following inequality holds:

$$f\left(\frac{2k_1 + \mu(k_2, k_1)}{2}\right) \leq \frac{B(\alpha)}{\alpha\mu(k_2, k_1)} \left[{}^{CF}I_{k_1}^\alpha \{f(k)\} + {}^{CF}I_{k_1 + \mu(k_2, k_1)}^\alpha \{f(k)\} - \frac{2(1 - \alpha)}{B(\alpha)} f(k) \right] \leq \frac{f(k_1) + f(k_2)}{2}$$

where $k \in [k_1, k_1 + \mu(k_2, k_1)]$.

For more information on various fractional operators and novel integral inequalities involving these operators, we recommend the following papers to readers: [1]-[21].

Suppose that

$$a, b, c, d > 0, \quad 0 < \theta < 1, \quad 0 < \beta < 1, \quad \theta + \beta = 1.$$

If $b < a, \quad d < c$, then

$$a^\theta b^\beta + c^\theta d^\beta \leq (a + c)^\theta + (b + d)^\beta \tag{1}$$

The fundamental inequality for integrable functions (1) can be given as:

Suppose f, g, h, r are integrable positive functions.

$$f(t), g(t), h(t), r(t) > 0, \quad 0 < \theta < 1, \quad 0 < \beta < 1, \quad \theta + \beta = 1.$$

If $g(t) < f(t), \quad r(t) < h(t)$, then

$$f(t)^\theta g(t)^\beta + h(t)^\theta r(t)^\beta \leq (f(t) + h(t))^\theta + (g(t) + r(t))^\beta.$$

This inequality is a very basic inequality that holds for real numbers. We will use this inequality to prove our main findings.

The paper demonstrates some new integral inequalities for integrable functions using the Caputo-Fabrizio fractional integral operator. Young's inequality was used in some analysis methods.

2. MAIN RESULTS

Theorem 2.1. Let $I \subseteq \mathbb{R}$. Suppose that $f, g, h, r : [a, b] \subseteq I \rightarrow \mathbb{R}^+$ integrable positive functions for $0 < \theta < 1, \theta + \beta = 1$. Then, for the Caputo-Fabrizio fractional integral operator, the following inequality holds:

$$\begin{aligned} & \frac{2(1 - \alpha)}{B(\alpha)} (f + h)^\theta(k) + \frac{\alpha}{B(\alpha)} \int_a^b [f(t)]^\theta \cdot [g(t)]^\beta dt + \frac{2(1 - \alpha)}{B(\alpha)} (g + r)^\beta(k) \\ & + \frac{\alpha}{B(\alpha)} \int_a^b [h(t)]^\theta [r(t)]^\beta dt \\ & \leq ({}^{CF}I_b^\alpha (f + h)^\theta)(k) + ({}^{CF}I_b^\alpha (f + h)^\theta)(k) + ({}^{CF}I_a^\alpha (g + r)^\beta)(k) + ({}^{CF}I_b^\alpha (g + r)^\beta)(k) \end{aligned}$$

where $B(\alpha) > 0$ is normalization function, $k \in [a, b]$ and $\alpha \in [0, 1]$.

Proof. We will start with

$$[f(t)]^\theta \cdot [g(t)]^\beta + [h(t)]^\theta [r(t)]^\beta \leq [f(t) + h(t)]^\theta + [g(t) + r(t)]^\beta.$$

By multiplying both sides of the above inequality with $\frac{\alpha}{B(\alpha)}$, we have

$$\frac{\alpha}{B(\alpha)} [f(t)]^\theta \cdot [g(t)]^\beta + \frac{\alpha}{B(\alpha)} [h(t)]^\theta [r(t)]^\beta \leq \frac{\alpha}{B(\alpha)} [f(t) + h(t)]^\theta + \frac{\alpha}{B(\alpha)} [g(t) + r(t)]^\beta.$$

By integrating both sides of the inequality over $[a, b]$ with respect to t , we get

$$\begin{aligned} \frac{\alpha}{B(\alpha)} \int_a^b [f(t)]^\theta \cdot [g(t)]^\beta dt + \frac{\alpha}{B(\alpha)} \int_a^b [h(t)]^\theta [r(t)]^\beta dt \\ \leq \frac{\alpha}{B(\alpha)} \int_a^b [f(t) + h(t)]^\theta dt + \frac{\alpha}{B(\alpha)} \int_a^b [g(t) + r(t)]^\beta dt \end{aligned}$$

and then we get

$$\begin{aligned} \frac{\alpha}{B(\alpha)} \int_a^b [f(t)]^\theta \cdot [g(t)]^\beta dt + \frac{\alpha}{B(\alpha)} \int_a^b [h(t)]^\theta [r(t)]^\beta dt \\ \leq \frac{\alpha}{B(\alpha)} \int_a^k [f(t) + h(t)]^\theta dt + \frac{\alpha}{B(\alpha)} \int_k^b [f(t) + h(t)]^\theta dt + \frac{\alpha}{B(\alpha)} \int_a^k [g(t) + r(t)]^\beta dt \\ + \frac{\alpha}{B(\alpha)} \int_k^b [g(t) + r(t)]^\beta dt. \end{aligned}$$

If we add $\frac{2(1-\alpha)}{B(\alpha)} (f + h)^\theta(k)$ and $\frac{2(1-\alpha)}{B(\alpha)} (g + r)^\beta(k)$ to both sides, we provide

$$\begin{aligned} \frac{2(1-\alpha)}{B(\alpha)} (f + h)^\theta(k) + \frac{\alpha}{B(\alpha)} \int_a^b [f(t)]^\theta \cdot [g(t)]^\beta dt + \frac{2(1-\alpha)}{B(\alpha)} (g + r)^\beta(k) \\ + \frac{\alpha}{B(\alpha)} \int_a^b [h(t)]^\theta [r(t)]^\beta dt \\ \leq \frac{(1-\alpha)}{B(\alpha)} (f + h)^\theta(k) + \frac{\alpha}{B(\alpha)} \int_a^k [f(t) + h(t)]^\theta dt + \frac{(1-\alpha)}{B(\alpha)} (f + h)^\theta(k) \\ + \frac{\alpha}{B(\alpha)} \int_k^b [f(t) + h(t)]^\theta dt + \frac{(1-\alpha)}{B(\alpha)} (g + r)^\beta(k) + \frac{\alpha}{B(\alpha)} \int_a^k [g(t) + r(t)]^\beta dt \\ + \frac{(1-\alpha)}{B(\alpha)} (g + r)^\beta(k) + \frac{\alpha}{B(\alpha)} \int_k^b [g(t) + r(t)]^\beta dt. \end{aligned}$$

We obtain

$$\begin{aligned} & \frac{2(1-\alpha)}{B(\alpha)}(f+h)^\theta(k) + \frac{\alpha}{B(\alpha)} \int_a^b [f(t)]^\theta \cdot [g(t)]^\beta dt + \frac{2(1-\alpha)}{B(\alpha)}(g+r)^\beta(k) \\ & \quad + \frac{\alpha}{B(\alpha)} \int_a^b [h(t)]^\theta [r(t)]^\beta dt \\ & \leq ({}^{CF}I_a^\alpha (f+h)^\theta)(k) + ({}^{CF}I_b^\alpha (f+h)^\theta)(k) + ({}^{CF}I_a^\alpha (g+r)^\beta)(k) + ({}^{CF}I_b^\alpha (g+r)^\beta)(k). \end{aligned}$$

which completes the proof.

Corollary 2.2. Under the assumptions of Theorem 2.1, if we choose $k = \frac{a+b}{2}$, then we have the following inequality:

$$\begin{aligned} & \frac{2(1-\alpha)}{B(\alpha)}(f+h)^\theta\left(\frac{a+b}{2}\right) + \frac{\alpha}{B(\alpha)} \int_a^b [f(t)]^\theta \cdot [g(t)]^\beta dt + \frac{2(1-\alpha)}{B(\alpha)}(g+r)^\beta\left(\frac{a+b}{2}\right) \\ & \quad + \frac{\alpha}{B(\alpha)} \int_a^b [h(t)]^\theta [r(t)]^\beta dt \\ & \leq ({}^{CF}I_a^\alpha (f+h)^\theta)\left(\frac{a+b}{2}\right) + ({}^{CF}I_b^\alpha (f+h)^\theta)\left(\frac{a+b}{2}\right) + ({}^{CF}I_a^\alpha (g+r)^\beta)\left(\frac{a+b}{2}\right) \\ & \quad + ({}^{CF}I_b^\alpha (g+r)^\beta)\left(k \frac{a+b}{2}\right). \end{aligned}$$

Corollary 2.3. Under the assumptions of Theorem 2.1, if we choose $\theta = \beta = \frac{1}{2}$, then we have the following inequality:

$$\begin{aligned} & \frac{2(1-\alpha)}{B(\alpha)}(f+h)^{\frac{1}{2}}(k) + \frac{\alpha}{B(\alpha)} \int_a^b \sqrt{f(t)g(t)} dt + \frac{2(1-\alpha)}{B(\alpha)}(g+r)^{\frac{1}{2}}(k) + \frac{\alpha}{B(\alpha)} \int_a^b \sqrt{h(t)r(t)} dt \\ & \leq ({}^{CF}I_a^\alpha (f+h)^{\frac{1}{2}})(k) + ({}^{CF}I_b^\alpha (f+h)^{\frac{1}{2}})(k) + ({}^{CF}I_a^\alpha (g+r)^{\frac{1}{2}})(k) \\ & \quad + ({}^{CF}I_b^\alpha (g+r)^{\frac{1}{2}})(k). \end{aligned}$$

Theorem 2.4. Let $I \subseteq R$. Suppose that $f, g, h, r : [a, b] \subseteq I \rightarrow R^+$ integrable positive functions for $0 < \theta < 1, \theta + \beta = 1$. Then, we have following inequality for Caputo-Fabrizio fractional integral operator:

$$\begin{aligned} & \frac{2(1-\alpha)}{B(\alpha)}(f+h)^{p\theta}(k) + \frac{p\alpha}{B(\alpha)} \int_a^b [f(t)]^\theta \cdot [g(t)]^\beta dt \\ & \quad + \frac{2(1-\alpha)}{B(\alpha)}(g+r)^{p\beta}(k) + \frac{p\alpha}{B(\alpha)} \int_a^b [h(t)]^\theta [r(t)]^\beta dt - \frac{2(b-a)}{q} \frac{p\alpha}{B(\alpha)} \\ & \leq ({}^{CF}I_a^\alpha (f+h)^{p\theta})(k) + ({}^{CF}I_b^\alpha (f+h)^{p\theta})(k) + ({}^{CF}I_a^\alpha (g+r)^{p\beta})(k) \\ & \quad + ({}^{CF}I_b^\alpha (g+r)^{p\beta})(k) \end{aligned}$$

where $B(\alpha) > 0$ is normalization function, $q > 1, \frac{1}{q} + \frac{1}{p} = 1, k \in [a, b]$ and $\alpha \in [0,1]$.

Proof. We can write

$$[f(t)]^\theta \cdot [g(t)]^\beta + [h(t)]^\theta [r(t)]^\beta \leq [f(t) + h(t)]^\theta + [g(t) + r(t)]^\beta.$$

By multiplying both sides of the above inequality with $\frac{p\alpha}{B(\alpha)}$, we get

$$\frac{p\alpha}{B(\alpha)} [f(t)]^\theta \cdot [g(t)]^\beta + \frac{p\alpha}{B(\alpha)} [h(t)]^\theta [r(t)]^\beta \leq \frac{p\alpha}{B(\alpha)} [f(t) + h(t)]^\theta + \frac{p\alpha}{B(\alpha)} [g(t) + r(t)]^\beta.$$

By integrating both sides of the inequality over $[a, b]$ with respect to t , we obtain

$$\begin{aligned} \frac{p\alpha}{B(\alpha)} \int_a^b [f(t)]^\theta \cdot [g(t)]^\beta dt + \frac{p\alpha}{B(\alpha)} \int_a^b [h(t)]^\theta [r(t)]^\beta dt \\ \leq \frac{p\alpha}{B(\alpha)} \int_a^b [f(t) + h(t)]^\theta dt + \frac{p\alpha}{B(\alpha)} \int_a^b [g(t) + r(t)]^\beta dt. \end{aligned}$$

If we apply the Young's inequality to the right -hand side of the inequality, we get

$$\begin{aligned} \frac{p\alpha}{B(\alpha)} \int_a^b [f(t)]^\theta \cdot [g(t)]^\beta dt + \frac{p\alpha}{B(\alpha)} \int_a^b [h(t)]^\theta [r(t)]^\beta dt \\ \leq \frac{p\alpha}{B(\alpha)} \left(\frac{1}{p} \int_a^k [f(t) + h(t)]^{p\theta} dt + \frac{1}{q} \int_a^k 1^q dt + \frac{1}{p} \int_k^b [f(t) + h(t)]^{p\theta} dt + \frac{1}{q} \int_k^b 1^q dt \right) \\ + \frac{p\alpha}{B(\alpha)} \left(\frac{1}{p} \int_a^k [g(t) + r(t)]^{p\beta} dt + \frac{1}{q} \int_a^k 1^q dt + \frac{1}{p} \int_k^b [g(t) + r(t)]^{p\beta} dt + \frac{1}{q} \int_k^b 1^q dt \right) \\ = \frac{p\alpha}{B(\alpha)} \left(\frac{1}{p} \int_a^k [f(t) + h(t)]^{p\theta} dt + \frac{k-a}{q} + \frac{1}{p} \int_k^b [f(t) + h(t)]^{p\theta} dt + \frac{b-k}{q} \right) \\ + \frac{p\alpha}{B(\alpha)} \left(\frac{1}{p} \int_a^k [g(t) + r(t)]^{p\beta} dt + \frac{k-a}{q} + \frac{1}{p} \int_k^b [g(t) + r(t)]^{p\beta} dt + \frac{b-k}{q} \right). \end{aligned}$$

This implies,

$$\begin{aligned} \frac{p\alpha}{B(\alpha)} \int_a^b [f(t)]^\theta [g(t)]^\beta dt + \frac{p\alpha}{B(\alpha)} \int_a^b [h(t)]^\theta [r(t)]^\beta dt - \frac{2(b-a)}{q} \frac{p\alpha}{B(\alpha)} \\ \leq \frac{p\alpha}{B(\alpha)} \left(\frac{1}{p} \int_a^k [f(t) + h(t)]^{p\theta} dt + \frac{1}{p} \int_k^b [f(t) + h(t)]^{p\theta} dt \right) \\ + \frac{p\alpha}{B(\alpha)} \left(\frac{1}{p} \int_a^k [g(t) + r(t)]^{p\beta} dt + \frac{1}{p} \int_k^b [g(t) + r(t)]^{p\beta} dt \right). \end{aligned}$$

If we add $\frac{2(1-\alpha)}{B(\alpha)} (f + h)^{p\theta}(k)$ and $\frac{2(1-\alpha)}{B(\alpha)} (g + r)^{p\beta}(k)$ to both sides of the inequality,

$$\begin{aligned} & \frac{p\alpha}{B(\alpha)} \int_a^b [f(t)]^\theta [g(t)]^\beta dt + \frac{p\alpha}{B(\alpha)} \int_a^b [h(t)]^\theta [r(t)]^\beta dt - \frac{2(b-a)}{q} \frac{p\alpha}{B(\alpha)} + \frac{2(1-\alpha)}{B(\alpha)} (f+h)^{p\theta}(k) \\ & + \frac{2(1-\alpha)}{B(\alpha)} (g+r)^{p\beta}(k) \\ & \leq \left(\frac{(1-\alpha)}{B(\alpha)} (f+h)^{p\theta}(k) + \frac{\alpha}{B(\alpha)} \int_a^k [f(t)+h(t)]^{p\theta} dt \right) \\ & + \left(\frac{(1-\alpha)}{B(\alpha)} (f+h)^{p\theta}(k) + \frac{\alpha}{B(\alpha)} \int_k^b [f(t)+h(t)]^{p\theta} dt \right) \\ & + \left(\frac{(1-\alpha)}{B(\alpha)} (g+r)^{p\beta}(k) + \frac{\alpha}{B(\alpha)} \int_a^k [g(t)+r(t)]^{p\beta} dt \right) \\ & + \left(\frac{(1-\alpha)}{B(\alpha)} (g+r)^{p\beta}(k) + \frac{\alpha}{B(\alpha)} \int_k^b [g(t)+r(t)]^{p\beta} dt \right). \end{aligned}$$

Therefore, we conclude

$$\begin{aligned} & \frac{p\alpha}{B(\alpha)} \int_a^b [f(t)]^\theta [g(t)]^\beta dt + \frac{p\alpha}{B(\alpha)} \int_a^b [h(t)]^\theta [r(t)]^\beta dt - \frac{2(b-a)}{q} \frac{p\alpha}{B(\alpha)} + \frac{2(1-\alpha)}{B(\alpha)} (f+h)^{p\theta}(k) \\ & + \frac{2(1-\alpha)}{B(\alpha)} (g+r)^{p\beta}(k) \\ & \leq ({}^{CF}I_a^\alpha (f+h)^{p\theta})(k) + ({}^{CF}I_b^\alpha (f+h)^{p\theta})(k) + ({}^{CF}I_a^\alpha (g+r)^{p\beta})(k) \\ & + ({}^{CF}I_b^\alpha (g+r)^{p\beta})(k) \end{aligned}$$

This completes the proof.

REFERENCES

1. Abdeljawad, T., Baleanu, D. (2017). Integration by parts and its applications of a new nonlocal fractional derivative with Mittag-Leffler nonsingular kernel. *J. Nonlinear Sci. Appl.*, 10, 1098–1107.
2. Abdeljawad, T., Baleanu, D. (2017). On fractional derivatives with exponential kernel and their discrete versions. *Reports on Mathematical Physics*, 80(1), 11-27.
3. Atangana, A., Baleanu, D. (2016). New fractional derivatives with non-local and non-singular kernel: Theory and Application to heat transfer model. *Thermal Science*, 20 (2), 763-769.
4. Tariq, M., Ahmad, H., Shaikh, A. G., Sahoo, S. K., Khedher, K. M., Gia, T. N. (2022). New fractional integral inequalities for preinvex functions involving Caputo Fabrizio operator. *AIMS Mathematics*, 7(3):3440–3455.
5. Caputo, M., Fabrizio, M. (2015). A new definition of fractional derivative without singular kernel. *Progress in Fractional Differentiation & Applications*, 1(2), 73-85.
6. Abdeljawad, T. (2015). On conformable fractional calculus. *Journal of Computational and Applied Mathematics*, 279, 57-66.

7. Akdemir, A.O., Aslan, S., Çakaloğlu, M.N. and Set, E. New Hadamard Type Integral Inequalities via Caputo-Fabrizio Fractional Operators. 4th International Conference on Mathematical and Related Sciences. Page (91) ICMRS 2021.
8. Akdemir, A., Aslan, S., Ekinçi, A. (2022). Novel Approaches for s-Convex Functions via Caputo-Fabrizio Fractional integrals. Proceedings of IAM, 11(1), 3-16.
9. Akdemir, A.O., Aslan, S., Çakaloğlu, M.N. and Ekinçi, A. Some New Results for Different Kinds of Convex Functions Caputo-Fabrizio Fractional Operators. 4th International Conference on Mathematical and Related Sciences. Page (92) ICMRS 2021.
10. Akdemir, A. O., Butt, S. I., Nadeem, M., Ragusa, M. A. (2021). New general variants of Chebyshev type inequalities via generalized fractional integral operators. Mathematics, 9(2), 122.
11. Akdemir, A. O., Ekinçi, A., Set, E. (2017). Conformable fractional integrals and related new integral inequalities, Journal of Nonlinear and Convex Analysis, 18 (4), 661-674.
12. Aslan, S. (2023). Some Novel Fractional Integral Inequalities for Different Kinds of Convex Functions. Eastern Anatolian Journal of Science, 9(1), 27-32.
13. Butt, S. I., Nadeem, M., Qaisar, S., Akdemir, A. O., Abdeljawad, T. (2020). Hermite–Jensen–Mercer type inequalities for conformable integrals and related results. Advances in Difference Equations, 2020(1), 1-24.
14. Butt, S. I., Umar, M., Rashid, S., Akdemir, A. O., Chu, Y. M. (2020). New Hermite–Jensen–Mercer-type inequalities via k-fractional integrals. Advances in Difference Equations, 2020, 1-24.
15. Caputo, M., Fabrizio, M. (2015). A new definition of fractional derivative without singular kernel. Progress in Fractional Differentiation & Applications, 1(2), 73-85.
16. Ekinçi, A., Özdemir, M.E. (2019). Some new integral inequalities via Riemann-Liouville integral operators. Applied and Computational Mathematics, 18(3), 288-295.
17. Rashid, S., Hammouch, Z., Kalsoom, H., Ashraf, R., Chu, Y. M. (2020). New investigation on the generalized k-fractional integral operators. Frontiers in Physics, 8, 25.
18. Rashid, S., Kalsoom, H., Hammouch, Z., Ashraf, R., Baleanu, D., Chu, Y. M. (2020). New multi-parametrized estimates having pth-order differentiability in fractional calculus for predominating h -convex functions in Hilbert space. Symmetry, 12(2), 222.
19. Samko, S. G. (1993). Fractional integrals and derivatives. Theory and Applications, Gordon and Breach.
20. Set, E. (2012). New inequalities of Ostrowski type for mappings whose derivatives are s-convex in the second sense via fractional integrals. Computers & Mathematics with Applications, 63(7), 1147-1154.
21. Set, E., Akdemir, A. O., Özdemir, E. M. (2017). Simpson type integral inequalities for convex functions via Riemann-Liouville integrals. Filomat, 31(14), 4415-4420.

IDUNAS	NATURAL & APPLIED SCIENCES JOURNAL	2023 Vol. 6 No. 2 (31-40)
--------	---------------------------------------	------------------------------------

Using CO₂ Laser, Optimization of Laser Power, Exposure Time and Frequency for Cavity Formation on Hardox Steel Plate

Research Article

Timur Canel^{1*} , Satılmış Ürgün² 

¹Department of Physics, Faculty of Arts and Science, Kocaeli University, 41380, Kocaeli, Türkiye

²Faculty of Aeronautics and Astronautics, Department of Aviation Electrics and Electronics,
Kocaeli University, Kocaeli, Türkiye.

Author E-mails

tcanel@kocaeli.edu.tr

urgun@kocaeli.edu.tr

T. Canel ORCID ID: 0000-0002-4282-1806

S. Ürgün ORCID ID: 0000-0003-3889-6909

*Correspondence to: Timur Canel, Department of Physics, Faculty of Arts and Science, Kocaeli University, Kocaeli, Türkiye
DOI: 10.38061/idunas.1358218

Received: 11.09.2023; Accepted: 07.12.2023

Abstract

The texture of the surfaces of materials causes changes in mechanical properties such as friction. Micro-scale cavities have been created on Hardox steel plate, which has recently been the focus of attention in demanding applications with its hardness, toughness, and wear resistance. A CO₂ laser was used in the cavitation process on the surface and the power, exposure, and frequency of the laser used were optimized to obtain a cavity with the desired geometry. Taguchi method was used in the optimization process. In addition to obtaining the optimum parameters, the effect ratios of the parameters were also calculated. Optimum laser parameters were obtained as 5 s for laser exposure duration, 60 W for laser power, and 50 kHz for laser frequency. According to the optimization calculations, the parameter with the highest effect on the result was laser exposure duration with a rate of 71,86 %. Laser power and laser frequency affected the result by 23.02 % and 5.12 % respectively.

Keywords: Laser machining, Optimization, Hardox Steel, Surface texturing.

1. INTRODUCTION

Developed by Swedish steelmaker SSAB, Hardox Steel is a brand covering a range of high-strength, wear-resistant steels that are widely used in a variety of industrial applications. These steels are renowned for their exceptional toughness, hardness, and wear resistance. This makes them an important material in environments subject to extreme wear and impact conditions [7]. This study aims to delve deeper into the properties, applications, and advantages of Hardox steel and shed light on its importance in modern

engineering and manufacturing. Hardox steel derives its superior properties from its unique composition and manufacturing process. These steels are typically alloyed with elements such as carbon, manganese, chromium, and other trace elements to achieve a fine balance between hardness and toughness [9]. The microstructure of Hardox steel consists of martensite, a hard crystalline structure that contributes to its exceptional hardness and toughness. In addition, the controlled heat treatment process further enhances the properties of the steel, resulting in a material with high impact resistance, excellent formability, and weldability [6].

The versatility of Hardox steel has led to its widespread adoption in numerous industrial sectors [8]. Hardox steel is used in the mining industry to manufacture buckets, dump truck bodies and crushing equipment where it resists abrasion from the movement of rocks and minerals. In construction and infrastructure projects, it finds use in excavator buckets, bulldozer blades, and concrete mixers, where its strength extends the service life of critical components. In addition, Hardox steel is a preferred choice in the production of agricultural machinery, forestry equipment, and waste management systems due to its ability to withstand the rigors of harsh working conditions [5]. The use of Hardox steel offers several notable advantages that contribute to increased operational efficiency and reduced maintenance costs. The exceptional wear resistance extends the life of components, minimizing the need for frequent replacement and downtime. Hardox steel's high strength-to-weight ratio enables the design of lightweight yet durable structures, resulting in increased load-carrying capacity and fuel efficiency. In addition, the steel's weldability facilitates ease of fabrication and repair, enabling manufacturers to adapt to changing requirements without compromising on quality [4]. Hardox steel is a prime example of advanced materials engineering, offering a unique combination of properties that meet the demands of industries grappling with severe wear and impact conditions. Its exceptional hardness, toughness, and wear resistance, combined with its widespread applicability, position Hardox steel as a vital resource in modern engineering and manufacturing. As industries continue to push the boundaries of performance and durability, Hardox Steel remains a steadfast partner in the pursuit of innovation and excellence.

Surface texturing of materials has emerged as a very important area of research and application in the field of materials science and engineering. The deliberate modification of a material's surface topography at micro, nano and even atomic scales has proven to provide numerous advantageous effects that influence properties such as friction, wear, adhesion, wettability, and optical properties. This study also aims to explore the techniques used in surface texturing, explain the benefits they offer, and examine their various applications in industries.

Surface texturing encompasses a range of techniques that impart specific patterns or structures to the surface of a material [10]. These techniques can be broadly categorized as mechanical, chemical, and physical methods. Mechanical techniques include processes such as grinding, polishing, and shot peening where controlled material removal or deformation results in desired surface topographies. Chemical techniques include processes such as etching and electrochemical methods that selectively remove material and create complex surface patterns. Physical techniques, on the other hand, include laser ablation, plasma treatment, and ion beam milling, which provide precise control over surface properties at nanometer scales. These techniques can be combined or modified to achieve a variety of surface textures tailored to specific applications.

Surface texturing provides a range of benefits to materials, making it a crucial tool in optimizing performance and functionality [1]. Enhanced oil retention and reduced coefficients of friction are achieved by retaining lubricants in textured surface structures, leading to improved wear resistance and energy efficiency in tribological applications. Enhanced hydrophobic or hydrophilic behavior can be achieved through controlled texturing, impact applications on self-cleaning surfaces, antifouling paints, and microfluidics. Surface texture also plays a crucial role in controlling light interaction, finding applications in optical devices, solar panels, and sensors [13]. Furthermore, tailored surface textures can influence cell adhesion and proliferation, making it a promising avenue in biomedical implants and tissue engineering.

The range of surface texturing applications is wide and covers various industrial sectors. In automotive engineering, textured engine components reduce friction and improve fuel efficiency. Aerospace applications benefit from improved aerodynamics and reduced ice accumulation on textured surfaces. In electronics, micro- and nano-textured materials contribute to improved heat dissipation and miniaturization. Furthermore, the renewable energy field uses surface texture to optimize light absorption and energy conversion in photovoltaic cells and light-emitting diodes. Biomedical applications include implants with improved osseointegration, drug delivery systems with controlled release profiles and diagnostic devices with enhanced precision.

Surface texturing of materials has evolved into a versatile discipline with far-reaching implications across industries. The techniques used, along with the numerous benefits offered, enable the tailoring of material surfaces to achieve specific performance improvements. As the field of research and innovation continues to move forward, surface texturing will undoubtedly remain a crucial strategy for enhancing material properties, optimizing functionality, and promoting advances in a wide range of technological fields.

Laser processing has emerged as a transformative process in modern manufacturing, enabling precision material removal and surface modification with unparalleled accuracy and versatility. This academic discourse aims to provide an in-depth investigation covering the fundamental principles of laser processing, its various techniques, and its wide-ranging applications across industries. This technology has revolutionized materials processing by leveraging the unique properties of laser light, offering a new paradigm for complex and efficient manufacturing processes. Laser processing is based on the principles of focused, high-intensity laser beams interacting with materials to trigger controlled material removal or replacement. The process begins with the generation of coherent, monochromatic laser light, usually by methods such as optical amplification or stimulated emission. The laser beam is then precisely focused onto the surface of the material, leading to localized heating and vaporization, cutting, or melting. The choice of laser wavelength, pulse duration, power density, and beam characteristics determine the extent and nature of material removal, providing fine-tuned control over the processing results. Laser processing encompasses several different techniques, each tailored to specific material types, geometries, and desired results. Laser cutting involves the use of focused laser beams to cut or melt materials along predefined paths resulting in precise and burr-free cuts. Laser cutting removes material by vaporization, leaving minimal heat-affected zones, making it suitable for delicate materials or high-precision applications. Laser engraving and marking uses controlled laser pulses to engrave patterns, text, or images onto surfaces, often used for product marking, labeling or aesthetic embellishments. Laser welding and cladding use localized heating and melting to fuse or coat materials, respectively, offering advantages in joining dissimilar materials or creating wear-resistant coatings. Laser processing applications span a wide range of industries, demonstrating its adaptability and transformative impact. In the automotive sector, laser cutting enables the production of complex and lightweight components, contributing to improved fuel efficiency and vehicle performance. The electronics industry utilizes precision laser ablation in microfabrication processes that produce miniaturized circuits, sensors, and semiconductor devices. Aerospace applications include laser drilling of cooling holes in turbine blades and the creation of complex aerospace structures. In addition, the medical field utilizes laser processing for precision ablation in surgeries to improve biocompatibility, in the manufacture of medical devices, and in the surface modification of implants. Laser processing is the cornerstone of modern manufacturing, offering an exceptional blend of precision, versatility, and efficiency. Leveraging the unique properties of laser light, this technology has revolutionized material processing across a range of industries. The ability to remove, surface modify and join complex materials with micron-level precision has paved the way for innovative advances in engineering, electronics, aerospace, and healthcare. As the field of laser processing continues to evolve through research and technological innovation, the potential to shape the future of materials processing remains limitless.

In traditional experimental methodology, each variable is examined separately. During this examination, the variable to be examined is changed while other variables are kept constant. This increases

the number of experiments and the time spent on the experiments. Optimization methods, on the other hand, aim to obtain optimum parameters with fewer experiments. In this study, the optimum parameters were obtained by the Taguchi method, which has given successful results in many engineering and research fields [3].

The Taguchi method is a design and analysis method used to optimize industrial and statistical quality control processes and improve product or service quality. It was developed by Genichi Taguchi.

In product and process design, the Taguchi method aims to improve quality by making the product's performance sensitive to environmental variables (e.g. temperature, humidity, pressure) and minimizing variance. This method assesses the sensitivity of product quality to certain factors and factor levels and attempts to determine the optimal parameter settings.

One of the key concepts is "quality loss". According to Taguchi, the further a product or service deviates from the design specifications of its characteristics, the greater the loss of quality perceived by the customer. His goal is to minimize quality loss by keeping product or process performance as close as possible to the specifications. The Taguchi method differs from traditional experimental design methods. For example, the Taguchi method uses a "multifactor" experimental design that evaluates the interaction of variables, not the effect of individual variables. The Taguchi method is used especially in engineering, manufacturing and quality control and contributes to continuous quality improvement processes. This method helps to design products and processes more effectively and efficiently by providing a quality-oriented approach. The Taguchi method is a design and analysis method used to optimize industrial and statistics.

2. MATERIALS & METHODS

In this study, the CO₂ laser parameters used to create dimples of various sizes and shapes on Hardox steel plates were investigated. These dimples were produced using three different laser parameters, with the goal of obtaining varied geometries on the Hardox plates. The specific parameters used, along with their levels, are detailed in Table 1.

The ratios of the smallest value of the cavity diameter to the largest value are given in Table 4. The ratios of the smallest value of the cavity diameter to the largest value are given in Table 3.

Table 1. Laser parameters and levels used in experiments.

	Laser Exposure duration (s)	Laser Power (Watt)	Laser Frequency (kHz)
1 st level	5	60	5
2 nd level	10	90	25
3 rd level	15	120	50

Laser power was studied between 60 and 120 watts. Since no cavity formation was observed on the Hardox material at laser power values lower than 60 W in the preliminary studies, the lowest value of the power was determined as 60 W. For similar reasons, the upper limit of the exposure time was set to 5 s, since no cavity formation was observed at laser exposure duration was less than 5 s. When the laser power exceeded 120 W and the laser exposure duration was higher than 15 s, more heat deformation was observed on the Hardox material due to excessive heat transfer.

2.1. Experimental Method

In an experimental design with three parameters and three levels for each parameter, the number of experiments required is 27. Optimization methods aim to obtain optimum results with the minimum number of trials possible instead of trying every combination [2]. With the Taguchi optimization method, the closest results to the optimum result can be obtained with 9 experiments instead of 27 experiments. In addition, the Taguchi method also calculates which parameter affects the result and to what extent. To achieve this, appropriate experimental sets are prepared by designing experiments by the Taguchi method [11, 12]. Thus, both experiment time and experiment cost are saved. The experiment sets are given in Table 2.

Table 2. Experiment sets according to the Taguchi optimization Method.

	Laser exposure duration (s)	Laser Power (Watt)	Laser Frequency (kHz)
1	5	60	5
2	5	90	25
3	5	120	50
4	10	60	25
5	10	90	50
6	10	120	5
7	15	60	50
8	15	90	5
9	15	120	25

The signal-to-noise ratio (S/N) used in the Taguchi method also represents the effects of noise from uncontrollable factors. Therefore, the highest signal-to-noise ratio is a desirable outcome. According to the Taguchi method, optimization can target one of three different states. The (S/N) is calculated for these different states ([14]) as given below.

- 1) highest is the best

$$\left(\frac{S}{N}\right) = -10\log_{10} \left[\frac{1}{n} \sum_{i=1}^n y_i^2 \right] \tag{1}$$

- 2) lowest is the best

$$\left(\frac{S}{N}\right) = -10\log_{10} \left[\frac{1}{n} \sum_{i=1}^n \frac{1}{y_i^2} \right] \tag{2}$$

- 3) the nominal value (defined value) is the best

$$\left(\frac{S}{N}\right) = -10\log_{10} \left[\frac{1}{n} \sum_{i=1}^n (y_i - m)^2 \right] \tag{3}$$

The y_i value in these equations represents the measurement results for each trial. Measurements were taken at any 5 locations on the dimple to reduce possible errors. In equation (3), “m” denotes the nominal value, which means the desired value.

3. RESULTS & DISCUSSION

Figure 1 shows examples of optical microscope images of cavities obtained on Hardox plates using the laser parameters listed in Table 3. Since the laser beam is circular and the material is assumed to be theoretically homogeneous, the geometry of the dimple should be close to a perfect circle. To verify this, the maximum and minimum values of the diameters of the dimples formed on Hardox plates were measured. The ideal circularity is achieved when the minimum diameter value is as close as possible to the maximum, ideally a ratio of '1', which was considered the best value. In order to minimize the rate of experimental systematic errors, each set of experiments was repeated five times. The ratios of the smallest value of the cavity diameter to the largest value are given in Table 3.

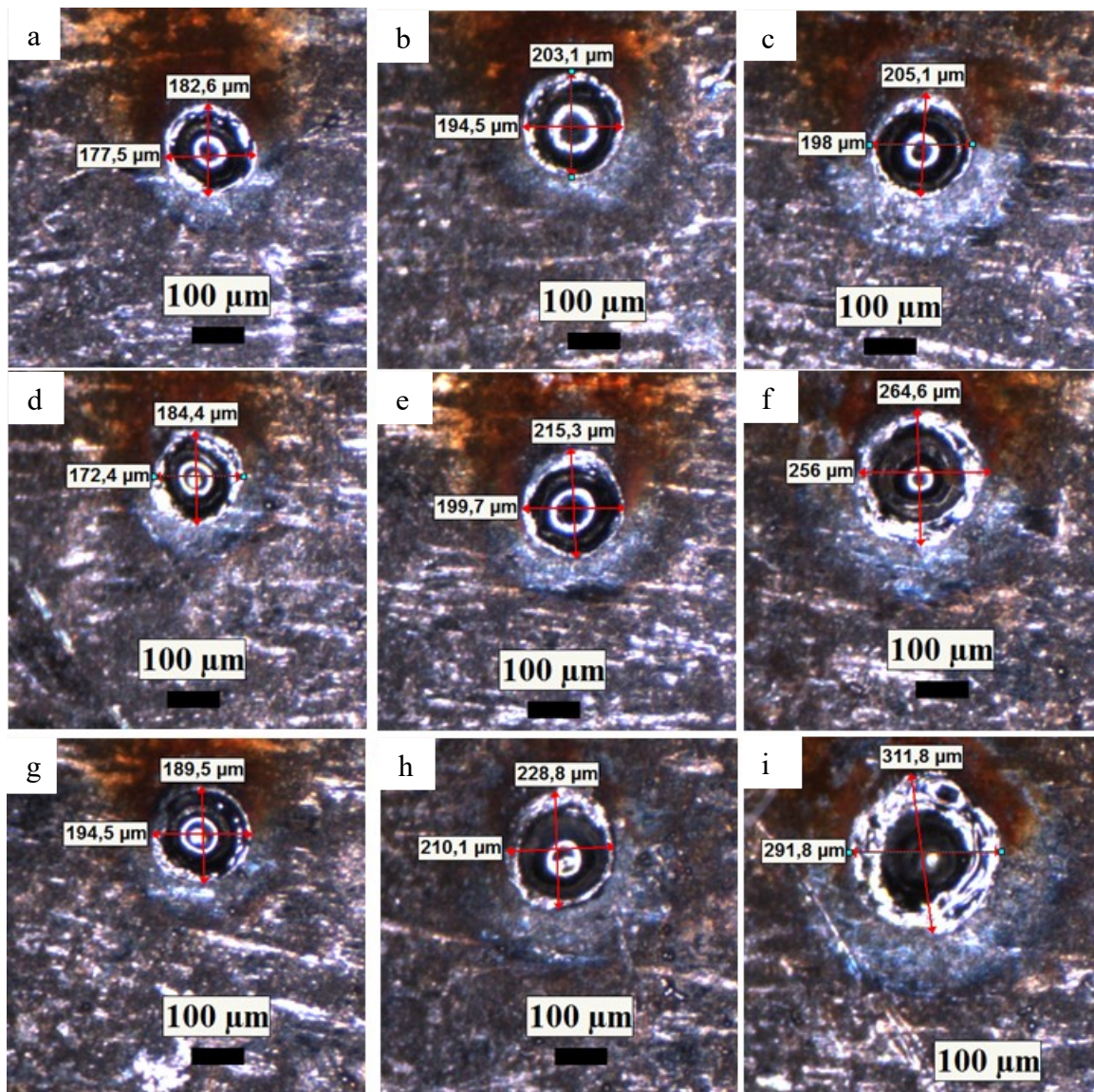


Figure 1. Optical microscope images of dimples obtained with the experimental sets in Table 2. (a) Experimental set number 1, (b) Experimental set number 2, (c) Experimental set number 3, (d) Experimental set number 4, (e) Experimental set number 5, (f) Experimental set number 6, (g) Experimental set number 7, (h) Experimental set number 8, (i) Experimental set number 9.

Since the result with the largest ratio of the minimum value of the measured cavity diameter to the maximum value is considered the best result, equation (1) was used to calculate the S/N ratio. S/N ratios calculated according to equation (1) are also given in Table 3.

Table 3. Ratios of the smallest value to the largest value of the cavity diameter and S/N values.

	1 st	2 nd	3 rd	4 th	5 th	S/N
1	0.98	0.94	0.94	0.98	0.97	-0.32
2	0.96	0.99	0.97	0.93	0.94	-0.38
3	0.99	0.96	0.98	0.97	0.90	-0.37
4	0.96	0.93	0.92	0.92	0.89	-0.67
5	0.88	0.94	0.93	0.92	0.96	-0.68
6	0.91	0.90	0.97	0.99	0.97	-0.47
7	0.95	0.98	0.97	0.98	0.93	-0.32
8	0.92	0.94	0.96	0.90	0.94	-0.64
9	0.97	0.93	0.94	0.92	0.97	-0.50

To identify the optimum parameters, an ANOVA table was prepared as shown in Table 4. This table, particularly its last column, details the optimum experimental parameters. Beyond simply identifying the optimum parameters, the Taguchi method is also capable of quantifying the impact of each parameter on the results. The sum of squares (SST) within the table represents the variance of the signal-to-noise ratio (S/N), as described by Yang and Tarng ([14]).

$$SS_T = \sum_{i=1}^n (\eta_i - \eta_m)^2 \tag{4}$$

The SS_T value is the sum of the squares of each factor ($SS_T=SS_A+SS_B+SS_C$) and it can also be obtained by equation (4).

$$SS_A = \sum_{i=1}^{k_A} n_{Ai} (\eta_{Ai} - \eta_m)^2 \tag{5}$$

Table 4 was obtained by using the data in equation (4) and the data in equation (5).

Table 4. ANOVA table for Optimum Ratio of Dimple diameter to HAZ diameter.

	Average S/N			Degree of Freedom	Effect Rate	Optimum Parameters
	1 st level	2 nd level	3 rd level			
Scan Speed (mm/s)	-0.36	-0.61	-0.49	4	71.86	50 mm/s
Power (W))	-0.44	-0.57	-0.45	4	23.02	120 W
Frequency (kHz)	-0.48	-0.52	-0.46	4	5.12	50 kHz
Total		-0.48			100	
Optimum S/N						-0.28
Optimum Ratio of Minimum Dimple diameter to HAZ diameter						0.97

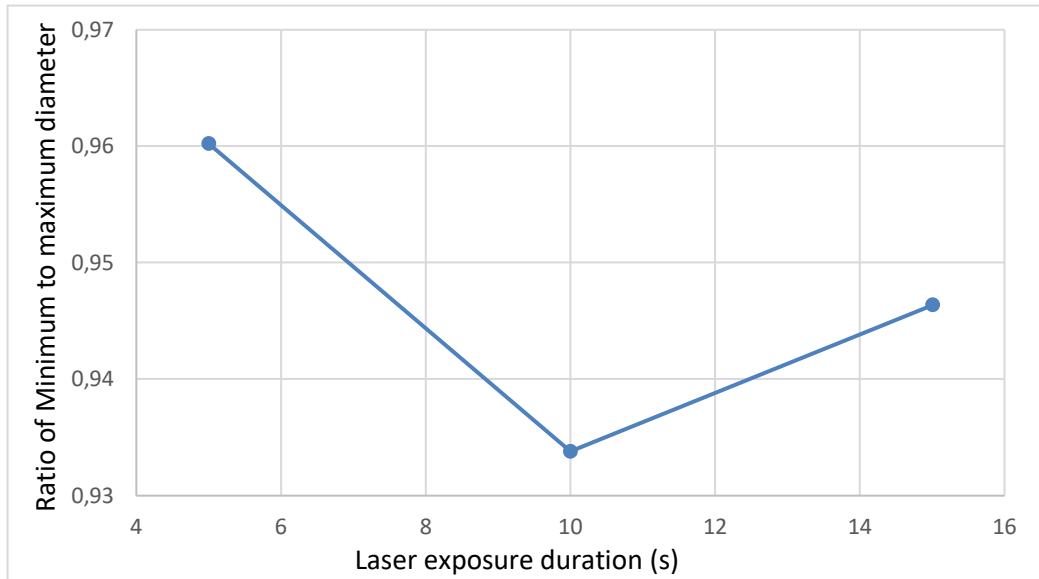


Figure 2. Main effect plot for laser power on the ratio of cavity diameter to HAZ diameter.

As shown in Figure 2, increasing the laser exposure duration from 5 seconds to 10 seconds results in a decrease in the diameter ratio. However, further increasing the duration from 10 seconds to 15 seconds leads to an increase in the width ratio, but at a slower rate than previously observed. The highest width-to-diameter ratio was recorded when the laser exposure duration was set at 5 seconds.

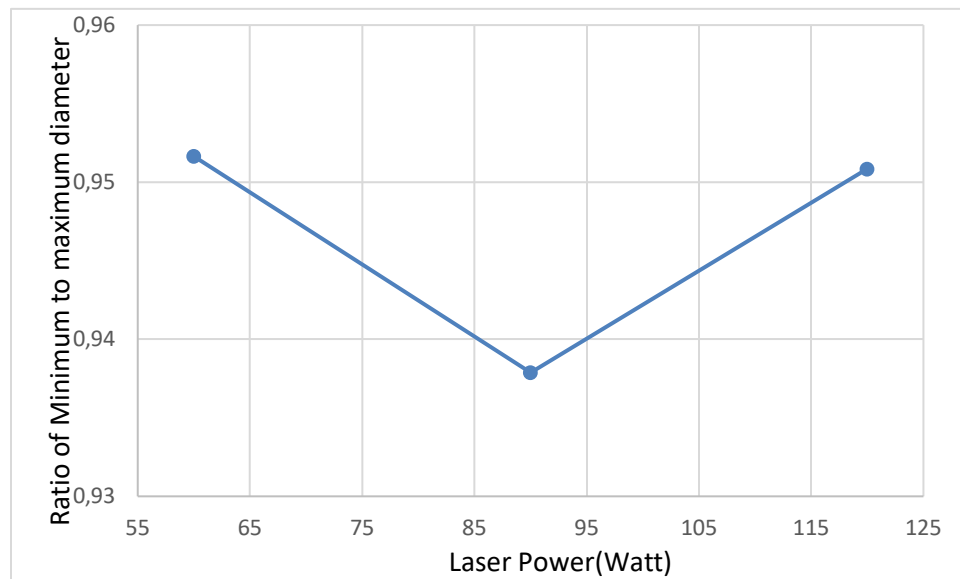


Figure 3. Main effect plot for laser power on the ratio of cavity diameter to HAZ diameter.

As seen in the Figure 3, increasing the laser power from 60 W to 90 W results in a decrease in the width ratio. Conversely, when the laser power is increased from 90 W to 120 W, the width ratio increases. The highest width ratio was observed at 60 W, but a nearly identical ratio was also reached at 120 W.

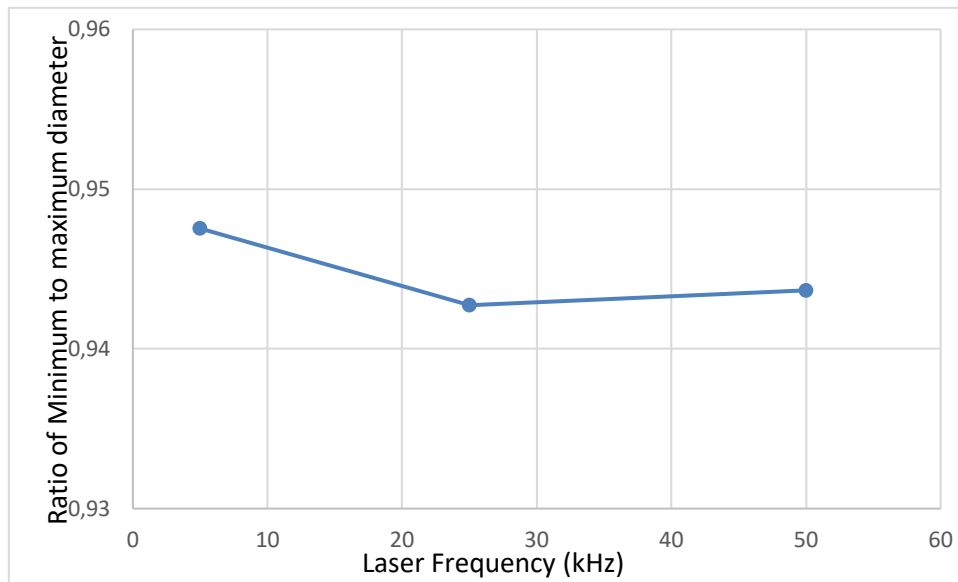


Figure 4. Main effect plot for laser frequency on the ratio of cavity diameter to HAZ diameter.

As seen in Figure 4, when the laser frequency is increased from 5 kHz to 25 kHz, the ratio of the widths decreases. However, when the frequency is increased from 25 kHz to 50 kHz, the width ratio increases. The highest ratio was observed when the frequency was 5 kHz.

4. CONCLUSION

The Taguchi method was used to optimize the largest cavity and the smallest heat-affected zone width in relation to this cavity. The optimum laser parameters were obtained as 5 s for laser exposure duration, 60 W for laser power, and 50 kHz for laser frequency.

As can be seen from the main effect plots, the ideal circularity has deviated from its optimal state at the middle values of all three parameters. Better results were observed at lower and high low and high values of the parameters compared to the middle values of the parameters. The best results can be obtained at low parameter values. However, cavity formation is not observed and becomes difficult at low values. In order to obtain deeper and circular dimples with better dimples, the laser should be applied for a longer time and the power of the applied laser beam should be high with equal quality. In addition, among the parameters analyzed in order to reach the desired result, the parameter that affected the result the most was calculated as laser exposure duration with a rate of 71,86 %. The influences of laser power and frequency on the results were comparatively lower, at 23.02% and 5.12% respectively.

5. CONFLICTS OF INTEREST

The authors declare no conflict of interest.

6. ACKNOWLEDGMENTS

The authors like to thank Sezgin Sac Ltd. Sti. for their help in providing the materials used.

REFERENCES

1. Arslan, A., Masjuki, H. H., Kalam, M. A., Varman, M., Mufti, R. A., Mosarof, M. H., Khuong, L. S., Quazi, M. M. (2016). Tribological Effect of Surface Texturing on Cutting Tool Performance: A Review, *Critical Reviews in Solid State and Materials Sciences*, 41; 448-481.
2. Canel, T., Kaya, A.U., Celik, B. (2012). Parameter optimization of nanosecond laser for microdrilling on PVC by Taguchi method, *Optics & Laser Technology*, 44; 2347–2353.
3. Canel, T., Zeren, M. Sinmazcelik, T. (2019). Laser parameters optimization of surface treating of Al 6082-T6 with Taguchi method, *Optics and Laser Technology*, 120; 105714.
4. Crouch I. G., Cimpoeru, S. J., Shanmugam D., Li, H. (2017). *Armour steels, The Science of Armour Materials* Woodhead Publishing in Materials, 55-115.
5. Khundyakov, A., Vaschennko, S., Banasiewicz, A., Wroblewski, A. (2021). Materials Selection and Design Options Analysis for a Centrifugal Fan Impeller in a Horizontal Conveyor Dryer, *Materials*, 14; 6696.
6. Konat, L. (2021). Technological, Microstructural and Strength Aspects of Welding and Post-Weld Heat Treatment of Martensitic, Wear-Resistant Hardox 600 Steel, *Materials*, 14; 4541.
7. Kuntoglu, M. (2022). Machining induced tribological investigations in sustainable milling of Hardox 500 steel: A new approach of measurement science, *Measurements*, 201; 111715.
8. Korkmaz., M. E. Gupta, M.K., Ross, N. M., Sivalingam, V., (2023). Sustainable Materials and Technologies, 36; e00641
9. Ligier, K., Zemlik, M., Lemecha, M., Konat, L., Napiorkowski, J. (2022). Analysis of Wear Properties of Hardox Steels in Different Soil Conditions, *Materials*, 15; 1-18.
10. Ramezani, M., Ripin, Z. M., Passang, T., Jiang, C. (2023). Surface Engineering of Metals: Techniques, Characterizations and Applications, *Metals*, 13; 1299.
11. Sahoo, S. K., Thirupathi, N., Saraswathamma, K. (2020). Experimental Investigation and Multi-Objective Optimization of Die sink EDM Process Parameters on Inconel-625 alloy by using Utility Function Approach, *Materials Today: Proceedings* 24; 995–1005.
12. Tarng, Y.S., Yang, W.H. (1998). Optimization of the weld bead geometry in gas tungsten arc welding by the Taguchi method, *Int. J. Adv. Manuf. Technol.* 14; 549–554.
13. Wang, W., Qi, L. (2019). Light Management with Patterned Micro- and Nanostructure Arrays for Photocatalysis, Photovoltaics, and Optoelectronic and Optical Devices, *Advanced Multifunctional Materials*, 29; 1807275.
14. Yang, W.H, Tarng Y.S. (1998). Design optimization of cutting parameters for turning operations based on the Taguchi method. *Journal of Materials Processing Technology* 164;122-129.

IDUNAS	NATURAL & APPLIED SCIENCES JOURNAL	2023 Vol. 6 No. 2 (41-48)
--------	---------------------------------------	------------------------------------

Homoderivations and Their Impact on Lie Ideals in Prime Rings

Research Article

Evrım Güven^{1*} 

¹Department of Mathematics, Kocaeli University, Kocaeli, Türkiye

Author E-mail
evrim@kocaeli.edu.tr
ORCID:0000-0001-5256-4447

*Correspondence to: Evrim Güven, Department of Mathematics, Kocaeli University, Kocaeli, Türkiye
DOI: 10.38061/idunas.1356057

Received: 06.09.2023; Accepted: 02.10.2023

Abstract

Assume we have a prime ring denoted as R , with a characteristic distinct from two. The concept of a homoderivation refers to an additive map H of a ring R that satisfies the property $H(r_1r_2) = H(r_1)r_2 + r_1H(r_2) + H(r_1)H(r_2), \forall r_1, r_2 \in R$. This article aims to obtain results for prime rings, ideals, and Lie ideals by utilizing the concept of homoderivation in conjunction with the established theory of derivations.

Keywords: Prime ring, Homoderivation, Lie ideal, Jordan ideal.

1. INTRODUCTION

Let R be a ring, with $Z(R)$ denoting its center. The commutator of r_1 and r_2 in R is denoted by $[r_1, r_2]$, while the anti-commutator is denoted by $r_1 \circ r_2 = (r_1, r_2)$. A nontrivial additive subset U within the ring R is referred to as a Lie ideal if it satisfies the condition $[U, R] \subset U$. A well-known result due to Bergen et al. (1981) is that if U is a Lie ideal of R such that $U \not\subseteq Z(R)$, then there exists an ideal I in R satisfying $[I, R] \subset U$ but $[I, R] \not\subseteq Z(R)$. Furthermore, in accordance with Sofy (2000), for any subset $A \subseteq R$, a function is $g: R \rightarrow R$ considered to preserve A if $g(A) \subseteq A$, and it is termed zero-power valued on A if it meets the criteria of preserving A , with the additional requirement that for each $a \in A$, there exists a positive integer $n(x) > 1$ such that $g^{n(x)} = 0$.

In the ring theory, derivations are additive mappings that satisfy the condition

$$D(r_1r_2) = D(r_1)r_2 + r_1D(r_2)$$

for all $r_1, r_2 \in R$.

The concept of a generalized derivation was introduced by Br̄esar ([18]) in the following manner: An additive mapping is referred to as a generalized derivation if there is a derivation ∂ such that

$$G(r_1r_2) = G(r_1)r_2 + r_1\partial(r_2)$$

for all $r_1, r_2 \in R$.

Throughout the last three decades, numerous authors have contributed to the establishment of the most fundamental theorems in ring theory by incorporating automorphisms or derivatives and proving commutation theorems for prime rings, semiprime rings, or suitable subsets. As the definition of derivation evolved, the field of study expanded to include generalized derivations, (α, β) -derivations, and semi-derivations. Recently, El Sofy proposed a new definition of homoderivations, which includes derivations as a special case [8]. By this definition,

$$h(r_1r_2) = h(r_1)h(r_2) + h(r_1)r_2 + r_1h(r_2)$$

is a homoderivation on R as additive mapping $h: R \rightarrow R$ for all $r_1, r_2 \in R$. An example of a homoderivation is $h(r) = \rho(r) - r$ for all $r \in R$, where ρ is an endomorphism on R . A recent study by Sofy showed that if $h(r)h(s) = 0$ for all $r, s \in R$, then $h = 0$, and Rehman et al. extended this result to I ideals of R [16].

In recent years, researchers have been exploring various generalizations of homoderivations on rings. One such generalization is the notion of generalized homoderivations, which extend the classical concept of homoderivations to noncommutative rings [1, 6, 14, 16]. As time progresses, one observes that generalizations of this derivative type are also beginning to be introduced [3, 7]. This paper explores implications for homoderivations of Lie ideals that have not been previously examined in the literature. Additionally, we have included some of the results obtained for ideals. Our work is motivated by several fundamental theorems in ring theory that involve automorphisms or derivatives and establish commutation theorems for prime rings, semiprime rings, or suitable subsets. Some notable inspirations for our work include ([15, 11, 12, 4]). We hope that our findings will contribute to the ongoing generalizations of the concept of homoderivations and their applications in ring theory.

2. RESULTS

In this section, we examine some basic properties using homoderivations under the conditions we assume for the ideals of the ring, and in particular for the Lie ideals.

Lemma 2.1. [5] A group cannot be represented as the union of two of its proper subgroups.

Lemma 2.2. [13] Let b and ab be in the center of a prime ring R . If b is not zero, then a is in $Z(R)$.

Lemma 2.3. [8] Let $h: R \rightarrow R$ be a homoderivation. If $h^2(R) = 0$ then $h = 0$.

Lemma 2.4. Let h_1 and h_2 be two nonzero homoderivations on R . If $h_1h_2(R) = 0$ then $h_1 = 0$ or $h_2 = 0$.

Proof. Let

$$h_1h_2(rs) = 0$$

for all $r, s \in R$. $0 = h_1(h_2(rs)) = h_1(h_2(r)s + rh_2(s) + h_2(r)h_2(s)) = h_2(r)h_1(s) + h_1(r)h_2(s)$. Hence, replacing $h_2(r)$ by r ,

$$h_2^2(r)h_1(s) = 0 \tag{1}$$

for all $r, s \in R$. By putting st instead of s , we have $h_2^2(r)sh_1(t) = 0$ for all $r, s, t \in R$. Thus,

$$h_2^2(R)Rh_1(R) = 0$$

Since R is a prime ring and from Lemma 2.3 it becomes $h_1 = 0$ or $h_2 = 0$.

Lemma 2.5. [8] Let h be a homoderivation of R . If $[h(R), a] = 0$ then $h = 0$ or $a \in Z(R)$.

Here are two apparent corollaries stemming from this lemma:

Corollary 2.6. Let h be a homoderivation of R . If $h(R) \subset Z(R)$ then $h = 0$ or R is commutative.

Corollary 2.7. Let h be a homoderivation and U be a Lie ideal of R . If $[h(R), U] = 0$ then $h = 0$ or $U \subset Z(R)$.

Lemma 2.8. [8] Assume R is a prime ring with a non-trivial two-sided ideal $I \neq (0)$. If R contains a nonzero homo derivation h that both commutes and exhibits zero power valuation on I , then R must be commutative.

Theorem 2.9. Let I and L be nonzero ideals of R . If h is a zero-power valued nonzero homoderivation on I and L such that $h(I) \subset Z(L)$ then R is commutative.

Proof. Let $h(I) \subset Z(L)$. According to this hypothesis $[h(xr), t] = 0, x \in I, t, r \in L$. Thus

$$0 = [h(x)h(r) + h(x)r + xh(r), t] = h(x)[h(r), t] + h(x)[r, t] + x[h(r), t] + [x, t]h(r) \quad (2)$$

In equation (2) replace r by t to get

$$0 = h(x)[h(t), t] + x[h(t), t] + [x, t]h(t) \quad (3)$$

Now, if we take rx instead of x in the Equation (3) equation, we find $0 = h(rx)[h(t), t] + rx[h(t), t] + [rx, t]h(t) = h(r)x[h(t), t] + rh(x)[h(t), t] + h(r)h(x)[h(t), t] + rx[h(t), t] + r[x, t]h(t) + [r, t]xh(t) = h(r)x[h(t), t] + h(r)h(x)[h(t), t] + [r, t]xh(t)$. If we choose to use t instead of r in this last equation

$$h(t)(x + h(x))[h(t), t] = 0 \quad (4)$$

Since h is zero-power valued on I , there exists an integer $n(x) > 1$ such that $h^{n(x)} = 0$, for all $x \in I$. Replacing x by $x - h(x) + h^2(x) + \dots + (-1)^{n(x)-1}h^{n(x)-1}$ in Equation (4), for all $x \in I, t \in L$

$$h(t)x[h(t), t] = 0$$

We put $K_1 = \{t \in L | h(t) = 0\}$ and $K_2 = \{t \in L | [h(t), t] = 0\}$. K_1 and K_2 both are additive subgroups of L . Through the Lemma 2.1 we arrive at $K_1 = L$ or $K_2 = L$. It is clear that if $K_1 = L$ then $h(L) = 0$. Since h is a nonzero homoderivation $[h(t), t] = 0$ for all $t \in L$ we see from Lemma 2.8 R is commutative.

Lemma 2.10. Let $h: R \rightarrow R$ be a nonzero homoderivation, a be a fixed element of R and $h(R \circ a) = 0$. Then $h(a) = 0$ or $a \in Z(R)$

Proof. Let $h(R \circ a) = 0$. Hence

$$0 = h(rs \circ a) = h(r(s \circ a) - [r, a]s)$$

for all $r, s \in R$. Replacing r by a we have $h(a)(s \circ a) = 0$. Replacing s by sx then $0 = h(a)(sx \circ a) = h(a)s[x, a]$ for all $x, s \in R$. We obtain $h(a) = 0$ or $a \in Z(R)$.

Lemma 2.11. Let $h: R \rightarrow R$ be a nonzero homoderivation and I be a nonzero ideal of R . If a and b are fixed elements of R such that $bh(I \circ a) = 0$ then $h(a) = 0$ or $b[b, a]=0$.

Proof. If $bh(I \circ a) = 0$ then $0 = bh((xa, a)) = bh((x, a)a) = b(x, a)h(a)$. From [10] $h(a) = 0$ or $b[b, a]=0$.

Lemma 2.12. Let h be a nonzero homoderivation, I be a nonzero ideal of R and μ be an automorphism of R . If a is a fixed element of R such that $h\mu(I, a) = 0$ then $a \in Z(R)$ or $h\mu(a) = 0$.

Proof. For all $x \in I$, $h\mu(xa, a) = h\mu((x, a)a) = h(\mu(x, a)\mu(a)) = h(\mu(x, a))h\mu(a) + h(\mu(x, a))\mu(a) + \mu(x, a)h\mu(a)$. So, we have $\mu(I, a)h\mu(a) = 0$. From [10], $a \in Z(R)$ or $h\mu(a) = 0$.

Lemma 2.13. Let $h: R \rightarrow R$ be a homoderivation and a be a fixed element of R . If $h([R, a]) = 0$ then $h = 0$ or $a \in Z(R)$.

Proof. If $h([R, a]) = 0$, for all $r \in R$, $h([ar, a]) = h(a)[r, a] = 0$. If we replace r with rx , $x \in R$

$$h(a)R[R, a] = 0$$

Since R is prime, we find that $a \in Z(R)$ or $h(a) = 0$. If $h(a) = 0$ then $0 = h([r, a]) = [h(r), a]$, for all $r \in R$. Thus $[h(R), a] = 0$. We obtain by Lemma 2.5 $h = 0$.

Corollary 2.14. Let $h: R \rightarrow R$ be a homoderivation and let U be a Lie ideal of R . If $h([R, U]) = 0$ then $h = 0$ or $U \subset Z(R)$.

Proof. Applying Lemma 2.13 and Corollary 2.7 sequentially makes the proof evident.

Lemma 2.15. Let $h: R \rightarrow R$ be a homoderivation. If I is a nonzero right ideal of R and for all $x \in I$, if $h(x) = x$, then $h(t) = 0$ for all $t \in R$.

Proof. By the hypothesis that for any $x \in I$, $t, s \in R$, $h(xst) = xst$, on the other hand, if we apply h homoderivation in this expression $h(xst) = h(xs)t + h(xs)h(t) + xsh(t) = xst$. Again, from our hypothesis we get $h(xs)h(t) + xsh(t) = 0$ and hence $2xsh(t) = 0$.

Since $char R \neq 2$, $xsh(t) = 0$. I is a nonzero ideal from hypothesis then $h(t) = 0$ for all $t \in R$.

Lemma 2.16. Let $h: R \rightarrow R$ be a nonzero homoderivation and let U be a Lie ideal on R . If $h(u) = u$ for all $u \in U$, then $U \subset Z(R)$.

Proof. By the hypothesis that $h(u) = u$ for all $u \in U$ we have $h([u, r]) = [u, r]$ for all $r \in R$, $u \in U$. Hence $h([u, r]) = [h(u), r] + [u, h(r)] + [h(u), h(r)] = [u, r]$. Now we get for all $r \in R$, $u \in U$

$$2[u, h(r)] = 0.$$

Since $\text{char}R \neq 2$ we have $[U, h(R)] = 0$. Hence from Corollary 2.7, $U \subset Z(R)$.

Lemma 2.17. [9] Let U be a Lie ideal of R . If $h(U) = 0$ then $h = 0$ or $U \subset Z(R)$.

Lemma 2.18. Let h be a nonzero homo derivation on R , a be a fixed element of R and θ be an automorphism on R . If $ah\theta(I) = 0$, then $a = 0$.

Proof. If $ah\theta(I) = 0$ then $0 = ah\theta(xr) = a\theta(x)h\theta(r)$. Thus $a\theta(I)h\theta(R) = 0$. Since $\theta(I)$ is a nonzero ideal of R , we obtain $a = 0$.

Theorem 2.19. Let h be a nonzero homoderivation a be a fixed element of R and let U be a noncentral Lie ideal on R . If $ah(U) = 0$ ($h(U)a = 0$) then $a = 0$.

Proof. In our hypothesis, we assumed that U is a noncentral Lie ideal. Under this assumption, there exists an $I \neq 0$ ideal in R such that $[I, R] \subset U$ but $[I, R] \not\subset Z(R)$ as stated in [4]. Thus, for all $x \in R, m \in I$, the relation $[xm, m] = [x, m]m \in U$ holds true due to $[R, I] \subset U$. Consequently, based on our hypothesis, we can conclude that

$$\begin{aligned} 0 &= ah([x, m]m) = a[x, m]h(m) = ah([x, m])h(m) = a[x, m]h(m) \\ & a[x, m]h(m) = 0. \end{aligned} \tag{5}$$

Taking here $h(u)x$ for x in Equation (5), we have

$$0 = a[h(u)x, m]h(m) = ah(u)[x, m]h(m) + a[h(u), m]xh(m)$$

for all $u \in U$, thus

$$a[h(U), m]Rh(m) = 0.$$

for all $m \in I$. Let $S_1 = \{m \in I | a[h(u), m] = 0\}$ and $S_2 = \{m \in I | h(m) = 0\}$. Utilizing Lemma 2.1, we see either $h(I) = 0$ or $a[h(U), I] = 0$. But h is a nonzero homoderivation of R we obtain

$$a[h(U), I] = 0$$

We have for all $m \in I, u \in U, a[h(u), m] = 0$. Hence, we arrive at $a = 0$ or $h(u) = 0$. By Lemma 2.17 $a = 0$ or $U \subset Z(R)$. Since $U \not\subset Z(R)$, we obtain $a = 0$.

(If the method described above is used it can also be easily shown that the same result will be obtained when $h(U)a = 0$.)

Theorem 2.20. Let $h: R \rightarrow R$ be a nonzero homoderivation and U be a noncentral Lie ideal on R . If $h(U) \subset Z(R)$, then $U \subset Z(R)$.

Proof. By Lemma 2.17 $h(U) \neq 0$. Let $r = [u, x] \in U$ for all $u \in U, x \in R$. then, $u[u, x] = ur \in U$. Thus

$$\begin{aligned} 0 &= [h(ur), y] = h(u)[r, y] + [u, y]h(r) \\ & h(u)[r, y] + [u, y]h(r) = 0 \end{aligned} \tag{6}$$

for all $u \in U, x, y \in R$. We substitute yu for y in this equation to obtain

$$h(u)[r, yu] + [u, yu]h(r) = h(u)y[r, u] + h(u)[r, y]u + [u, y]uh(r) = 0$$

for all $u \in U, x, y \in R$. Since $h(r) \in Z(R)$ using the relation Equation (6) we obtain $h(u)y[r, u] = 0$. Hence

$$h(u)R[r, u] = 0$$

for all $u \in U, x \in R (r = [u, x])$. Let $T_1 = \{u \in U | [u, x]u = 0\}$ and $T_2 = \{u \in U | h(u) = 0\}$. Through the T_1 and T_2 additive subgroups of R , from Lemma 2.1 and $h(U) \neq 0$, we arrive at

$$[[u, x], u] = 0$$

for all $u \in U$. If $U \not\subset Z(R)$ then $u \notin Z(R)$ for at least one $u \in U$. Let define a nonzero inner derivation $d_u: R \rightarrow R$ induced by u . Hence

$$d_u(d_u(x)) = [u, [u, x]] = 0$$

for all $x \in R$. That is $U \subset Z(R)$ by [17].

Example. Let $R = \left\{ \begin{bmatrix} k_1 & k_2 \\ 0 & k_3 \end{bmatrix} \mid k_1, k_2, k_3 \in \mathcal{J}, \text{ the set of integers} \right\}$ be a ring, on this case $U = \begin{bmatrix} k_1 & k_2 \\ 0 & k_1 \end{bmatrix}$ is a Lie ideal on R .

Let $a = \begin{bmatrix} 0 & 1 \\ 0 & 0 \end{bmatrix} \in R$. Defining h is follows:

$$h \begin{bmatrix} k_1 & k_2 \\ 0 & k_3 \end{bmatrix} = \begin{bmatrix} 0 & k_3 - k_1 \\ 0 & 0 \end{bmatrix}$$

It can be seen that h is a homoderivation. However, the condition of the above theorem is not satisfied. It is important that the ring is a prime.

Theorem 2.21. Let $h: R \rightarrow R$ be a nonzero homoderivation and U be a Lie ideal on R . If h preserves U and $h^2(U) = 0$ then $U \subset Z(R)$.

Proof. Assume that U is a noncentral Lie ideal on the ring R . By [4], $S = [U, U]$ is a noncentral Lie Ideal of R . If we show that $S \subset Z(R)$, we have what we want. From [4], there exists a nonzero ideal I ideal in R which satisfies the condition $[I, R] \subset U$ but at the same time $[I, R] \not\subset Z(R)$. For $m \in [I, R] \subset U \cap I$ and $u \in S$ we get $\omega = h(u) \in h(S) \subset U$. By the hypothesis $h(\omega) = 0$. Thus,

$$\begin{aligned} 0 &= h^2([m\omega, y]) = h^2(m[\omega, y] + [m, y]\omega) \\ &= h\{h(m)[\omega, y] + mh[\omega, y] + h(m)h[\omega, y] + h[m, y]\omega + [m, y]h(\omega) + h[m, y]h(\omega)\} \\ &= 2h(m)h[\omega, y] \end{aligned}$$

for all $y \in R$. Since $char R \neq 2$, for all $m \in [I, R]$ gives $h(m)h[\omega, y] = 0$.

$$h([I, R])h[\omega, y] = 0$$

for all $y \in R$. Since $[I, R]$ is a noncentral Lie ideal of R , by Lemma 2.19, we get

$$h[\omega, y] = h[h(u), y] = 0$$

for all $u \in S, y \in R$.

$$0 = h[h(u), y] = [h^2(u), y] + [h(u), h(y)] + [h^2(u), h(y)] = [h(u), h(y)]$$

and that is

$$[h(u), h(y)] = 0$$

for all $u \in S, y \in R$. By Lemma 2.5 we have $h(u) \in Z(R)$, for all $u \in S = [U, U]$. That is $S = [U, U] \subset Z(R)$. Let's remember our acceptance $U \not\subset Z(R)$. Then there exist elements a and b in U such that neither of them belongs to the center of R ($Z(R)$). Now let's define two mappings $d_a(x) = [a, x]$ and $d_b(x) = [b, x]$ in R . Since $[a, x] \in U$ $[a, x], b \in Z(R)$. $[a, x], b = [a, [x, b]] + [[a, b], x] = [a, [x, b]] \in Z(R) \in Z(R)$ and so, we have $d_a d_b(R) \subset Z(R)$. By Lee and Lee [9], we see that R is commutative. This result contradicts of $U \not\subset Z(R)$. Therefore, $U \subset Z(R)$.

Theorem 2.22. Let $h: R \rightarrow R$ be a nonzero homoderivation and U be a Lie ideal of R . If $[U, h(U)] \subset Z(R)$, then $U \subset Z(R)$.

Proof: Let v be an element of U . For all $u \in U$ we have $[u, h(v)] \in Z(R)$. Thus

$$0 = [[u, h(v)], r] = [u, [h(v), r]] + [[u, r], h(v)] \in Z(R)$$

for all $r \in R$. Hence $[u, [h(v), r]] \in Z(R)$. For two inner derivations $d_1(x) = [u, x]$ and $d_2(x) = [h(v), x]$ by u and $h(v)$ of R , we have $d_1 d_2(x) = [u, [h(v), x]] \in Z(R)$ for all $x \in R$. That is by [2] $d_1 = 0$ or $d_2 = 0$. Hence Theorem 2.20 yields that $U \subset Z(R)$.

4. CONCLUSION

In this article, algebraic identities are obtained, including homoderivations on prime rings. We also examine algebraic identities involving homoderivations for an ideal of the prime ring or the Lie ideal. We establish that the Lie ideal, conforming to the identities elaborated upon in this section, resides within the core of the prime ring. In future studies, the hypotheses in this study can be examined using homoderivations of the prime ring and Jordan ideals.

5. CONFLICTS OF INTEREST

The authors declare no conflict of interest.

REFERENCES

1. Alharfie E. F., Muthana N. M. (2018). The commutativity of prime rings with homoderivations, *Int. J. of Adv. and App. Sci.*, 5(5), 79-81.
2. Awtar R. (1984). Lie ideals and Jordan derivations of prime rings, *Proc. Amer. Math. Soc.*, 90, 1, 9-14.
3. Atteya M. J. (2022). Homogeneralized (σ, τ) -Derivations of Associative Rings, *Studies on Scientific Developments in Geometry, Algebra, and Applied Mathematics*, 52.
4. Bergen J., Herstein I. N., Kerr J. (1981). Lie Ideals and derivations of Prime Rings, *Journal of Algebra*, 71, 259-267.
5. Divinsky N. (1965). *Rings and Radicals*, University of Toronto Press, Toronto.
6. Ebrahimi M. M., Pajooohesh H. (2003). Inner derivations and homoderivations on \mathfrak{q} -Rings, *Acta Math. Hungar.*, 100, 157-165.
7. El-Soufi M. M. and Ghareeb A. (2022). Centrally Extended α -Homoderivations on Prime and Semiprime Rings, *Journal of Mathematics*.
8. El Sofy, M. M. (2000). Rings with some kinds of mappings, M.Sc. Thesis, Cairo University, Branch of Fayoum, Egypt.
9. Engin A., Aydın, N. (2023). Homoderivations in Prime Rings, *Journal of New Theory*, 43, 23-24.
10. Güven E. (2019). Some Results on Left (σ, τ) -Jordan Ideals and one sided Generalized Derivations, *TWMS J. App. and Eng. Math.*, 9, 1, 22-29.
11. Herstein, I.N. (1979). A Note On Derivations II, *Canad. Math. Bull.*, 22 (4), 509-511.
12. Lee P. H., Lee T.K., (1981). On Derivations of Prime Rings *Chinese Journal of Mathematics*, 9, 2, 107-110.
13. Mayne, J. H. (1984). Centralizing Mappings of Prime Rings, *Canadian Mathematical Bulletin* 27 (1), 122--126.
14. Mouhssine S. and Boua A. (2021). Homoderivations and Semigroup Ideals in 3-Prime Near-Rings, *Algebraic Str. and Their App.* 8, No. 2, 177-194.
15. Posner E. C. (1957). Derivations in prime rings, *Proc. Amer. Math. Soc.* 8, 1093-1100.
16. Rehman N., Mozumder M. R., Abbasi A. (2019). Homoderivations on ideals of prime and semiprime rings, *The Aligarh Bull. of Math.*, 38-1, 77-87.
17. Aydın N., Kaya K. (1992). Some Generalizations in Prime Rings with (σ, τ) -Derivation, *Doğa-Tr. J. Mathematics*, 16, 169-176.
18. Bresar M. (1991). On the distance of the composition of two derivations to the generalized derivations, *Glasgow Math. J.*, 33, 89-93.

IDUNAS	NATURAL & APPLIED SCIENCES JOURNAL	2023 Vol. 6 No. 2 (49-60)
--------	---------------------------------------	------------------------------------

Determination of the CO₂ Laser Parameters on Dimple Geometry on Al₂O₃ Ceramic Surface

Research Article

Çağla Pilavcı^{1,4*}, Satılmış Ürgün^{3*}, Yasemin Tabak^{2*}, Timur Canel^{4*}

¹TUBITAK Marmara Research Center Life Sciences, Kocaeli, Türkiye

²TUBITAK Marmara Research Center Material Technologies, Kocaeli, Türkiye

³Faculty of Aeronautics and Astronautics, Department of Aviation Electrics and Electronics, Kocaeli University, Kocaeli, Türkiye.

⁴Department of Physics, Faculty of Arts and Science, Kocaeli University, 41380, Kocaeli, Türkiye

Author E-mails:

cagla.pilavci@gmail.com

urgun@kocaeli.edu.tr

yasemin.tabak@tubitak.gov.tr

tcanel@kocaeli.edu.tr

Ç. Pilavcı ORCID ID: 0009-0005-5237-9598

S. Ürgün ORCID ID: 0000-0003-3889-6909

Y. Tabak ORCID ID: 0000-0002-4912-8828

T. Canel ORCID ID: 0000-0002-4282-1806

*Correspondence to: Çağla Pilavcı, TUBITAK Marmara Research Center Life Sciences, Kocaeli, Türkiye

DOI: 10.38061/idunas.1363477

Received: 20.09.2023; Accepted: 06.12.2023

Abstract

Dimples on Al₂O₃ ceramic plates were created with a CO₂ laser using different laser parameters. The effects of the laser parameters used on the dimple geometry were investigated and the necessary laser parameters were optimized to obtain the desired dimple geometry. Taguchi method was used in the optimization process. The effects of laser power, scan speed and laser frequency from laser parameters were investigated. Optimum laser parameters were determined as a result of the Taguchi Optimization method. In addition, the laser parameter with the highest effect on the result was determined. Optimum laser parameters were obtained as 60 W for laser power, 35 s for laser exposure duration and 50 kHz for laser frequency.

Keywords: Al₂O₃, Ceramics, Optimization, Laser texturing, Laser parameters.

1. INTRODUCTION

Aluminum oxide, commonly known as Al₂O₃, is a versatile ceramic material with a wide range of applications in various industries (Sarkar et al., 2004). Its unique combination of exceptional mechanical, thermal, and electrical properties make it an ideal choice for numerous high-performance applications. Al₂O₃ ceramics are characterized by their high hardness, excellent wear resistance, and outstanding

corrosion resistance, making them suitable for use in harsh environments where other materials might fail. These ceramics are composed of a stable crystal structure, primarily consisting of corundum, which contributes to their remarkable stability and robustness.

One of the most notable properties of Al_2O_3 ceramics is their exceptional thermal resistance. With a melting point of approximately 2050°C , Al_2O_3 exhibits remarkable thermal stability, making it an ideal material for high-temperature applications. Additionally, its low thermal expansion coefficient ensures minimal dimensional changes under varying temperatures, reducing the risk of thermal stress-induced failures. As a result, Al_2O_3 ceramics find extensive use in industries, such as aerospace, metallurgy, and manufacturing, where high-temperature processes and demanding thermal conditions are prevalent [37].

Apart from its exceptional mechanical and thermal properties, Al_2O_3 ceramics possess excellent dielectric and insulating characteristics [48]. This makes them highly desirable for electronic and electrical applications, including semiconductor packaging, high-power electrical insulators, and substrates for microelectronics. Their ability to withstand high voltages and resist electrical breakdown allows for efficient and reliable operation in demanding electrical environments. Moreover, Al_2O_3 ceramics can be tailored for specific electrical properties through dopants, offering engineers and researchers a degree of flexibility in designing electronic components.

In the biomedical field, Al_2O_3 ceramics have garnered considerable attention for their biocompatibility and bio-inertness. When used as medical implants or prosthetics, Al_2O_3 ceramics exhibit excellent resistance to chemical reactions with body fluids and tissues, ensuring minimal adverse reactions. Furthermore, their high strength and wear resistance make them suitable for load-bearing applications in orthopedics and dentistry [34]. The biocompatibility, combined with the material's inert nature, contributes to its widespread use in hip joint replacements, dental implants, and other medical devices.

Despite the numerous advantages, Al_2O_3 ceramics do present some challenges in their fabrication and processing. The material's high hardness can make shaping and machining difficult, requiring specialized manufacturing techniques, such as diamond grinding or laser cutting. Additionally, the inherent brittleness of ceramics poses concerns for their fracture toughness, which must be carefully considered in structural applications subjected to impact or dynamic loading [5]. Researchers continue to explore various techniques, including sintering additives and advanced processing methods, to enhance the fracture toughness and overall mechanical performance of Al_2O_3 ceramics.

In conclusion, Al_2O_3 ceramics stand as a remarkable class of materials with diverse applications across numerous industries. Their exceptional properties, including high hardness, thermal stability, electrical insulation, and biocompatibility, make them indispensable in a wide range of critical applications. As researchers and engineers push the boundaries of material science, continued advancements in processing techniques and material design hold the promise of unlocking even more potential for Al_2O_3 ceramics in the future.

Laser surface texturing is a cutting-edge technique used to modify the surface topography of materials through controlled laser ablation [24]. This involves the precise application of laser energy to create micro or nano-scale patterns, roughness, or features on the surface. The fundamental principle behind laser surface texturing lies in the interaction of the laser beam with the material, which leads to localized melting, vaporization, or solid-state phase changes. The resulting surface textures offer a myriad of advantages, including improved tribological properties, enhanced wettability, reduced friction, and tailored optical characteristics. As a versatile and non-contact method, laser surface texturing has gained widespread attention in various industries, from automotive and aerospace to biomedical and energy sectors.

One of the key benefits of laser surface texturing is its ability to tailor surface properties based on specific requirements. By adjusting laser parameters, such as pulse duration, energy density, and spot size, engineers can precisely control the depth, shape, and spatial distribution of the textured features. For instance, in the automotive industry, laser texturing has been applied to engine cylinder walls to create specific patterns that improve oil retention and reduce friction, leading to enhanced fuel efficiency and

reduced emissions [9, 40]. In the field of microfluidics, laser-textured channels have been utilized to control fluid flow and optimize mixing, offering novel solutions for lab-on-a-chip devices and microreactors.

The influence of laser wavelength and material characteristics on the surface texturing process cannot be overlooked. Different materials exhibit varying responses to laser energy, affecting the ablation mechanism and resulting surface features. Metals, ceramics, polymers, and even transparent materials can be textured using lasers with appropriate wavelengths and pulse characteristics[30]. Moreover, advances in ultrafast laser technology have enabled the creation of sub-wavelength surface structures, leading to unique optical properties, such as antireflection and light-trapping effects. These developments have opened up exciting possibilities for photovoltaic applications and laser-induced periodic surface structures (LIPSS) in photonics.

However, challenges remain in the widespread adoption of laser surface texturing. The process demands precise control and stability of laser parameters to achieve consistent and repeatable results. Additionally, the high-power laser systems required for certain applications can be costly, limiting accessibility for some industries. Furthermore, the impact of laser-induced heat on the material's mechanical properties and potential surface damage necessitates a comprehensive understanding of the material's response to laser energy. To address these concerns, ongoing research efforts are focused on optimizing laser texturing techniques, developing cost-effective systems, and investigating new materials suitable for laser texturing.

In conclusion, laser surface texturing has emerged as a powerful tool for surface modification, offering a wide range of possibilities for improving material performance and tailoring surface characteristics to meet specific application requirements. From enhancing the efficiency of mechanical systems to revolutionizing optical devices and microfluidics, the versatility of laser surface texturing holds significant promise for various industrial sectors. As research continues to advance, and technology becomes more accessible, the field of laser surface texturing is likely to witness even greater innovation and integration into diverse fields of science and engineering.

Surface patterns play a crucial role in determining the mechanical and tribological properties of materials [43]. By altering the topographical features at the micro and nano scales, surface patterns can significantly affect the friction, wear resistance, and mechanical behavior of materials. The interaction between contacting surfaces is governed by these surface patterns, and their influence is of particular importance in engineering applications where reducing friction and wear is essential for improving the overall performance and lifespan of components. Understanding the relationship between surface patterns and mechanical/tribological properties is pivotal for tailoring materials to meet specific functional requirements across various industries.

The topographical characteristics of a surface pattern directly influence its mechanical properties. The presence of micro-scale asperities, such as surface roughness, can enhance the interlocking between contacting surfaces, increasing the load-bearing capacity and overall strength of the material. In contrast, nano-scale surface patterns, nanoindentations, or nanocavities, can introduce stress concentration sites, affecting the material's fracture toughness and fatigue resistance. Additionally, the distribution and arrangement of surface patterns significantly impact the contact area and stress distribution during loading, which in turn affects the material's deformation behavior, hardness, and elastic modulus.

Surface patterns also exert a profound influence on the tribological properties of materials, especially in sliding and rolling contact scenarios. The creation of specific surface textures can reduce friction and wear rates by promoting the formation of a lubricating film, trapping wear debris, or facilitating hydrodynamic lubrication [13]. In some cases, laser-textured surfaces with controlled roughness have shown improved boundary lubrication properties, leading to reduced friction and enhanced wear resistance. Moreover, the presence of well-defined surface patterns can alter the coefficient of friction and wear mechanisms, allowing for tailored solutions based on specific application requirements.

The effect of surface patterns on mechanical and tribological properties is highly dependent on the material's composition and the nature of the applied loads. For example, in metal alloys, surface patterns

can lead to strain-hardening effects, where localized plastic deformation strengthens the material near the surface. However, in brittle materials like ceramics, surface patterns can exacerbate crack initiation and propagation, leading to reduced wear resistance. Understanding the trade-offs and limitations associated with different surface patterns is crucial for selecting the most appropriate texture for a given application.

In conclusion, surface patterns play a vital role in determining materials' mechanical and tribological properties. Their influence extends to various aspects, such as load-bearing capacity, friction, wear resistance, and deformation behavior. By carefully designing and controlling surface patterns, engineers can tailor the properties of materials to achieve desired outcomes in specific applications. The optimization of surface patterns holds significant potential for improving the efficiency and reliability of engineering systems, making it a topic of ongoing research and exploration in the fields of material science and surface engineering.

In this study, laser beams with different laser power and different exposure time were sent on the Al_2O_3 ceramic surface. Images of the cavities were taken with a high-resolution microscope to examine the effect of laser power and the effect of laser exposure time on the cavity sizes. Cavity sizes were measured using the images obtained.

Optimization methods are mathematical and computational methods that aim to find the best or non-worst values of an objective function under certain constraints. In general, optimization methods attempt to optimize an objective function (usually a maximum or minimum) by adjusting the values of variables in a given problem. Such methods are used in many different fields and disciplines, such as Engineering, Economics, Data Mining and Machine Learning, Transport and Logistics, Energy Management, and Healthcare, in addition to scientific research. Optimization methods may include different types of techniques, usually mathematical algorithms, heuristics, or meta-heuristics. These methods may require different approaches depending on the nature, size, and complexity of the problem. The most widely used optimization algorithms include gradient-based methods, genetic algorithms, simulation-based optimization, surface response methodology, etc.

The Taguchi Method, developed by Dr. Genichi Taguchi, is a reliable method for designing experiments and optimizing parameters, which is widely used in engineering and scientific studies. This method, which is a product of statistical science, provides a systematic approach to optimize multi-parameter systems. The main objective of the Taguchi Method is to optimize a smaller number of parameters.

In the Taguchi Method, one of the three basic elements is the controllable factors called "signal", i.e. parameters. The second is the so-called "noise", which is uncontrollable, i.e. undesirable. The third element is what is aimed as a result of the experiments. Although the objective is usually a numerical value, in some cases it may be a non-numerical parameter. In the Taguchi method, the parameter is numerical and orthogonal arrays are designed according to the number of levels of each parameter. According to these orthogonal arrays, experimental sets and the number of experiments are determined. The Taguchi method not only minimizes the time and resources required for the experiment but also ensures the robustness and reliability of the results obtained. The optimization process involves maximizing the S/N ratio to improve the desired characteristics of the system while minimizing sensitivity to noise factors.

2. MATERIALS & METHODS

In this study, dimples were formed using a CO_2 laser on 10 mm thick Al_2O_3 ceramic plates prepared at TUBITAK Marmara Research Center. The wavelength of the CO_2 laser used is 10600 μ and the maximum power is 130 watts. The effects of laser power and laser exposure time on the dimple geometry were investigated. Laser beams with different laser power and different frequency were sent at different times on Al_2O_3 ceramic plates. The levels of the analyzed parameters are given in Table 1.

Table 1. Parameters and Levels.

	1 st level	2 nd level	3 th level
Power (W)	40	80	120
Exposure Time (s)	5	20	35
Frequency (kHz)	5	25	50

In experiments with classical experimental designs, $3^3=27$ experiments are required to examine the effect of each parameter on the result. Taguchi method offers different solutions, such as the relationship between parameters or which parameter is more effective, as well as obtaining the same result with fewer experiments. By performing fewer experiments, both the material used, and time are saved.

According to Taguchi, experimental design, the optimum parameter levels can be determined by using the L_9 orthogonal index. Experimental sets designed according to the L_9 orthogonal index are given in Table 2.

Table 2. Parameter and Levels.

Parameters → Exp. Sets ↓	Power (W)	Time (s)	Frequency (kHz)
1	30	5	5
2	30	20	25
3	30	35	50
4	60	5	25
5	60	20	50
6	60	35	5
7	90	5	50
8	90	20	5
9	90	35	25

When the laser power was less than 30 W, no cavity formation was observed on the ceramic material. When the laser power was greater than 90 W, uncontrollable deformation occurred due to overheating. Similarly, cavity formation was not observed at low power values when the laser exposure time was less than 5 seconds. When the laser exposure time was 35 seconds, excessive thermal deformation occurred due to the excessive amount of energy transferred to the material. When the frequency was more than 50 kHz, the frequency was limited to 50 kHz since no visible difference could be obtained.

With the 3 parameters used and 3 levels of each of these parameters, 27 experiments should be done with classical test methods. However, with the Taguchi optimization method, the same result can be obtained with 9 experiments and 1 confirmation experiment with a total of 9 experiments.

According to the Taguchi method, the target must be defined first. There can be three different targets. There is a separate calculation method for each target. These; quality in Taguchi Design of Experiment method the criterion used in measuring and evaluating the characteristics is the ratio of signal (S) to noise factor (N). The signal value is the value given by the system and desired to be measured. The real value and the noise factor are the measured values. Represents the share of undesirable factors in it does. Experiments in calculating the signal/noise ratio and the quality value targeted to be achieved as a result feature is also important. There are three important categories;

1) Larger the Better

$$S/N_i = -10 \log_{10} \left[\frac{1}{n} \sum_{i=1}^n \frac{1}{y_i^2} \right] \quad (1)$$

2) Smaller the Better

$$S/N_i = -10 \log_{10} \left[\frac{1}{n} \sum_{i=1}^n y_i^2 \right] \quad (2)$$

3) Nominal the Best

$$S/N_i = -10 \log_{10} \left[\frac{1}{n} \sum_{i=1}^n (y_i - m)^2 \right] \quad (3)$$

In these equations, n is the number of trials, y_i is the measurement result, and m is the target value. The Taguchi method suggests an L_9 orthogonal array for 3 parameters and 3 levels. Experimental sets according to the L_9 orthogonal index are given in Table 2.

3. RESULTS & DISCUSSION

Figure 1 shows the micro-sized dimples obtained with each set of experiments. The cavity diameters and Heat Affected Zone diameters of the dimples were measured using the images obtained. The ratio of the diameters of the dimples to the HAZ diameters was considered to be the best. In other words, the aim of this experiment is to have the highest ratio of the cavity size to the HAZ size when the Heat Affected Zone size is compared with the cavity size. Accordingly, "Larger the better" characteristic was used when calculating the S/N ratio. In order to minimize the error rate in the experiments, 3 repetitions of each set of experiments were performed. The measurement results, calculated ratios, and S/N ratios obtained using these ratios are given in Table 3.

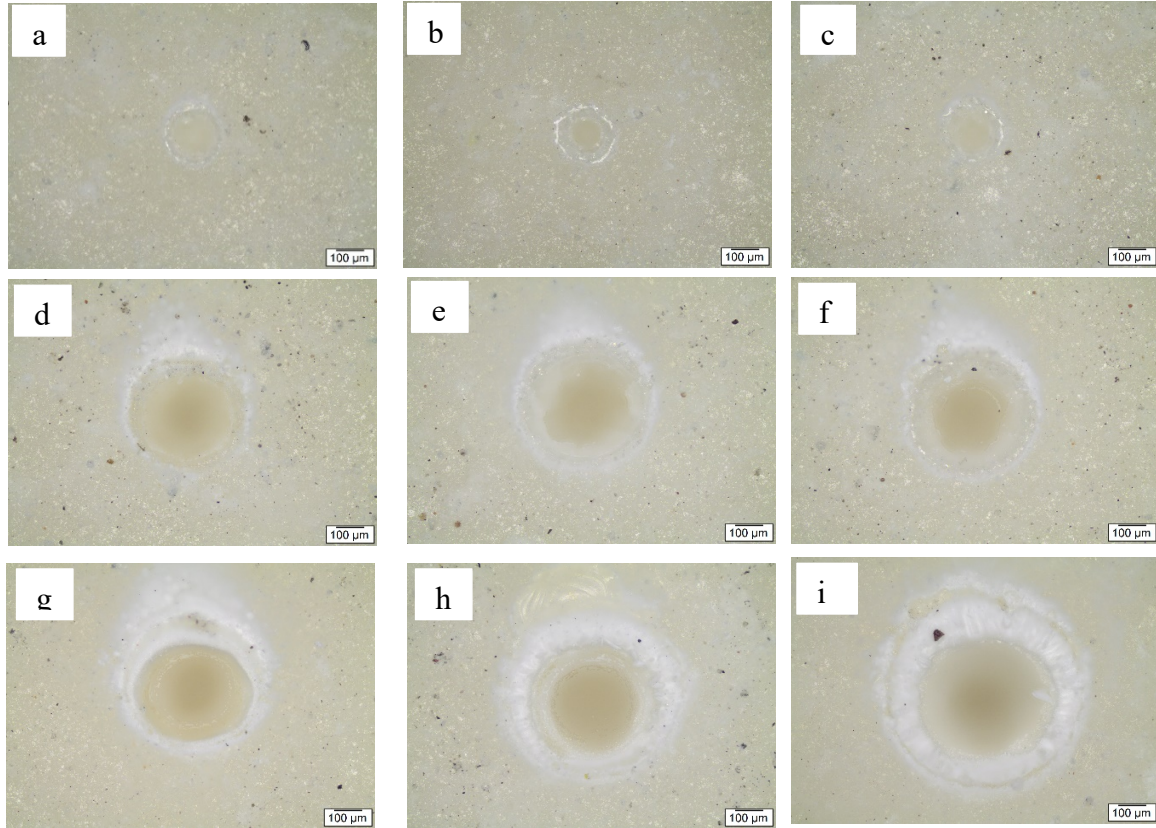


Figure 1. Optical microscope images of dimples obtained with the experimental sets in Table 2. (a) Experimental set number 1, (b) Experimental set number 2, (c) Experimental set number 3, (d) Experimental set number 4, (e) Experimental set number 5, (f) Experimental set number 6, (g) Experimental set number 7, (h) Experimental set number 8, (i) Experimental set number 9.

Table 3. Size ratios of three measurements with calculated S/N ratios. Cavity diameter to HAZ diameter Ratio of Dimple.

	1 st	2 nd	3 rd	S/N
1	0,54	0,70	0,74	-3,86
2	0,57	0,50	0,68	-4,87
3	0,68	0,68	0,57	-3,87
4	0,74	0,71	0,67	-3,06
5	0,70	0,74	0,75	-2,70
6	0,66	0,73	0,67	-3,29
7	0,65	0,65	0,68	-3,58
8	0,90	0,59	0,72	-3,03
9	0,68	0,70	0,82	-2,79

In addition to finding the optimum parameters, the Taguchi method can also calculate how much the parameters used affect the result. The sum of squares (SST) indicates the variance of S/N [3].

$$SS_T = \sum_{i=1}^n (\eta_i - \eta_m)^2 \tag{4}$$

The SST value is actually the sum of the squares of each factor ($SS_T=SS_A+SS_B+SS_C$), and it can also be obtained by equation (4) as

$$SS_A = \sum_{i=1}^{k_A} n_{Ai}(\eta_{Ai} - \eta_m)^2 \tag{5}$$

Table 4 was obtained by using the data in Table 3, equation (4) and equation (5).

Table 4. ANOVA table for Optimum Ratio of Dimple diameter to HAZ diameter.

	Average S/N			Degree of Freedom	Effect Rate	Optimum Parameters
	1 st level	2 nd level	3 rd level			
Power (W)	-4,20	-3,02	-3,13	2	94,44	60 W
Exposure Time (s)	-3,50	-3,53	-3,32	2	2,93	35 s
Frequency (kHz)	-3,39	-3,58	-3,38	2	2,63	50 kHz
Total		-3,45			100	
Optimum S/N						-2,82
Optimum Ratio of Dimple diameter to HAZ diameter						0,72

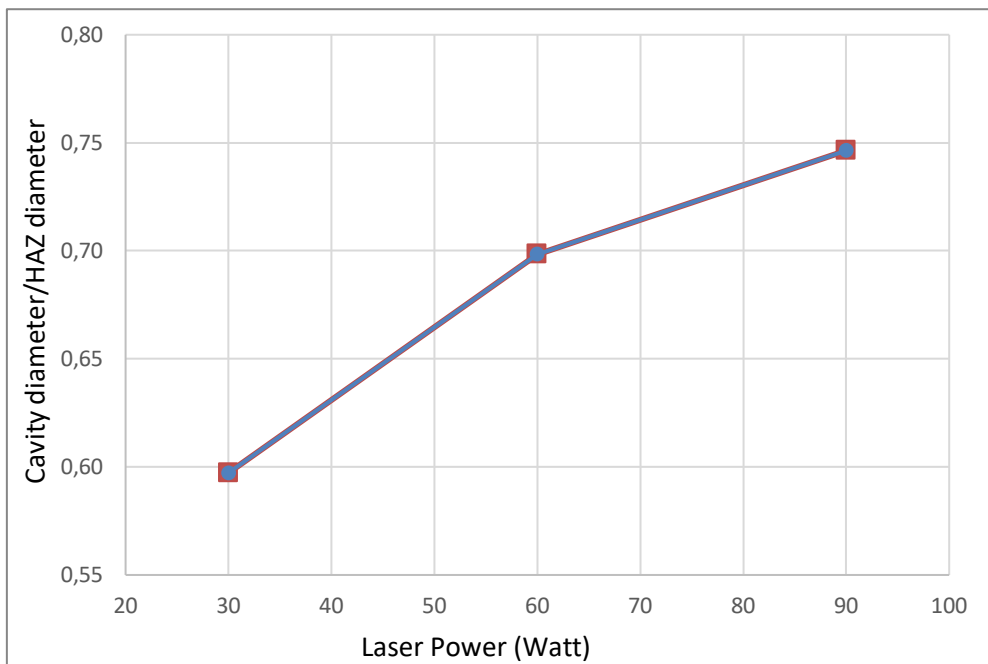


Figure 2. Main effect plot for laser power on the ratio of cavity diameter to HAZ diameter.

As can be seen in the Main effect plot for laser power, when the laser power is increased from 30 W to 60 W, the ratio of widths increases. However, when the speed was increased from 60 W to 90 W, the width ratio also increased but slower than the previous stage. The highest ratio was observed when the laser power was 90 W.

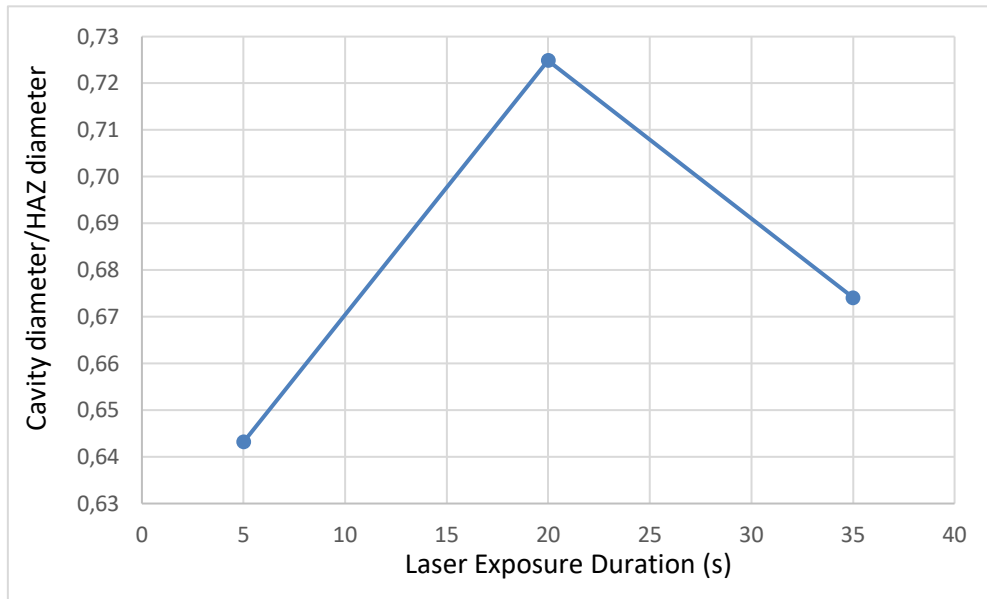


Figure 3. Main effect plot for laser exposure duration on the ratio of cavity diameter to HAZ diameter.

As seen in the Main effect plot for Laser exposure duration, when the Laser exposure duration is increased from 5 s to 20 s, the ratio of widths increases. However, when the Laser exposure duration is increased from 20 s to 35 s, the ratio of widths decreases. The highest ratio was observed when the Laser exposure duration was 20 s.

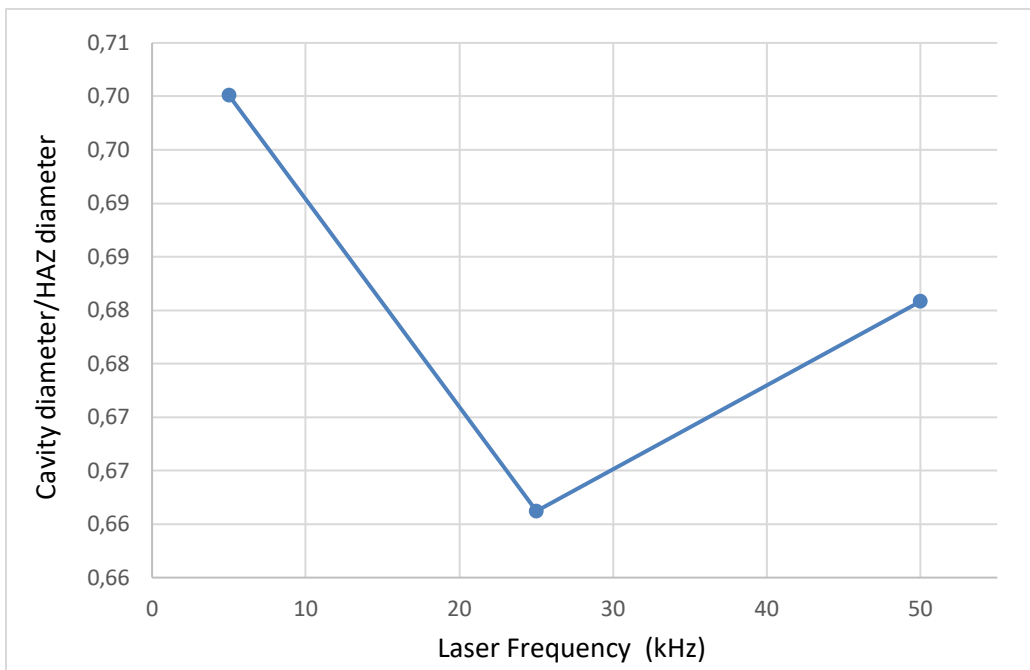


Figure 4. Main effect plot for laser frequency on the ratio of cavity diameter to HAZ diameter.

As seen in the Main effect plot for laser frequency, when the laser frequency is increased from 5 kHz to 25 kHz, the ratio of the widths decreases. However, when the frequency is increased from 25 kHz to 50 kHz, the width ratio increases. The highest ratio was observed when the frequency was 5 kHz.

4. CONCLUSION

The Taguchi method was applied to achieve two objectives: optimizing the size of the largest possible cavity and minimizing the width of the heat-affected zone adjacent to this cavity. Optimum laser parameters were obtained as 60 W for laser power, 35 s for laser exposure duration, and 50 kHz for laser frequency. In addition, among the parameters analyzed in order to reach the desired result, the parameter that affected the result the most was calculated as laser power with a rate of 94.44%. The rate of laser exposure duration and laser frequency affecting the result is quite low. Laser exposure duration and laser frequency affected the result by 2.93% and 2.63% respectively.

REFERENCES

- Alhassan, I., Gashua, A. G., Sunday, D. O. G. O., & Mahmud, S. A. N. I. (2018). Physical properties and organic matter content of the soils of Bade in Yobe State, Nigeria. *International Journal of Agriculture Environment and Food Sciences*, 2(4), 160-163.
- Arshad, M. A., Lowery, B., & Grossman, B. (1997). Physical tests for monitoring soil quality. *Methods for assessing soil quality*, 49, 123-141.5.
- Bhatt, R. (2019). Importance of Soil Texture. (retrieved from <https://www.scribd.com> on 30 December 2019)
- Canel, T., Kaya, A. U., & Celik, B. (2012). Parameter optimization of nanosecond laser for microdrilling on PVC by Taguchi method. *Optics & Laser Technology*, 44(8), 2347-2353.
- Chaudhari, P. R., Ahire, D. V., Ahire, V. D., Chkravarty, M., & Maity, S. (2013). Soil bulk density as related to soil texture, organic matter content and available total nutrients of Coimbatore soil. *International Journal of Scientific and Research Publications*, 3(2), 1-8.
- Chu, B., Liu, Q., Liu, L., Lai, X., & Mei, H. (2020). A Rate-Dependent Peridynamic Model for the Dynamic Behavior of Ceramic Materials. *CMES-Computer Modeling in Engineering & Sciences*, 124(1).
- Dawaki, U. M., Dikko, A. U., Noma, S. S., & Aliyu, U. (2013). Heavy metals and physicochemical properties of soils in Kano urban agricultural lands. *Nigerian Journal of Basic and Applied Sciences*, 21(3), 239-246.
- Deckers, S., Dondeyne, S., Vandekerckhoven, L., & Raes, D. (1995). Major soils and their formation in the West-African Sahel. *Irrigated rice in the Sahel: Prospects for sustainable development*, 23-35.
- EPA, U. (2002). Supplemental guidance for developing soil screening levels for superfund sites, Appendix A—Generic SSLs for the residential and commercial/industrial scenarios. Washington DC: Office of Emergency and Remedial Response, United States Environmental Protection Agency, 9355-4.
- Erdemir, A. (2005). Review of engineered tribological interfaces for improved boundary lubrication. *Tribology International*, 38(3), 249-256.
- Estefan, G. (2013). Methods of soil, plant, and water analysis: a manual for the West Asia and North Africa region.
- Eswaran, H., Lal, R., & Reich, P. F. (2001). Land degradation: an overview. Responses to Land Degradation. In Proc. 2nd International Conference on Land Degradation and Desertification. Khon Kaen, Thailand, edited by E. Bridges, I. Hannam, L. Oldeman, F. Penning de Vries, S. Scherr, and S. Sompatpanit. New Delhi: Oxford Press.
- FAO/WHO. (2001). Food additives and contaminants. Joint Codex Alimentarius Commission. FAO/WHO Food Standards Programme, ALINORM 01/12A.
- Gachot, C., Rosenkranz, A., Hsu, S. M., & Costa, H. L. (2017). A critical assessment of surface





- texturing for friction and wear improvement. *Wear*, 372, 21-41.
14. Hengl, T., Leenaars, J. G., Shepherd, K. D., Walsh, M. G., Heuvelink, G. B., Mamo, T., ... & Kwabena, N. A. (2017). Soil nutrient maps of Sub-Saharan Africa: assessment of soil nutrient content at 250 m spatial resolution using machine learning. *Nutrient Cycling in Agroecosystems*, 109, 77-102.
15. Horneck, D. A., Sullivan, D. M., Owen, J. S., & Hart, J. M. (2011). *Soil test interpretation guide*.
16. Hunt, N., & Gilkes, R. (1992). *Farm Monitoring Handbook—A practical down-to-earth manual for farmers and other land users*. University of Western Australia: Nedlands, WA, and Land Management Society: Como, WA.
17. Ibrahim, A. K., Usman, A., Abubakar, B., & Aminu, U. H. (2011). Extractable micronutrients status in relation to other soil properties in Billiri Local Government Area. *Journal of Soil Science and Environmental Management*, 3(10), 282-285.
18. Idera, F., Omotola, O., Adedayo, A., & Paul, U. J. (2015). Comparison of acid mixtures using conventional wet digestion methods for determination of heavy metals in fish tissues. *J. Sci. Res. Rep*, 8(7), 1-9.
19. Kabata-Pendias, A. (2000). *Trace elements in soils and plants*. CRC press.
20. Kihara, J., Bolo, P., Kinyua, M., Rurinda, J., & Piikki, K. (2020). Micronutrient deficiencies in African soils and the human nutritional nexus: opportunities with staple crops. *Environmental Geochemistry and Health*, 42, 3015-3033.
20. Lal, R. (2006). *Encyclopedia of Soil Science*. Taylor and Francis, Florida, USA.
21. Lavado, R. S., & Porcelli, C. A. (2000). Contents and main fractions of trace elements in Typic Argiudolls of the Argentinean Pampas. *Chemical Speciation & Bioavailability*, 12(2), 67-70.
22. Liu, G., Simonne, E. H., & Li, Y. (2011). Nickel nutrition in plants. *IFAS Extension University of Florida*, 6.
23. Ma, Y., & Hooda, P. S. (2010). Chromium, nickel and cobalt. *Trace elements in soils*, 461-479.
24. Mao, B., Siddaiah, A., Liao, Y., & Menezes, P. L. (2020). Laser surface texturing and related techniques for enhancing tribological performance of engineering materials: A review. *Journal of Manufacturing Processes*, 53, 153-173.
25. McKenzie, N. N., Jacquier, D. D., Isbell, R. R., & Brown, K. K. (2004). *Australian soils and landscapes: an illustrated compendium*. CSIRO publishing.
26. Mulima, I. M., Shafiu, M., Ismaila, M., & Benisheikh, K. M. (2015). Status and Distribution of Some Available Micronutrients in Sudan and Sahel Savanna Agro-Ecological Zones of Yobe State, Nigeria. *Journal of Environmental Issues and Agriculture in Developing Countries*, 7(1), 18.
27. Mustapha, S., Voncir, N., Umar, S., & Abdulhamid, N. A. (2011). Status and Distribution of some Available Micronutrients in the Haplic usferts of Akko Local Government Area, Gombe State, Nigeria. *International Journal of Soil Science*, 6(4), 267.
28. Negasa, T., Ketema, H., Legesse, A., Sisay, M., & Temesgen, H. (2017). Variation in soil properties under different land use types managed by smallholder farmers along the toposequence in southern Ethiopia. *Geoderma*, 290, 40-50.
30. Obilor, A. F., Pacella, M., Wilson, A., & Silberschmidt, V. V. (2022). Micro-texturing of polymer surfaces using lasers: A review. *The International Journal of Advanced Manufacturing Technology*, 120(1-2), 103-135.
31. Ogundele, D. T., Adio, A. A., & Oludele, O. E. (2015). Heavy metal concentrations in plants and soil along heavy traffic roads in North Central Nigeria. *Journal of Environmental & Analytical Toxicology*, 5(6), 1.

32. Oluwadare, D. A., Voncir, N., Mustapha, S., & Mohammed, G. U. (2013). Evaluation and enhancement of available micronutrients status of cultivated soil of Nigeria guinea savanna using organic and inorganic amendments. *IOSR Journal of Agriculture and Veterinary Science*, 3(5), 62-68.
33. Oyinlola, E. Y., & Chude, V. O. (2010). Status of available micronutrients of the basement complex rock-derived alfisols in northern Nigeria savanna. *Tropical and subtropical Agroecosystems*, 12(2), 229-237. *Tropical and Subtropical Agroecosystems*, 12(2):229-237.
34. Patel, N. R., & Gohil, P. P. (2012). A review on biomaterials: scope, applications & human anatomy significance. *Int. J. Emerg. Technol. Adv. Eng*, 2(4), 91-101.
35. R Core Team, A., & R Core Team. (2022). R: A language and environment for statistical computing. R Foundation for Statistical Computing, Vienna, Austria. 2012.
36. Sarkar, P., De, D., & Rho, H. (2004). Synthesis and microstructural manipulation of ceramics by electrophoretic deposition. *Journal of Materials Science*, 39, 819-823.
37. Shukla, U. C., & Gupta, B. L. (1975). Response to Mn application and evaluation of chemical extractants to determine available Mn in some arid brown soils of Haryana (India). *Journal of the Indian Society of Soil Science (India)*.
38. Singh, L., Sehgal, S., & Kuldeep, K. S. (2021). Behavior of Al₂O₃ in aluminum matrix composites: An overview. In *E3S Web of Conferences* (Vol. 309, p. 01028). EDP Sciences.
39. Srivastava, J. P., English, J. C., & Lal, R. (1993). *Conserving soil moisture and fertility in the warm seasonally dry tropics*. Washington, DC: World Bank.
40. Sundararajan, G., Joshi, S. V., & Krishna, L. R. (2016). Engineered surfaces for automotive engine and power train components. *Current opinion in chemical engineering*, 11, 1-6.
41. Tabi, F. O., & Ogunkunle, A. O. (2007). Spatial variation of some soil physico-chemical properties of an Alfisol in Southwestern Nigeria. *Nigerian Journal of Soil and Environmental Research*, 7, 82-91.
42. Tabor, N. J., Myers, T. S., & Michel, L. A. (2017). *Sedimentologist's guide for recognition, description, and classification of paleosols. In Terrestrial depositional systems* (pp. 165-208). Elsevier.
43. Tichy, J. A., & Meyer, D. M. (2000). Review of solid mechanics in tribology. *International Journal of Solids and Structures*, 37(1-2), 391-400.
44. Tilahun, G. (2007). Soil fertility status as influenced by different land uses in Maybar areas of South Wello Zone, North Ethiopia. Haramaya University, Ethiopia.
45. Ufot, U. O., Iren, O. B., & Chikere Njoku, C. U. (2016). Effects of land use on soil physical and chemical properties in Akokwa area of Imo State, Nigeria. *International Journal of Life Sciences Scientific Research*, 2(3), 273-278.
46. Weil, R. R. and Brady, N. C. (2017). *Nature and Properties of Soils*, 15th edition. Pearson Education, Inc. Delhi, India.
47. Yusuff, R. O., & Sonibare, J. A. (2004). Characterization of textile industries' effluents in Kaduna, Nigeria and pollution implications. *Global nest: the int. J*, 6(3), 212-221.
48. Zha, J. W., Dang, Z. M., Li, W. K., Zhu, Y. H., & Chen, G. (2014). Effect of micro-Si₃N₄-nano-Al₂O₃ co-filled particles on thermal conductivity, dielectric and mechanical properties of silicone rubber composites. *IEEE Transactions on Dielectrics and Electrical Insulation*, 21(4), 1989-1996.

IDUNAS	NATURAL & APPLIED SCIENCES JOURNAL	2023 Vol. 6 No. 2 (61-69)
---------------	---	------------------------------------

A Generalization of The Prime Radicals of Rings

Research Article

Didem Karalarlıoğlu Camcı^{1*} , Didem Yeşil² , Rasie Mekera³ , Çetin Camcı⁴ 

^{1,2,3,4}Department of Mathematics, Çanakkale Onsekiz Mart University, Çanakkale, Türkiye.

Author E-mails:

didemk@comu.edu.tr

dyesil@comu.edu.tr

rasiemekera@gmail.com

ccamci@comu.edu.tr

D. K. Camcı ORCID ID: 0000-0002-8413-3753

D. Yeşil ORCID ID: 0000-0003-0666-9410

R. Mekera ORCID ID: 0000-0002-0092-2991

Ç. Camcı ORCID ID: 0000-0002-0122-559X

*Correspondence to: Didem Karalarlıoğlu Camcı, Department of Mathematics, Çanakkale Onsekiz Mart University, Çanakkale, Türkiye.

DOI: 10.38061/idunas.1401075

Received: 06.12.2023; Accepted: 18.12.2023

Abstract

Let R be a ring, I be an ideal of R and \sqrt{I} be a prime radical of I . This study generalizes the prime radical of \sqrt{I} which denotes by ${}^{n+1}\sqrt{I}$, for $n \in \mathbb{Z}^+$. This generalization is called the n -prime radical of ideal I . Moreover, this paper demonstrates that R is isomorphic to a subdirect sum of ring H_i where H_i are n -prime rings. Furthermore, two open problems are presented.

Keywords: Prime ring, Prime ideal, Semiprime ideal, Prime radical.

1. INTRODUCTION

Let R be a ring and I be an ideal of R . The prime radical of the ideal I is

$$\sqrt{I} = \{r \in R : \text{for every } m - \text{system } M \text{ containing } r, M \cap I \neq \emptyset\}$$

and the radical of ring R is also defined as $\beta(R) = \sqrt{0}$ [11].

The reason for studying radicals is that a ring R is isomorphic to a subdirect sum of prime rings if and only if $\beta(R) = (0)$ [11]. Due to this feature, problems in rings can be transferred to prime rings by using the prime radical of a ring.

In generalizing the classical notion of the radical in a ring, different kinds of radicals have been defined by many authors, including Köthe [8], Baer [5], Levitzki [9], Jacobson [7], Brown-McCoy [6], Azumaya [4] and McCoy [10]. Moreover, different generalizations of the prime radical have also been tried to be accomplished [13], [12].

This study constructs a different generalization of the prime radical which is represented by ${}^{n+1}\sqrt{I}$ and analyzes the properties of ${}^{n+1}\sqrt{I}$. It also attempts to characterize the n -radical of a ring and denoted it by $\beta^n(R)$.

2. BASIC CONCEPTS AND NOTIONS

The current section provides the following basic definitions in [1, 11].

Definition 2.1. Let R be a ring and I be a semigroup ideal of R . If $aRb \subset I$ implies $a \in I$ or $b \in I$, then I is called a semigroup prime ideal.

Definition 2.2. Let I be an ideal of ring R . If $aRb \subset I$ implies $a \in I$ or $b \in I$, then I is called a prime ideal.

Definition 2.3. Let I be a semigroup ideal of ring R . I is called a semigroup semiprime ideal, if $aRa \subset I$ implies $a \in I$.

Definition 2.4. Let I be an ideal of ring R . I is called semiprime ideal, if $aRa \subset I$ implies $a \in I$.

Definition 2.5. [3] Let R be a ring and $\emptyset \neq I$ be an ideal of R . In [1], the set $\mathcal{L}_R(I)$ is defined as follows:

$$\mathcal{L}_R(I) = \{a \in R : aRa \subset I\}$$

Motivated by this set,

$$\mathcal{L}_R^n(I) = \{a \in R : aRa \subset \mathcal{L}_R^{n-1}(I), n \in \mathbb{N}\}$$

Definition 2.6. [3] Let I be an ideal of ring R . I is called an n -prime ideal if $\mathcal{L}_R^n(I)$ is a semigroup prime ideal.

Definition 2.7. [3] Let I be an ideal of ring R . I is called an n -semiprime ideal if $\mathcal{L}_R^n(I)$ is a semigroup semiprime ideal.

Definition 2.8. [3] R is called an n -prime ring if $\mathcal{L}_R^n(0)$ is a semigroup prime ideal.

Definition 2.9. [3] R is called an n -semiprime ring if $\mathcal{L}_R^n(0)$ is a semigroup semiprime ideal.

3. A GENERALIZATION OF THE PRIME RADICAL

Key definitions and notations essential for the generalization of radicals are presented below.

Notation 1. Let I be a semigroup semiprime ideal. Then, from [3], $\mathcal{L}_R^n(I) = I$. Accordingly,

$$A^n(I) = \{J \subset R : J \text{ semigroup ideal and } \mathcal{L}_R^n(J) = I\} \tag{1}$$

is not an empty set because of $I \in A^n(I)$.

Lemma 3.1. Let J and \bar{J} be two ideals of ring R . Then, $\mathcal{L}_R^n(J \cap \bar{J}) = \mathcal{L}_R^n(J) \cap \mathcal{L}_R^n(\bar{J})$.

Proof. Since $\mathcal{L}_R^0(J) = J$ and $\mathcal{L}_R^0(\bar{J}) = \bar{J}$, for $n = 0$, the proof is obtained evidently. Let $n = 1$. If $x \in \mathcal{L}_R(J) \cap \mathcal{L}_R(\bar{J})$, then $xrx \in \mathcal{L}_R^0(J) = J$ and $xrx \in \mathcal{L}_R^0(\bar{J}) = \bar{J}$, for all $r \in R$. Hence, $xrx \in J \cap \bar{J} = \mathcal{L}_R^0(J \cap \bar{J})$. Therefore, $x \in \mathcal{L}_R(J \cap \bar{J})$. Accordingly, $\mathcal{L}_R(J) \cap \mathcal{L}_R(\bar{J}) \subseteq \mathcal{L}_R(J \cap \bar{J})$. Conversely, if $x \in \mathcal{L}_R(J \cap \bar{J})$, then $xrx \in J \cap \bar{J} = \mathcal{L}_R^0(J \cap \bar{J})$. From here, $xrx \in \mathcal{L}_R^0(J) = J$ and $xrx \in \mathcal{L}_R^0(\bar{J}) = \bar{J}$, for all $r \in R$. This means $x \in \mathcal{L}_R(J) \cap \mathcal{L}_R(\bar{J})$. Consequently, $\mathcal{L}_R(J \cap \bar{J}) \subseteq \mathcal{L}_R(J) \cap \mathcal{L}_R(\bar{J})$. Assume that

$$\mathcal{L}_R^n(J \cap \bar{J}) = \mathcal{L}_R^n(J) \cap \mathcal{L}_R^n(\bar{J})$$

for an arbitrary $n \in \mathbb{N}$.

Let $x \in \mathcal{L}_R^{n+1}(J) \cap \mathcal{L}_R^{n+1}(\bar{J})$. Then, $xrx \in \mathcal{L}_R^n(J)$ and $xrx \in \mathcal{L}_R^n(\bar{J})$, for all $r \in R$. Therefore, $xrx \in \mathcal{L}_R^n(J) \cap \mathcal{L}_R^n(\bar{J})$ for all $r \in R$. From here, $xrx \in \mathcal{L}_R^n(J \cap \bar{J})$. As a result, $x \in \mathcal{L}_R^{n+1}(J \cap \bar{J})$. Thus, $\mathcal{L}_R^{n+1}(J) \cap \mathcal{L}_R^{n+1}(\bar{J}) \subseteq \mathcal{L}_R^{n+1}(J \cap \bar{J})$. The converse is similar. Hence, $\mathcal{L}_R^{n+1}(J \cap \bar{J}) = \mathcal{L}_R^{n+1}(J) \cap \mathcal{L}_R^{n+1}(\bar{J})$.

Corollary 3.2. $\{J_i\}_{i \in \Lambda}$ is a set of ideals of ring R . Then, $\mathcal{L}_R^n(\bigcap_{i \in \Lambda} J_i) = \bigcap_{i \in \Lambda} \mathcal{L}_R^n(J_i)$.

Proof. The proof is evident from induction.

Theorem 3.3. Let I be a semigroup semiprime ideal. $J \cap \bar{J} \in A^n(I)$, for every $J, \bar{J} \in A^n(I)$.

Proof. If $J, \bar{J} \in A^n(I)$, then $\mathcal{L}_R^n(J) = \mathcal{L}_R^n(\bar{J}) = I$. From Lemma 3.1,

$$I = \mathcal{L}_R^n(J) \cap \mathcal{L}_R^n(\bar{J}) = \mathcal{L}_R^n(J \cap \bar{J})$$

Then, $J \cap \bar{J} \in A^n(I)$.

Lemma 3.4. Let I be a semigroup semiprime ideal of ring R . Then, $A^n(I) \subset A^{n+1}(I)$, for all $n \in \mathbb{N}$.

Proof. Let $J \in A^n(I)$. Thus, $\mathcal{L}_R^{n+1}(J) = \mathcal{L}_R(\mathcal{L}_R^n(J)) = \mathcal{L}_R(I) = I$. Therefore, $J \in A^{n+1}(I)$ and $A^n(I) \subset A^{n+1}(I)$.

Notation 2. Let I_α be a semigroup semiprime ideal, for all $\alpha \in \Lambda$. Consider the set

$$\left\{ J = \bigcap_{\alpha \in \Lambda} J_\alpha : J_\alpha \in A^n(I_\alpha), \alpha \in \Lambda \right\}$$

From Notation 1, since $I_\alpha \in A^n(I_\alpha)$, for all $\alpha \in \Lambda$, then $\bigcap_{\alpha \in \Lambda} I_\alpha$ is an element of this set. Let's symbolize this set with $\overline{\bigcap_{\alpha \in \Lambda} A^n(I_\alpha)}$.

Theorem 3.5. Let I_α be a semigroup semiprime ideal, for all $\alpha \in \Lambda$. Then,

$$\overline{\bigcap_{\alpha \in \Lambda} A^n(I_\alpha)} \subset A^n\left(\bigcap_{\alpha \in \Lambda} I_\alpha\right)$$

Proof. Let $J \in \overline{\bigcap_{\alpha \in \Lambda} A^n(I_\alpha)}$. Then, $J = \bigcap_{\alpha \in \Lambda} J_\alpha$ where $J_\alpha \in A^n(I_\alpha)$, for all $\alpha \in \Lambda$. Hence, from Corollary 3.2,

$$\mathcal{L}_R^n(J) = \mathcal{L}_R^n\left(\bigcap_{\alpha \in \Lambda} J_\alpha\right) = \bigcap_{\alpha \in \Lambda} \mathcal{L}_R^n(J_\alpha) = \bigcap_{\alpha \in \Lambda} I_\alpha$$

Accordingly, $J \in A^n(\bigcap_{\alpha \in \Lambda} I_\alpha)$.

Example 1. Let $(F, +, \cdot)$ be a field and $R = \left\{ \begin{pmatrix} a & b & c \\ 0 & d & e \\ 0 & 0 & 0 \end{pmatrix} : a, b, c, d, e \in F \right\}$ be a ring.

$$I_1 = \left\{ \begin{pmatrix} a & b & c \\ 0 & 0 & e \\ 0 & 0 & 0 \end{pmatrix} : a, b, c, e \in F \right\}, I_2 = \left\{ \begin{pmatrix} 0 & b & c \\ 0 & d & e \\ 0 & 0 & 0 \end{pmatrix} : b, c, d, e \in F \right\},$$

$$I_3 = \left\{ \begin{pmatrix} a & b & c \\ 0 & 0 & 0 \\ 0 & 0 & 0 \end{pmatrix} : a, b, c \in F \right\}, I_4 = \left\{ \begin{pmatrix} 0 & b & c \\ 0 & 0 & d \\ 0 & 0 & 0 \end{pmatrix} : b, c, d \in F \right\},$$

$$I_5 = \left\{ \begin{pmatrix} 0 & b & c \\ 0 & 0 & 0 \\ 0 & 0 & 0 \end{pmatrix} : b, c \in F \right\}, I_6 = \left\{ \begin{pmatrix} 0 & 0 & c \\ 0 & 0 & d \\ 0 & 0 & 0 \end{pmatrix} : c, d \in F \right\} \text{ and}$$

$$I_7 = \left\{ \begin{pmatrix} 0 & 0 & c \\ 0 & 0 & 0 \\ 0 & 0 & 0 \end{pmatrix} : c \in F \right\} \text{ are semigroup semiprime ideals of } R. \text{ From here,}$$

$\mathcal{L}_R(I_1) = I_1, \mathcal{L}_R(I_2) = I_4, \mathcal{L}_R(I_3) = I_1, \mathcal{L}_R(I_4) = I_4, \mathcal{L}_R(I_5) = I_4, \mathcal{L}_R(I_6) = I_4, \mathcal{L}_R(I_7) = I_4$ and $\mathcal{L}_R(0) = I_5 \cup I_6$. Besides that, I_1 and I_2 are prime ideals. Moreover, $I_1 \cap I_2 = I_4$ is a semiprime ideal. Thus, $A(I_1) = \{I_1\}$ and $A(I_2) = \{I_2, I_3\}$.

Consider with $\Lambda = \{1, 2\}$, $\overline{\bigcap_{\alpha \in \Lambda} A(I_\alpha)} = \{I_4, I_5\}$.

Because of $\bigcap_{\alpha \in \Lambda} I_\alpha = I_1 \cap I_2 = I_4$,

$$A\left(\bigcap_{\alpha \in \Lambda} I_\alpha\right) = \{I_4, I_5, I_6, I_7\}$$

is provided.
Therefore,

$$\overline{\bigcap_{\alpha \in \Lambda} A(I_\alpha)} \subset A\left(\bigcap_{\alpha \in \Lambda} I_\alpha\right).$$

Notation 3. Let I be a semigroup semiprime ideal. Then,

$$\mathcal{L}_R^{-n}(I) = \bigcap_{J \in A^n(I)} J.$$

Theorem 3.6. If I is a semigroup semiprime ideal, then $\mathcal{L}_R^{-n}(I) \in A^n(I)$.

Proof. Let I be a semigroup semiprime ideal.

$$\mathcal{L}_R^n(\mathcal{L}_R^{-n}(I)) = \mathcal{L}_R^n\left(\bigcap_{J \in A^n(I)} J\right) = \bigcap_{J \in A^n(I)} \mathcal{L}_R^n(J) = I$$

Hence, $\mathcal{L}_R^{-n}(I) \in A^n(I)$. Since I is a semigroup semiprime ideal, $\mathcal{L}_R^{-n}(I) \in A^n(I)$. Therefore, $\mathcal{L}_R^{-n}(I) \subset J$ for all $J \in A^n(I)$.

Definition 3.7. If I is a semigroup semiprime ideal of R , then $\mathcal{L}_R^{-n}(I)$ is called an n -minimal semigroup semiprime ideal of $A^n(I)$.

Lemma 3.8. [3] Let R and S be two rings and $\varphi: R \rightarrow S$ be an endomorphism and P be an ideal with $\text{Ker}\varphi = K \subset P$. If P is a n -semiprime ideal of ring R , then $\varphi(P)$ is a n -semiprime ideal of ring R .

Lemma 3.9. [3] Let R and S be two rings and $\varphi: R \rightarrow S$ be an endomorphism and P be an ideal with $\text{Ker}\varphi = K \subset P$. If P is a n -prime ideal of ring R , then $\varphi(P)$ is a n -prime ideal of ring R .

Theorem 3.10. Let I_α be a semigroup semiprime ideal, for all $\alpha \in \Lambda$. Then,

$$\mathcal{L}_R^{-n}\left(\bigcap_{\alpha \in \Lambda} I_\alpha\right) \subset \bigcap_{\alpha \in \Lambda} \mathcal{L}_R^{-n}(I_\alpha)$$

Proof. From Theorem 3.5,

$$\mathcal{L}_R^{-n}\left(\bigcap_{\alpha \in \Lambda} I_\alpha\right) = \bigcap_{J \in A^n(\bigcap_{\alpha \in \Lambda} I_\alpha)} J \subset \bigcap_{J \in \overline{\bigcap_{\alpha \in \Lambda} A^n(I_\alpha)}} J.$$

Therefore,

$$\bigcap_{J \in \overline{\bigcap_{\alpha \in \Lambda} A^n(I_\alpha)}} J = \bigcap_{\alpha \in \Lambda} \mathcal{L}_R^{-n}(I_\alpha).$$

Example 2. Adopting the Example 1,

$$\mathcal{L}_R^{-1}(I_1) = \bigcap_{J \in A(I_1)} J = I_2,$$

$$\mathcal{L}_R^{-1}(I_2) = \bigcap_{J \in A(I_2)} J = I_5,$$

$$\bigcap_{\alpha \in \Lambda} \mathcal{L}_R^{-1}(I_\alpha) = \mathcal{L}_R^{-1}(I_1) \cap \mathcal{L}_R^{-1}(I_2) = I_5$$

and

$$\mathcal{L}_R^{-1}\left(\bigcap_{\alpha \in \Lambda} I_\alpha\right) = \mathcal{L}_R^{-1}(I_1 \cap I_2) = I_7.$$

Therefore,

$$\mathcal{L}_R^{-1}\left(\bigcap_{\alpha \in \Lambda} I_\alpha\right) = I_7 \subset I_5 = \bigcap_{\alpha \in \Lambda} \mathcal{L}_R^{-1}(I_\alpha).$$

This means that equality may not be achieved.

Definition 3.11. Let I be an ideal of ring R and \sqrt{I} be the prime radical of I . Then, the n -prime radical of I is characterized as

$${}^{n+1}\sqrt{I} = \mathcal{L}_R^{-(n-1)}(\sqrt{I}), \quad \text{for } n \in \mathbb{Z}^+$$

where 1-prime radical of I is equivalent to $\sqrt{I} = \mathcal{L}_R^0(\sqrt{I})$. Moreover, the n -prime radical of ring R can be defined as n -radical of the ring

$$\beta^n(R) = {}^{n+1}\sqrt{(0)}$$

where $n \geq 1$, $n \in \mathbb{N}$, and 1-radical of ring R is equivalent to $\beta(R)$.

Theorem 3.12. Let I be an ideal of ring R . Then,

$${}^{n+1}\sqrt{I} \subset {}^n\sqrt{I}$$

for $n \in \{2, 3, \dots\}$.

Proof. Let I be an ideal of R . Then, from Lemma 3.2, $A^{n-1}(\sqrt{I}) \subset A^n(\sqrt{I})$. Accordingly,

$${}^{n+1}\sqrt{I} = \mathcal{L}_R^{-(n-1)}(\sqrt{I}) = \bigcap_{J \in A^{n-1}(\sqrt{I})} J \subset \bigcap_{J' \in A^n(\sqrt{I})} J' = \mathcal{L}_R^{-(n)}(\sqrt{I}) = {}^n\sqrt{I}.$$

Corollary 3.13. Let I be an ideal of ring R . Then,

$$\dots \subset {}^{n+1}\sqrt{I} \subset {}^n\sqrt{I} \subset \dots \subset \sqrt[4]{I} \subset \sqrt[3]{I} \subset \sqrt{I} \subset I$$

Proof. The proof is obvious from induction.

Corollary 3.14. Let I be an ideal of ring R . Then,

$${}^{n+1}\sqrt{I} = \bigcap_{I \subset P, P \text{ prime}} \mathcal{L}_R^{-(n-1)}(P).$$

Proof. $\sqrt{I} = \bigcap_{I \subset P, P \text{ prime}} P$. Then,

$${}^{n+1}\sqrt{I} = \mathcal{L}_R^{-(n-1)}(\sqrt{I}) = \mathcal{L}_R^{-(n-1)}\left(\bigcap_{I \subset P, P \text{ prime}} P\right) = \bigcap_{I \subset P, P \text{ prime}} \mathcal{L}_R^{-(n-1)}(P).$$

Example 3. For the \mathbb{Z}_{36} ring, let's examine n-prime radicals $\beta^n(\mathbb{Z}_{36})$.

I_i ideal	$\mathcal{L}_{\mathbb{Z}_{36}}(I_i)$
$I_0 = (0), I_6 = (6), I_{12} = (12), I_{18} = (18)$	$\mathcal{L}_{\mathbb{Z}_{36}}(I_0) = \mathcal{L}_{\mathbb{Z}_{36}}(I_6) = \mathcal{L}_{\mathbb{Z}_{36}}(I_{12}) = \mathcal{L}_{\mathbb{Z}_{36}}(I_{18}) = (6)$
$I_1 = (1) = \mathbb{Z}_{36}$	$\mathcal{L}_{\mathbb{Z}_{36}}(I_1) = \mathbb{Z}_{36}$
$I_2 = (2), I_4 = (4)$	$\mathcal{L}_{\mathbb{Z}_{36}}(I_2) = \mathcal{L}_{\mathbb{Z}_{36}}(I_4) = (2)$
$I_3 = (3), I_9 = (9)$	$\mathcal{L}_{\mathbb{Z}_{36}}(I_3) = \mathcal{L}_{\mathbb{Z}_{36}}(I_9) = (3)$
$I_8 = (8)$	$\mathcal{L}_{\mathbb{Z}_{36}}(I_8) = (4)$
$I_{16} = (16)$	$\mathcal{L}_{\mathbb{Z}_{36}}(I_{16}) = (8)$

Since $I_{12} \cap I_{18} = (0)$,

$$\mathcal{L}_{\mathbb{Z}_{36}}(I_{12} \cap I_{18}) = \mathcal{L}_{\mathbb{Z}_{36}}(0) = I_6.$$

In this case, $\beta(\mathbb{Z}_{36}) = \sqrt{(0)} = I_2 \cap I_3 = I_6$. Furthermore,

$$\mathcal{L}_{\mathbb{Z}_{36}}^{-1}(\sqrt{(0)}) = I_0 \cap I_6 \cap I_{12} \cap I_{18} = (0)$$

and

$$\beta^2(\mathbb{Z}_{36}) = \sqrt[3]{(0)} = \sqrt[1+2]{(0)} = \mathcal{L}_{\mathbb{Z}_{36}}^{-1}(\sqrt{(0)}) = \mathcal{L}_{\mathbb{Z}_{36}}^{-1}((6)) = (0)$$

and $\mathbb{Z}_{36} / \beta^2(\mathbb{Z}_{36}) \cong \mathbb{Z}_{36}$. Therefore,

$$\beta^2(\mathbb{Z}_{36} / \beta^2(\mathbb{Z}_{36})) = (0).$$

Example 4. Let $(F, +, \cdot)$ be a field and $R = \left\{ \begin{pmatrix} a & b & c \\ 0 & d & e \\ 0 & 0 & 0 \end{pmatrix} : a, b, c, d, e \in F \right\}$ be a ring. Then,

$$\beta(R) = \sqrt{(0)} = \left\{ \begin{pmatrix} 0 & a & b \\ 0 & 0 & c \\ 0 & 0 & 0 \end{pmatrix} : a, b, c \in F \right\},$$

$$\mathcal{L}_R^{-1}(\sqrt{(0)}) = \left\{ \begin{pmatrix} 0 & 0 & a \\ 0 & 0 & 0 \\ 0 & 0 & 0 \end{pmatrix} : a \in F \right\}$$

and

$$\beta^2(R) = \sqrt[3]{(0)} = \sqrt[2+1]{(0)} = \mathcal{L}_R^{-1}(\sqrt{(0)}) = \left\{ \begin{pmatrix} 0 & 0 & a \\ 0 & 0 & 0 \\ 0 & 0 & 0 \end{pmatrix} : a \in F \right\}.$$

Quotient ring as

$$\bar{R} = \left\{ \begin{pmatrix} a & b & c \\ 0 & d & e \\ 0 & 0 & 0 \end{pmatrix} + \beta^2(R) : a, b, c, d, e \in F \right\} = \left\{ \begin{pmatrix} a & b & 0 \\ 0 & d & e \\ 0 & 0 & 0 \end{pmatrix} : a, b, d, e \in F \right\}$$

where

$$\begin{pmatrix} a & b & 0 \\ 0 & c & d \\ 0 & 0 & 0 \end{pmatrix} + \begin{pmatrix} x & y & 0 \\ 0 & z & t \\ 0 & 0 & 0 \end{pmatrix} = \begin{pmatrix} a+x & b+y & 0 \\ 0 & c+z & d+t \\ 0 & 0 & 0 \end{pmatrix}$$

and

$$\begin{pmatrix} a & b & 0 \\ 0 & c & d \\ 0 & 0 & 0 \end{pmatrix} \begin{pmatrix} x & y & 0 \\ 0 & z & t \\ 0 & 0 & 0 \end{pmatrix} = \begin{pmatrix} ax & ay + bz & bt \\ 0 & cz & ct \\ 0 & 0 & 0 \end{pmatrix}.$$

Thus, $I_1 = \left\{ \begin{pmatrix} a & b & 0 \\ 0 & 0 & e \\ 0 & 0 & 0 \end{pmatrix} : a, b, e \in F \right\}$, $I_2 = \left\{ \begin{pmatrix} 0 & b & 0 \\ 0 & d & e \\ 0 & 0 & 0 \end{pmatrix} : b, d, e \in F \right\}$,

$I_3 = \left\{ \begin{pmatrix} a & b & 0 \\ 0 & 0 & 0 \\ 0 & 0 & 0 \end{pmatrix} : a, b \in F \right\}$, $I_4 = \left\{ \begin{pmatrix} 0 & b & 0 \\ 0 & 0 & e \\ 0 & 0 & 0 \end{pmatrix} : b, e \in F \right\}$,

$I_5 = \left\{ \begin{pmatrix} 0 & b & 0 \\ 0 & 0 & 0 \\ 0 & 0 & 0 \end{pmatrix} : b \in F \right\}$, $I_6 = \left\{ \begin{pmatrix} 0 & 0 & 0 \\ 0 & 0 & e \\ 0 & 0 & 0 \end{pmatrix} : e \in F \right\}$ are semiprime ideals of \bar{R} . Then, $\mathcal{L}_{\bar{R}}(I_1) =$

I_1 , $\mathcal{L}_{\bar{R}}(I_2) = I_4$, $\mathcal{L}_{\bar{R}}(I_3) = I_1$, $\mathcal{L}_{\bar{R}}(I_4) = I_4$, $\mathcal{L}_{\bar{R}}(I_5) = I_4$, $\mathcal{L}_{\bar{R}}(I_6) = I_4$, and $\mathcal{L}_{\bar{R}}(0) = I_4$. Herefrom,

$$I_2 = \left\{ \begin{pmatrix} 0 & b & 0 \\ 0 & d & e \\ 0 & 0 & 0 \end{pmatrix} : b, d, e \in F \right\} \text{ and } I_1 = \left\{ \begin{pmatrix} a & b & 0 \\ 0 & 0 & e \\ 0 & 0 & 0 \end{pmatrix} : a, b, e \in F \right\}$$

are prime ideal. Moreover, $I_1 \cap I_2 = I_4$ is a semiprime ideal. $A(I_2) = \{I_2\}$ and $A(I_1) = \{I_1, I_3\}$ are obtained. It is observed that

$$\beta(\bar{R}) = \sqrt{(0)} = I_4$$

Since $\mathcal{L}_{\bar{R}}^{-1}(\sqrt{(0)}) = (0)$, $\beta^2(\bar{R}) = (0)$. Thus,

$$\beta^2(\bar{R} / \beta^2(\bar{R})) = \beta^2(\bar{R}) = (0).$$

Theorem 3.15. If I is an ideal of R , then $\mathcal{L}_R(I) \subset \sqrt{I}$.

Proof. For all $a \in \mathcal{L}_R(I)$, $aRa \subset I \subset \sqrt{I}$. Since \sqrt{I} is a semiprime ideal, $a \in \sqrt{I}$. Hence, $\mathcal{L}_R(I) \subset \sqrt{I}$.

Theorem 3.16. If I is an ideal of R , then $\mathcal{L}_R^n(I) \subset \sqrt{I}$, for all $n \in \mathbb{N}$.

Proof. From Theorem 6, $\mathcal{L}_R(I) \subset \sqrt{I}$, for $n = 1$. Let

$$\mathcal{L}_R^n(I) \subset \sqrt{I}$$

for all $n \in \mathbb{N}$. Therefore,

$$\mathcal{L}_R(\mathcal{L}_R^n(I)) = \mathcal{L}_R^{n+1}(I) \subset \mathcal{L}_R(\sqrt{I}) = \sqrt{I}.$$

Theorem 3.17: Let R be a ring and let $\{H_i\}_{i \in \Lambda}$ be a n -prime ring family. If R is isomorphic to a subdirect sum of ring H_i , then $\beta(R) = \mathcal{L}_R^n(0)$.

Proof. Since R is isomorphic to a subdirect sum of ring H_i , there is an ideal K_i of R such that $R / K_i \simeq H_i$ and $\bigcap_{i \in \Lambda} K_i = (0)$.

On the other hand, from [[3], Theorem 4], $\pi^{-1}(\mathcal{L}_{H_i}^n(0)) = \mathcal{L}_R^n(K_i)$ is a prime ideal. Therefore,

$$\beta(R) = \bigcap_{j \in \Lambda} P_j \subset \bigcap_{i \in \Lambda} \mathcal{L}_R^n(K_i) = \mathcal{L}_R^n\left(\bigcap_{i \in \Lambda} K_i\right) = \mathcal{L}_R^n(0).$$

Hence we get $\beta(R) = \mathcal{L}_R^n(0)$.

Theorem 3.18. Let R be a commutative ring with identity. Suppose that $(\mathcal{L}_R^n(0))^2 = (0)$ and each ideal of ring R has pairwise comaximal ideals in R . If $\beta(R) = \mathcal{L}_R^n(0)$, then R is isomorphic to a subdirect sum of ring H_i where H_i are n -prime rings.

Proof. Suppose that $\mathcal{L}_R^n(0) = \beta(R)$. Hence,

$$\mathcal{L}_R^n(0) = \bigcap_{i \in \Lambda} P_i$$

where P_i is a prime ideal, for all $i \in \Lambda$. Since P_i is a pairwise comaximal ideals in R ,

$$\bigcap_{i \in \Lambda} P_i^2 = \left(\bigcap_{i \in \Lambda} P_i \right)^2 = (\mathcal{L}_R^n(0))^2 = (0)$$

Thus, $\bigcap_i K_i = 0$ where $P_i^2 = K_i$, for all $i \in \Lambda$. On the other hand, since $\mathcal{L}_R^n(K_i) = \mathcal{L}_R^n(P_i^2) = P_i$, $\mathcal{L}_R^n(K_i)$ is a prime ideal and the set $R / K_i \simeq H_i$ is a n -prime ring. Let $\pi_i: R \rightarrow R / K_i$ be a natural epimorphism with $\pi_i(r) = 0$, for all $i \in \Lambda$ and $0 \neq r$. As a consequence, $r \in \bigcap_{i \in \Lambda} K_i = (0)$. This is a contradiction.

Remark 1. If $\beta(R) = \mathcal{L}_R^n(0)$, then $\beta^n(R/\beta^n(R)) = (0)$.

Proof. If $\mathcal{L}_R^n(0) = \mathcal{L}_R(\mathcal{L}_R^{n-1}(0)) = \beta(R)$, then $(0) \in A^{n-1}(\beta(R))$. Therefore,

$$\beta^n(R) = \sqrt[n+1]{(0)} = \mathcal{L}_R^{-(n-1)}(0) = \bigcap_{J \in A^{n-1}(\beta(R))} J = (0)$$

and

$$\beta^n(R/\beta^n(R)) = (0).$$

4. CONCLUSION

This article attempts to generalize the prime radical in a promising way. It also investigates the properties of the basic notions essential for this generalization specifically $A^n(I)$ and $\mathcal{L}_R^{-n}(I)$. The paper introduces the definitions of n -minimal semigroup semiprime ideal, n -prime radical of ideal I , and n -prime radical of ring R . Future research could extend these results to different rings, utilizing the generalization of prime radicals, thereby contributing significantly to ring theory. Additionally, the paper highlights open problems that may guide future studies.

5. OPEN PROBLEMS

1. Minimal $(n - 1) -$ prime radical is a subideal of intersection of $(n - 1) -$ prime ideals.
2. Let R be a ring. Then, $\beta^n(R/\beta^n(R)) = (0)$.

REFERENCES

1. Karalarlıoğlu Camcı, D. (2017). Source of semiprimeness and multiplicative (generalized) derivations in rings, Doctoral Thesis, Çanakkale Onsekiz Mart University, Çanakkale, Turkey.
2. Aydın, N., Demir, Ç., Karalarlıoğlu Camcı, D. (2018). The source of semiprimeness of rings, Communications of the Korean Mathematical Society, 33(4), 1083-1096.
3. Karalarlıoğlu Camcı, D., Yeşil, D., Mekera, R., Camcı, Ç. A Generalization of Source of Semiprimeness, Submitted.

4. Azumaya, G. (1948). On generalized semi-primary rings and Krull-Remak-Schmidt's theorem, *Japanese Journal of Mathematics*, 19, 525-547.
5. Baer, R. (1943). Radical ideals, *American Journal of Mathematics*, 65, 537-568.
6. Brown B., McCoy, N. H. (1947). Radicals and subdirect sums, *American Journal of Mathematics*, 67, 46-58.
7. Jacobson, N. (1945). The radical and semi-simplicity for arbitrary rings, *American Journal of Mathematics*, 76, 300-320.
8. Köthe, G. (1930). Die Struktur der Ringe deren Restklassenring nach den Radikal vollständigreduzibel ist, *Mathematische Zeitschrift*, 32, 161-186.
9. Levitzki, J. (1943). On the radical of a ring, *Bulletin of the American Mathematical Society*, 49, 462-466.
10. McCoy, N. H. (1949). Prime ideals in general rings, *American Journal of Mathematics*, 71, 833-833.
11. McCoy, N. H. (1964). *The Theory of Rings*. The Macmillan Co.
12. Harehdashti, J. B., Moghimi, H. F. (2017). A Generalization of the prime radical of ideals in commutative rings, *Communication of the Korean Mathematical Society*, 32 (3), 543–552.
13. Clark, W. E. (1968). Generalized Radical Rings, *Canadian Journal of Mathematics* , 20, 88 - 94.